國立交通大學

電信工程研究所

碩 士 論 文

共存干擾之管理

On the Management of In-Device Coexistence
Interference

研 究 生：賴勇先

指導教授：蘇育德　教授

謝世福　教授

中 華 民 國 一 百 零 一 年 七 月

共存干擾之管理

On the Management of In-Device Coexistence Interference

研 究 生：賴勇先　　　　Student：Yung-shian Lai

指導教授：蘇育德　　　　Advisor：Dr. Yu T. Su

　　　　　謝世福　　　　　　　　Dr. Shih F. Hsieh

國 立 交 通 大 學

電信工程研究所

碩 士 論 文

A Thesis

Submitted to the Institute of Communications Engineering

in Partial Fulfillment of the Requirements

for the Degree of

Master of Science

in

Communications Engineering

at the

National Chiao Tung University

July 2012

Hsinchu, Taiwan

中華民國 一百零一年七月

共存干擾之管理

學生：賴勇先　　　　　　　　　　　　　　　　　指導教授：蘇育德博士

　　　　　　　　　　　　　　　　　　　　　　　　　　　　謝世福博士

國立交通大學電信工程研究所碩士班

摘　　　要

　　為了完全利用有多個無線電系統共存的異質網路，使用者應該有能力去選擇最有效率的系統；其中效率的測度為單位傳輸功率的吞吐量。這樣一來，使用者裝置需搭載多種傳收器以因應不同的環境並選擇當下最適當的系統。例如：藉由選擇無線區域網路（Wi-Fi）或藍芽（Bluetooth）來代替一般的巨型蜂巢式系統以連接公眾網路，減少網路端和用戶端的單位頻寬功率消耗。一個擁有多種無線電傳輸能力的使用者設備，也可以被當作大型和小型無線系統之間的中繼站，來降低大型無線網路流量的負載。

　　在上述的應用中，除非這些無線電使用的頻帶間距夠遠，否則會有嚴重的干擾問題。這是因為正在傳送信號的無線電會干擾到其他無線電的接收端。找出消除此共存干擾的解決方案正是這篇論文的主要目的。我們將集中討論在長期演進發展技術（LTE）和 Wi-Fi 之間的共存干擾問題。這個議題在第三代合作夥伴計劃（3GPP）的標準 36.816 [1]已經被密集的討論過，主要可歸納為三種候選方案：功率控制（PC）、分頻多工（FDM）、分時多工（TDM）等技術。藉由兼容這三者的優點，即同時利用 FDM 方案使兩個無線電操作頻段盡可能遠離、藉由 TDM 避免多個無線電同時啟用並將傳送功率控制在可容忍的範圍內，可以得到一個最佳解決方案。然而，如此做法可能因為與現有的標準相容性的問題而變得不可行，故尚需更進一步的探討。

　　非連續接收機制（DRX）原本設計是為了省電，使用者只能在每周期的一段固定時間內進行通訊，而在剩下的時間睡眠來達到省電的效果。而這樣的周期性的開關機制卻讓二個無線電可以分別在不同時間進行通訊。因為 DRX 已納入 LTE 標準，相容性的考量讓以 DRX 為基礎的 TDM 解決方顯得較為實用。但由於 DRX 機制會將時間資源分別給 LTE 和 Wi-Fi 傳收端，使得二者的系統吞吐量都下降。因此，我們不希望太早啟用這種機制以盡可能地避免吞吐量下降；另一方面，如果太晚啟用，沒有被處理的共存干擾又會降低訊號干擾雜訊比（SINR）並且導致封包遺失。我們試著找出啟動與解除 DRX 機制的最佳時間點，並且在正確的時間點傳

送觸發訊號給基地台。我們利用在適當時間區間量測到的 SINR 來決定是否要啟上述機制並回報 DRX 的相關參數給基地台。根據模擬結果，在 LTE 下傳吞吐量的效能上，我們提出的方法會比以下另外二種方式來得好：第一種是當 Wi-Fi 一開啟就立即啟用 DRX 機制；第二種則是不啟用任何的共存干擾解決方案。我們的方法不但可以同時滿足 LTE 和 Wi-Fi 的吞吐量要求，也可使 LTE 下傳吞吐量達到最大。

正如前述，為了要決定何時要啟動 DRX 機制，我們需要量測 SINR 的比值，因此如何在實體層精準地量測 SINR 是我們要探討的另一個議題。我們利用二階回歸模型[3]來同時估測通道增益和其對應的 SINR。根據模擬結果，這種做法會比傳統的最小平方誤差通道估計器效能更好。

我們分別用電腦模擬和數學分析來估算和比較開啟 DRX 後 LTE 和 Wi-Fi 吞吐量，根據這些分析結果我們可以評價各種 DRX 參數對於吞吐量的影響。我們推導得到了傳送一個封包所費時間的機率密度函數，以及其相關的變異數以及平均吞吐量。雖然 Wi-Fi 系統只可在 DRX 的睡眠期間啟動，它可以趁這期間結束前，根據已知剩餘可用的時間調整封包大小。在這種情況下，Wi-Fi 平均的吞吐量大約會等於睡眠時間和 DRX 週期的比值，此理論推導也藉由模擬得到驗證。另外，我們採用 FD-PF[15]公平資源排程機制來進行 LTE 吞吐量分析，模擬結果符合 LTE 可用時間比例與吞吐量一同增加的預期。我們可以從模擬結果發現此排程機制所導致的一些特徵，並利用它們來建立可同時滿足 LTE 和 Wi-Fi 吞吐量需求的 DRX 參數選擇方針。

On the Management of In-Device Coexistence Interference

Student : Yung-Shian Lai   Advisor : Yu T. Su and Shih F. Hsieh

Department of Communications Engineering

National Chiao Tung University

Abstract

To make the most of a heterogeneous network in which multiple radio systems co-exist, an user equipment (UE) should have the capability to select the most efficient system where the efficiency is measured by the throughput/power ratio. Such a capability requires that UEs are equipped with built-in multiple transceivers so that it can adapts to the environment and choose, for example, Wi-Fi or Bluetooth, to connect to the network instead of a regular macro-cellular system, resulting in power/bandwidth saving for both the UE and network. A device with such multiple radio capability can also be used as a relay between a macro system and a small cell to offload the network traffic.

A serious interference problem arises when applications similar to the latter scenario are called for unless the assigned bands for these radios are sufficiently separated. When both transceivers in the same device are active, the transmitting radio signal will interfere the other radio's receiver. It is the purpose of this thesis to find solutions for mitigating this in-device coexistence interference(IDCI). We focus on IDCI between LTE and Wi-Fi systems. This particular issue has been intensively discussed in 3GPP specification 36.816 [1] from which three major candidates solutions have emerged, namely, Power control solution, Frequency Division Multiplexing (FDM) solution, and Time Division Multiplexing (TDM) solution. An optimal one would bear the flavors of all three

approaches, i.e., one invokes the FDM solution to select the available bands as far apart as possible, and the TDM solution to avoid simultaneous activation while control the transmit power to a tolerable range. Unfortunately, such a solution is often not realizable as it may not compatible with the existing LTE standard and modifications are needed.

As a result, the Discontinue Reception (DRX) based TDM solution is much more practical as DRX had been standardized by LTE. DRX is originally designed for energy-saving purpose that allows only a fractional wake-up interval within each predetermined period. However, such a periodic on-off clock can be used to serve two radios in disjoint time intervals.

Since the DRX based solution divides the time resources into two parts for the LTE and Wi-Fi transceivers, it will degrade the throughput of both systems. Hence we do not want to activate such an IDCI solution too early to avoid degradation of throughput as much as possible. On the other hand, if we invoke the IDCI solution too late, the coexistence interference will reduce SINR and cause packet loss. In this study, we try to optimize the activation time for the DRX based solution, sending a trigger signal to eNB at the right time. We also find the optimal deactivation time. Based on measured SINR over a proper time period, we decide whether or not to trigger the IDC solution and report the associated DRX parameters to the serving eNB.

For determining when to trigger the DRX based solution, we need to measure the signal quality such as Signal to Interference plus Noise Ratio (SINR). Hence, how to measure SINR accurately in the physical layer is another issue we want to discuss. We use the regression model based approach of [3] to jointly estimate the channel gain and the correspondent SINR. It is shown that this approach outperforms the conventional least square (LS) based channel estimator.

Our simulations indicate that the LTE DL throughput performance of the proposed solution is better than the other two alternatives: the first one triggers the DRX based

solution whenever WiFi is on while the second one does not employ any IDCI solution. Our method not only satisfies the LTE and WiFi throughput constraints but also maximizes the LTE DL throughput.

The WiFi and LTE throughput performance is estimated by both computer simulation and analysis. The analytical results enable us to assess the effects of the DRX parameters on the throughput performance. We derive the probability density function (pdf) of the packet transmission time and evaluate the mean throughput and the associated variance. As WiFi can use only the off-duration of the DRX clock, it can adjust the packet size according the timing information. In that case, the average throughput is approximately equal to the fraction of the off-duration. The theoretical derivations are verified by simulations. For the LTE throughput analysis, we adopt the fairness-aware FD-PF scheduling scheme. The simulation results are consistent with the anticipation that the throughput improves with the increase availability of the LTE time resource. We establish guidelines for the system to select appropriate DRX parameters to meet both LTE and WiFi's throughput requirements.

Contents

List of Figures

List of Tables

Chapter 1

Introduction

1.1 The coexistence interference problem

The LTE-A (Long Term Evolution-Advanced) mobile standard supported by 3GPP (3rd Generation Partnership Project) shall provide downlink data rates greater than or equal to 1 Gbps and 100 Mbps for low and high mobilities, respectively. LTE downlink shall adapt the Orthogonal Frequency Division Multiple Access (OFDMA) technology while Single Carrier Orthogonal Frequency Division Multiple Access (SC-OFDMA) is the uplink air interface technology. Both technologies provide many attractive features that include robustness against frequency selective fading, high spectral efficiency, great flexibility in radio resource allocation and scheduling.

Due to the increasing popularity and proliferation of the Wireless Local Area Networks (WLANs), it has become a desired feature that a mobile phone can access to both cellular and WLAN systems. One prefers to make a phone call through cellular system, access the Internet through WiFi, and connect a portable handset (earphone) through Bluetooth. In some applications, one would like to access these heterogenous systems simultaneously which unfortunately causes inter-radio interference. This is because the operation band of the so-called industrial, scientific, and medical (ISM) band and band 40 of LTE are close to one another, the coexistence of two types of radio transceivers

will result in adjacent channel interference. We refer to the interference issue associated with this scenario as In-device coexistence interference (IDCI) problem.
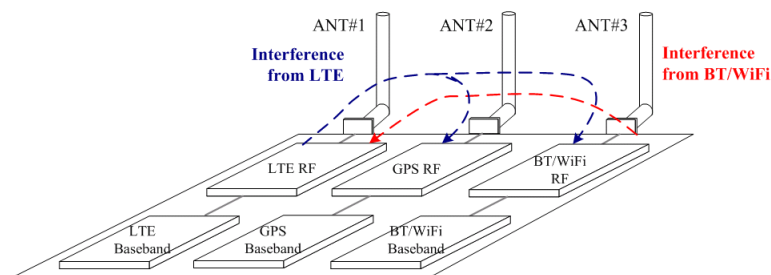
Figure 1.1: Coexistence interference within the same UE.

Fig. 1.1 shows an example in which many radio transceivers are embedded in the same UE chip. The transmit power from a radio transmitter is often much higher than the power received by another radio while both are located in the same chip. Because of insufficient frequency separation and isolation between the transmit and receive units, the transmit signal causes serious interference. The current filter technology can not provide enough rejection and it is difficult to solve interference problem by RF design. Alternative methods by baseband design should therefore be considered. The above in-device coexistence interference (IDCI) problem in power, time, and frequency domains is illustrated in Fig. 1.2. An ISM band transmitter sends signal to AP, and the LTE receiver receives signal from eNB at the same time. Typically, the spurious emission by the ISM transmitter is much higher than the received LTE signal strength.

Fig. 1.3 plots the 3GPP frequency bands around 2.4GHz ISM band. Three radio technologies discussed in 3GPP 36.816 [1] result in coexistence with LTE, namely, WiFi, Bluetooth, and GNSS. We discuss these three operating scenarios in the following section.

1.2 Operation Scenarios for IDCI
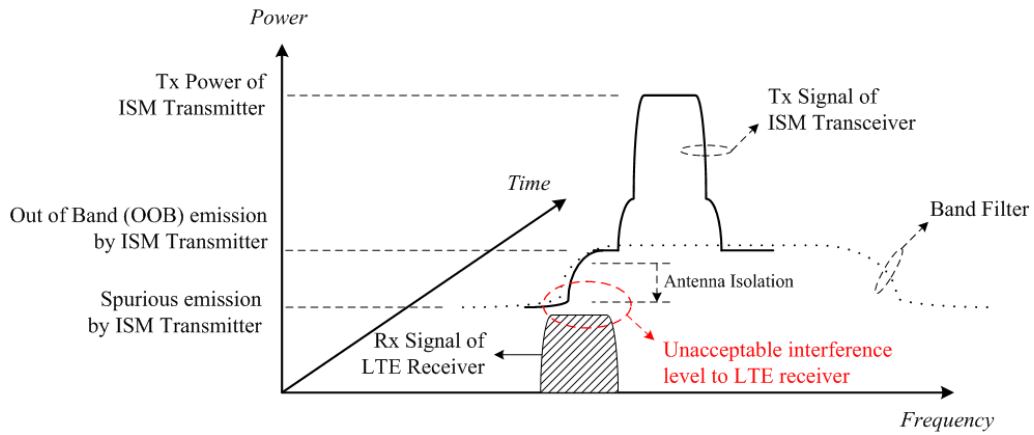
Figure 1.2: Coexistence interference from the in-device ISM transmitter to the E-UTRA receiver.
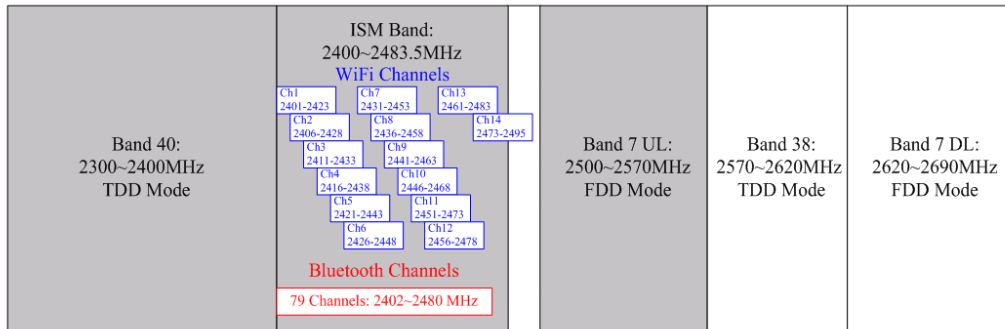
Figure 1.3: 3GPP frequency bands around the ISM band.

1.2.1 IDCI caused by coexistence of LTE and WiFi

When an IDC user transmits a WiFi waveform and receive data from the LTE network to provide real time traffic service, WiFi uplink data to AP will interfere with LTE receiving data from eNB, and LTE uplink data will also interfere with the WiFi receiving data from AP because LTE band 40 operates at TDD mode, and it will uplink and downlink data at the same frequency band. WiFi has 14 channels in ISM band, and each channel bandwidth is 22MHz. Channel 1 starts with 2401MHz, and channel 14 ends at 2495MHz. Each channel separates from adjacent channel by 5MHz. There is an exception in channel number 14 where separation is 12MHz. Channel number 14 is defined beyond ISM band,

and it is only used in Janpan. The transmitter of WiFi will affect receiver of LTE band 40 and vice-versa. Since LTE band 7 is a FDD band, it will affect WiFi receiver. However, WiFi doesn't affect LTE receiver at LTE band 7 downlink.
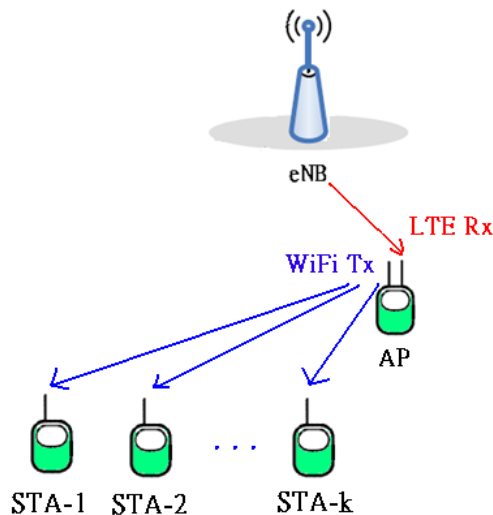
Figure 1.4: LTE + WiFi portable router.

1.2.1.1 LTE + WiFi portable router

Fig. 1.4 can express this scenario. In this figure, it shows the situation for LTE downlink data from eNB to IDC-UE and for WiFi of IDC-UE downlink data to many stations, and the transmission of WiFi will interfere LTE receiver. UE uses LTE which is considered as a backhaul link to access the Internet to download data from network, and the UE shares the data by WiFi to other local WiFi stations which connect with it. Therefore, the UE becomes a portable AP which has full control on frequency channel and transmitting power. The UE can move WiFi signal away from LTE band by itself. If this is not sufficient to solve IDCI problem, UE can inform eNB and require an IDCI solution. If we use TDM solution to solve the IDCI problem, it will allocate scheduled period and unscheduled period for LTE. During DL from eNB to UE, the worst case is that if a packet arrives at the eNB at the beginning of the LTE unsched-

4

uled period, the resulting delay is the sum of the LTE unscheduled period (waiting for LTE scheduling) and the LTE scheduling period (waiting for WiFi scheduling). It is the delay which begins with eNB receiving packet from Internet and ends with WiFi starting to transmit this packet to the station. The situation is similar to the UL. The scheduling/unscheduled periods can be made as small as 1 ms to minimize delay, but it is unusable because it doesn't consider the impact on retransmissions and other timelines on both LTE and WiFi, and it also can't satisfy WiFi transmission time which may excess 1ms. Therefore, the scheduling/unscheduled periods should be balanced between the timeline requirements and the needs of the specific Quality of service (QoS). The scheduling periods and unscheduled periods should use the following guidelines:

1. Scheduling periods and unscheduled periods should be typically not more than [20-60] ms.

2. The scheduling and unscheduled periods should be large enough to conform reasonable operation of the LTE and WiFi timelines.

3. Since LTE has typically lower data rate than the WiFi link, the LTE scheduling periods should be longer than the unscheduled periods in order to achieve roughly the same throughput on both links.

The coexistence interference case 1-3 of section 1.2 may happen in this scenario.

1.2.1.2 LTE + WiFi offload

Fig. 1.5 can express this scenario. It shows the situation for WiFi uplink data to AP and for LTE downlink data from eNB to UE, and the transmission of WiFi will interfere with LTE receiver. LTE UE can offload traffic from LTE to WiFi, and the WiFi transceiver of the UE operates as a terminal (not AP) in infrastructure mode. For example, UE performs video conference. The video stream can be divided into image packets and VoIP packets. And it uses WiFi radio to transmit image packets for
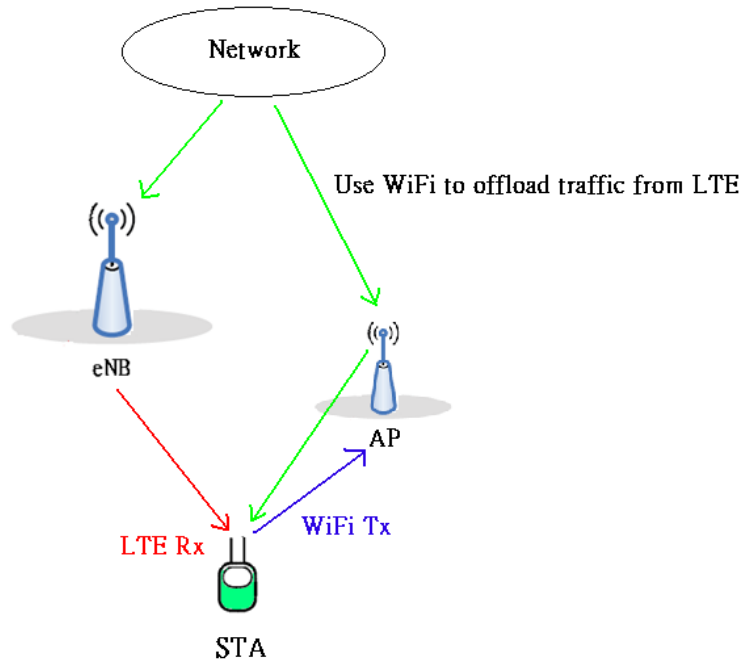
Figure 1.5: LTE + WiFi offload.

offloading load of LTE and uses LTE radio to transmit VoIP packets for guaranteeing Qos (delay). Because WiFi radio is not AP, it is difficult for the WiFi radio to change the configured frequency channel. In addition, the WiFi radio has to keep listening to the beacon signal transmitted from WiFi AP for maintaining connection. In this scenario, if we use time domain solution, the requirements for the scheduling period and the unscheduled periods will be analyzed as following three observations:

First observation is that UE in WiFi client mode must receive WiFi beacon. In order to receive beacons properly, the LTE unscheduled period needs to align with the WiFi beacons. Besides, in order to provide for beacon reception, the scheduling period of LTE should be no longer than 100ms.

Second observation is that the packet from network can choose one link (WiFi for offload packets, and LTE for non-offload packets) to transmit to UE. For offload packets, the largest delay will be scheduling periods, and vice versa. Comparing to WiFi portable router, the WiFi offload has larger scheduling periods and unscheduled periods with the

same delay requirements.

Third observation is that the traffic volume of the non-offloaded and offloaded traffic should be matched by the ratio of the scheduling and unscheduled periods.

Synthesizing the above observations, we conclude that the scheduling periods and the unscheduled periods shall find a balance between the QoS (delay) requirements and the requirements of the acknowledgement/timeline of LTE and WiFi (HARQ timer, beacon duration, and so on). In summary, the following guidelines are useful.

1. The scheduling and unscheduled periods should typically not be more than [40-100] ms.

2. The scheduling and unscheduled periods should be large enough to conform reasonable operation of the LTE and WiFi timelines.

3. WiFi beacons are important messages, LTE unscheduled period should align with them.

4. The ratio of the scheduling and unscheduled periods should be aligned to the ratio of the volume of non-offloaded and offloaded traffic.

The coexistence interference case 1-3 of section 1.2 may happen in this scenario.

1.2.2   IDCI Arisen from Coexistence of LTE and Bluetooth

When an IDC user uses LTE for VoIP service and Bluetooth earphones as a part of a hands-free mobile phone, inter-radio interfere results. Bluetooth has 79 channels which are separated by 1 MHz and are in ISM band. The first channel starts with 2402 MHz , and the last channel ends at 2480 MHz. Similar to WiFi case, the LTE band 40 will be disturbed by BT and vice versa. The FDD LTE band 7 will affect BT receiver, but BT won't affect FDD LTE band 7 receiver.

1.2.3   LTE coexisting with GNSS

Examples of Global Navigation Satellite System (GNSS) include GPS, Modernized GPS, Galileo, GLONASS, Space Based Augmentation Systems (SBAS), and Quasi Zenith Satellite System (QZSS). The LTE UL band 7/13/14 will interfere some operating bands of GNSS system. The problematic cases between LTE and GNSS include:

1. Because LTE band 13/14 is uplink and the operation of frequency band is in 777-787 MHz/788-798 MHz respectively. It will cause interference to L1/E1 frequency of GNSS at 1575.42 MHz because of second harmonics which are produced by LTE band 13/14.

2. The frequency band of Galileo operates at 2.5 GHz for GNSS, which will be affected by LTE band 7 which operates in 2500-2570 MHz;

3. IRNSS (Indian Regional Navigation Satellite System) are transmitted on L5 (1164-1215 MHz) and S (2483.5-2500 MHz) bands. The S bands will be affected by LTE band 7 which operates in 2500-2570 MHz;

1.2.4   Summary of in-device coexistence interference scenarios

Based on the above analysis, the problematic coexistence scenarios will be reorganized by following four cases:

- Case 1: LTE Band 40 radio Tx causing interference to ISM radio Rx;

- Case 2: ISM radio Tx causing interference to LTE Band 40 radio Rx;

- Case 3: LTE Band 7 radio Tx causing interference to ISM radio Rx;

- Case 4: LTE Band 7/13/14 radio Tx causing interference to GNSS radio Rx.

We will identify the different usage scenarios to observe coexistence interference situation, and it will contribute to different solutions for collocated behavior of LTE and other technologies radio.

1.3 Coexistence interference avoidance
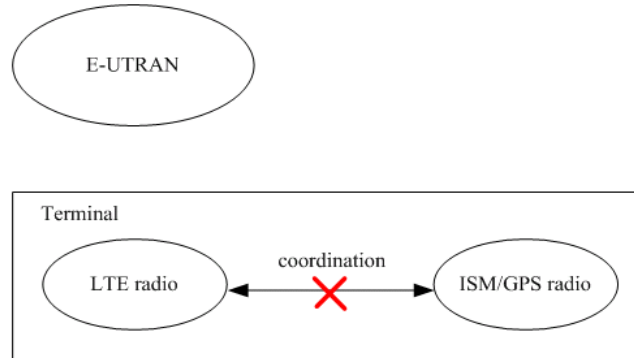
Figure 1.6: Uncoordinated mode.

1.3.1 Coexistence operation modes

(1) Uncoordinated mode:

In Fig. 1.6, it illustrates that the LTE radio operates independently of the ISM radio and there is no cooperation between the two radios and the LTE radio does not inform the E-UTRAN about coexistence interference problem. In this mode, if coexistence interference occurs, the only solution is using better filter to diminish the interference from another radio. In this case, UE must cost more money to make an accurate filter design; even so, the improvement is still restricted.

(2) Coordinated within UE only: Fig. 1.7 illustrates the scenario that an LTE radio is cooperating with an ISM radio without informing the E-UTRAN about the possible coexistence interference problem. In this situation, if coexistence interference occurs, the UE can use LTE denial (limit LTE transmission) or WiFi denial (limit WiFi transmission) to let one radio transmitter not collide with another radio receiver in time domain. In some cases, UE must receive important control information from WiFi AP (beacon) or LTE eNB (synchronous signal), so it is important for UE to use LTE or WiFi
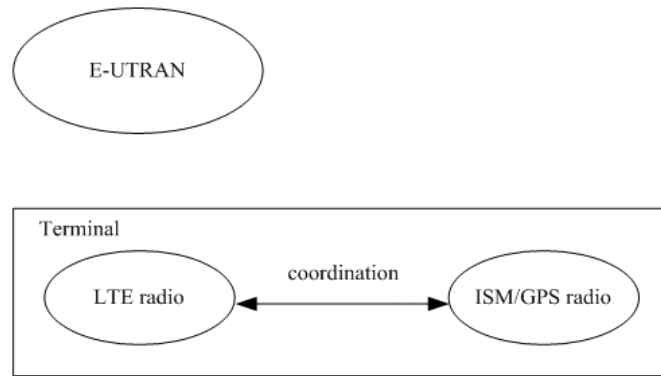
Figure 1.7: Coordinated within UE only.

denial sometimes. Since the E-UTRAN is not informed of the LTE denial message, E-UTRAN will transmit data even if the UE is in the LTE denial. The eNB may use lower modulation coding scheme because the transmission is failed by LTE denial, which will cause performance loss.
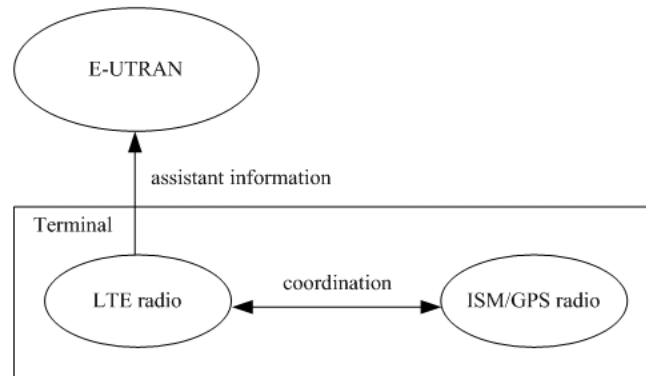
Figure 1.8: Coordinated with network level.

(3) Coordinated with network level:

Fig. 1.8 illustrates the case when an LTE radio is cooperating with an ISM radio while informing the E-UTRAN about the coexistence interference problem. In this situation, if coexistence interference occurs, the UE can request E-UTRAN for IDCI solution to solve coexistence interference problem. The IDCI solution is one of the Power control(PC) solution, the FDM solution, and the TDM solution which will be illustrated in next

section. The WiFi radio can also use WiFi denial to assist the process of TDM solution, and WiFi only transmits in the unscheduling period.

1.3.2   Frequency Division Multiplexing (FDM)

The UE informs the E-UTRAN when transmission/reception of LTE signal or other radio signal (e.g. WiFi) would be impaired because LTE doesn't use certain carriers or frequency resources. The UE will indicate which frequencies are unusable due to in-device coexistence and which frequencies are usable to eNB so that eNB can select appropriate frequency bands for FDM solution. We consider two candidate options.

Case 1: Move LTE signal away from ISM band
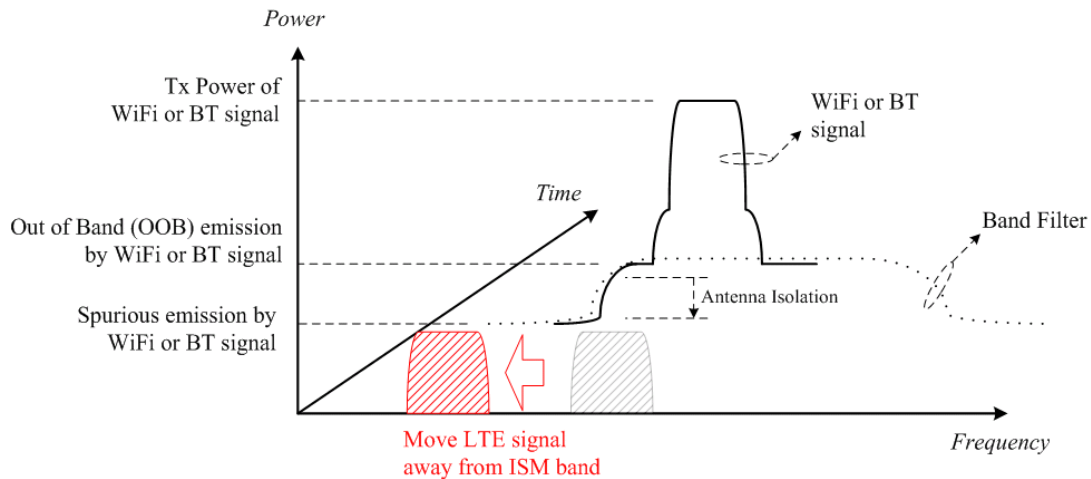
Figure 1.9: Potential solutions to move LTE signal away from ISM band.

This scenario is illustrated in Fig 1.9. The WiFi transmits data to AP, and LTE receives data from eNB. However, the WiFi signal will leak out to LTE receiver since existing filter restriction. By informing eNB about coexistence interference problem, if the eNB chooses FDM solution to solve IDCI problem, it will move LTE signal away from ISM band. In that way, it can reduce the LTE interference from WiFi signal.

Case 2: Move ISM radio signal away from LTE frequency band

The WiFi transmits data to AP and LTE receives data from eNB, the situation
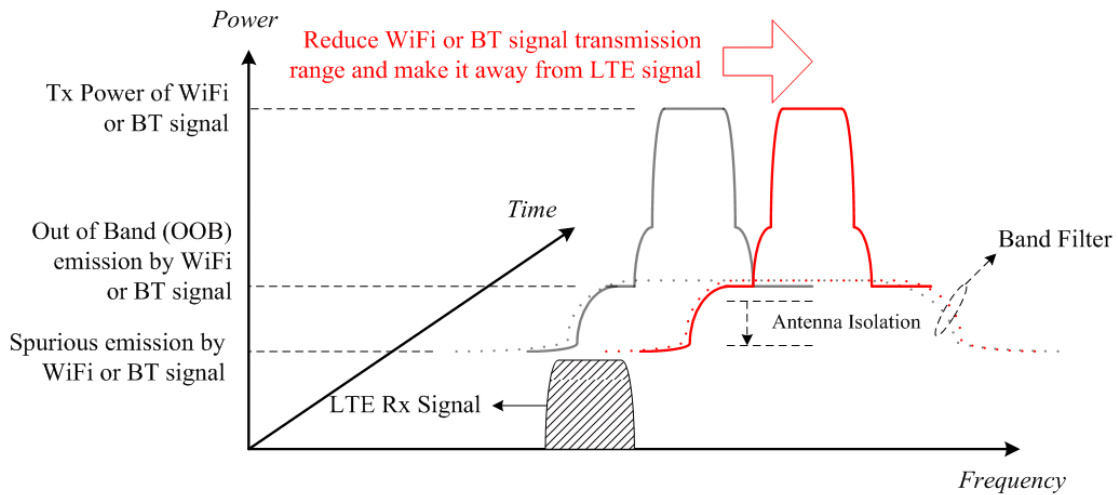
Figure 1.10: Move WiFi radio signal away from LTE frequency band.

can be shown in Fig 1.10. However, the WiFi signal will leak out to LTE receiver since existing filter restriction. By reducing WiFi or BT signal transmission range and making it away from LTE signal, it can reduce the LTE interference from WiFi signal. The WiFi station shall request AP for new operating frequency band. In order to help WiFi radio complete these necessary procedures, LTE also needs to avoid coexistence interference with WiFi radio during the initial stage (e.g. Using LTE denial).

1.3.3 Time Division Multiplexing (TDM)

As shown in Fig 1.11, though the LTE operating band is very close to the WiFi band, there is no interfere since the two radios use orthogonal time resources, e.g., the WiFi transmits signal between t_0 and t_1 while the LTE receives signal after t_1.

DRX based solution for LTE and WiFi

DRX is a discontinuous reception mechanism. When this mechanism is active, it will have a period for LTE to transmit and receive datum , known as the on-duration, and it will also have another period for LTE to not do any action, known as the off-duration (sleep period). In the off-duration, eNB will not allocate any resources to the UE, so the UE can't uplink data. Besides, eNB will also not downlink data to the UE. The UE

12
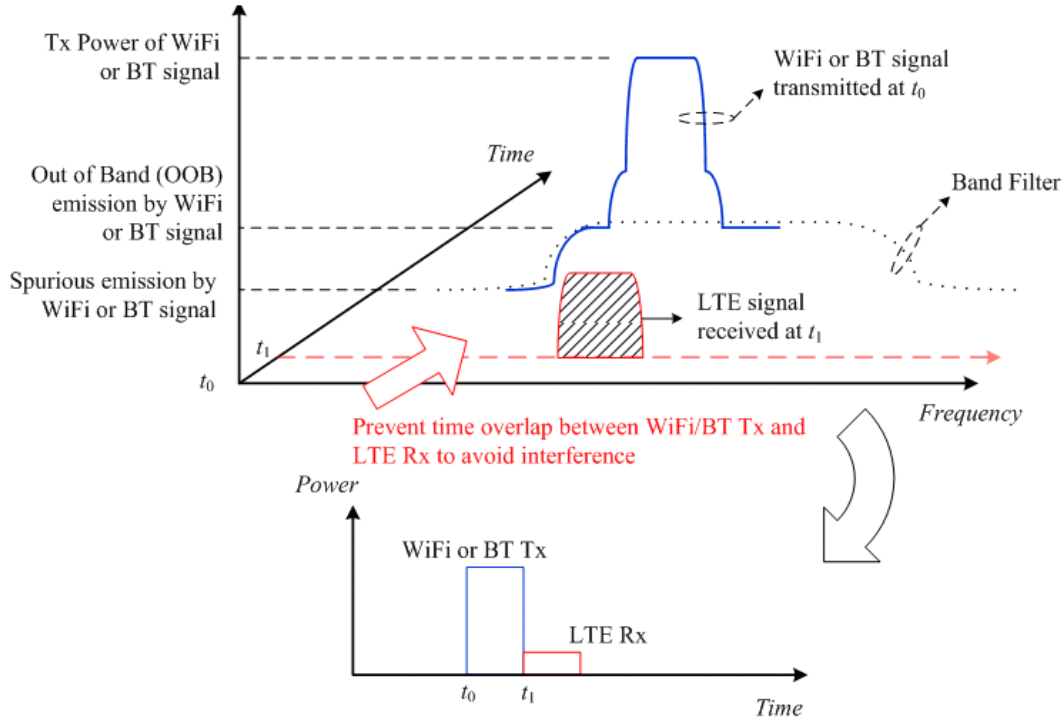
Figure 1.11: Time division multiplexing for coexistence interference avoidance.

will not transmit and receive during off-duration, so it can sleep to save battery power.

During the DRX operation, an LTE user can't send and receive actions in sleep mode. Therefore, in this period, we can use WiFi transmission and reception. Both sides will not be affected by the other side interference. Since the DRX mechanism already exists in current LTE system, using this mechanism to resolve the in-device coexistence interference problem is a good method. It can reduce the opportunity to modify LTE standards and make the operation become more simpler.

When the UE encounters the IDCI problem, it will inform eNB about this situation and require IDC solution. The UE will also provide the eNB with a desired TDM pattern. For example, the parameters related to the TDM pattern may consist of periodicity of the TDM pattern and scheduling period (or unscheduled period). The UE can suggest TDM pattern (e.g. Fig. 1.12). The configuration of scheduling/unscheduled period can

be designed by usage of LTE and WiFi. For example, if WiFi traffic is more frequent than LTE traffic, then the unscheduled period shall be longer than scheduling period. However, this configuration shall also satisfy both radio QoS and throughput constraint. If the unscheduled period is too long, the LTE delay requirement may not be satisfied, and it will result in packet loss.

The final DRX configuration is controlled by eNB (see Fig. 1.13) which can be based on the UE suggested TDM pattern and other possible criteria (e.g. traffic type). The scheduling period corresponds to the active time of DRX operation, while unscheduled period corresponds to the inactive time. The eNB should try to guarantee the unscheduled period by existing mechanisms, (e.g. appropriate UL/DL scheduling, DRX Command MAC control element usage, and etc). It means that flexibility principles from existing DRX mechanism will be applied (i.e. variable scheduling/unscheduled period is possible) and that no impact on UE HARQ operation is assumed so far. During inactive time, UE is allowed to delay the initiation of dedicated scheduling request and/or RACH procedure.
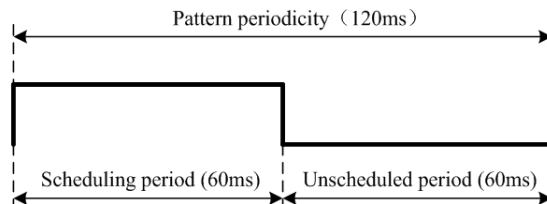
Figure 1.12: Example of UE suggested TDM pattern.

Introduction of DRX scheme

UE is active during the on-duration while listening to the physical downlink control channel (PDCC) to learn if eNB has data to be transmitted to it. After the activation of the on duration timer, the UE enters Inactive timer. During this timer, UE still listens to the control channel, and the timer will down count with time. The inactive timer will be reset once the eNB has data to transmit. If inactive timer counts to zero, and there
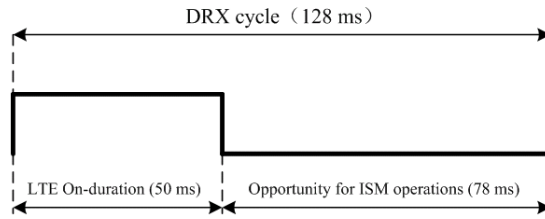
Figure 1.13: Example of DRX configured by eNB to enable TDM.
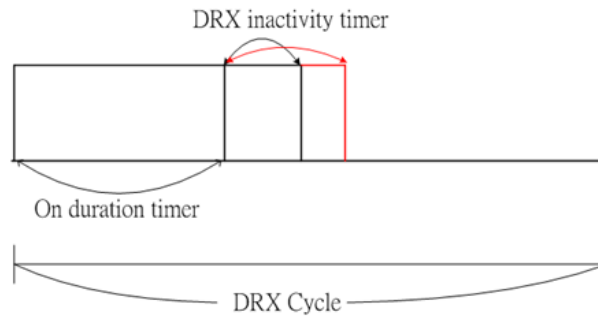
Figure 1.14: DRX scheme.

is no data buffer in eNB, then UE will enter power saving mode to save power. During this mode, UE can only listen to downlink control message, and it can't transmit or receive data during this period. Therefore, UE can transmit WiFi signal in this period. In addition to DRX solution pattern, WiFi of UE must use WiFi denial in DRX active time to avoid interfering with LTE. Combining DRX scheme and WiFi denial, WiFi and LTE will not interfere with each other.

1.3.4 Power control (PC)

When there is interference from WiFi uplink, UE can reduce the transmit WiFi power to mitigate the interference to LTE, but it will induce the degradation of WiFi SINR. The WiFi power which UE can adjust must conform with WiFi throughput constraint. To diminish LTE coexistence interference to ISM or GNSS downlink reception, the UE can report the need for power reduction to the eNB. The UE can adjust the power control parameters locally and report the power change value by existing mechanism. How the

15

report is transmitted (e.g. via RRC or MAC) and what information (e.g. interference type, power reduction value, and etc) should be transmitted to eNB are still not clear for 3GPP. The eNB can adjust the UE transmission power by existing mechanism, e.g. PDCCH or RRC signalling upon eNB receives the report from UE.

This method has two cases:

Case1: LTE power control

In this scenario LTE can reduce transmission power to mitigate interference with WiFi.
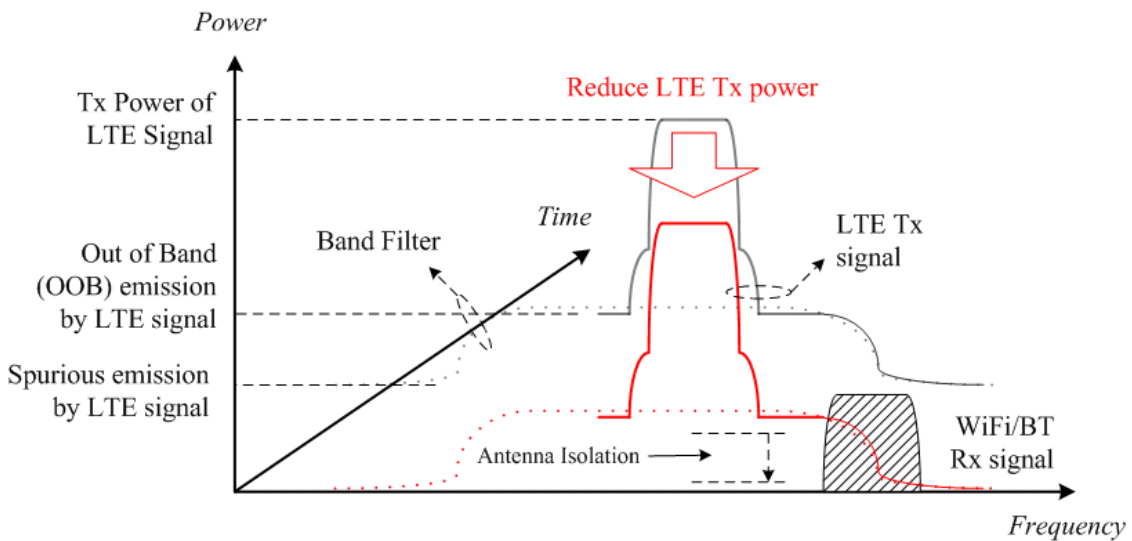
Figure 1.15: LTE power control for coexistence interference mitigation.

Case2: ISM power control

In this scenario WiFi can reduce transmission power to mitigate interference with LTE.

1.3.5 Summary for coexistence interference problem solution

Power control

WiFi uplink power reduction will result in WiFi SINR degradation and also lower WiFi UL throughput. If the coexistence interference problem is serious, the WiFi power
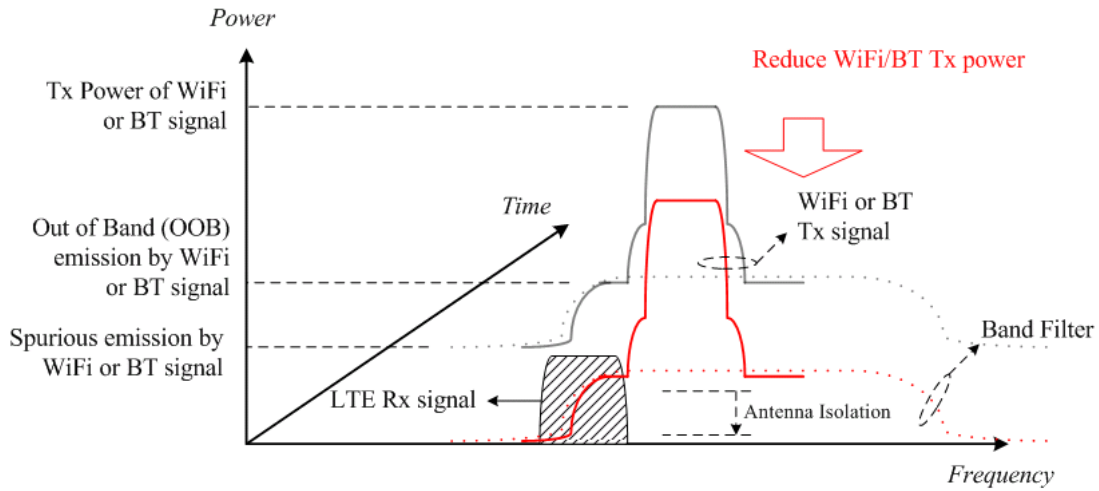
Figure 1.16: ISM power control for coexistence interference mitigation.

may need to be reduced by 20dB or even 60dB. Thus, it makes the WiFi throughput very low or even to be zero, and the power control solution becomes unsuitable. It is useful only if IDCI is relatively small.

FDM solution

FDM solution is done by shifting the operating frequency band to degrade interference from one another. However, this method can only degrade interference, it can't mitigate interference absolutely. When the IDC user is near the cell edge, the remaining interference still can't be endured by this user, so FDM solution is still not enough to solve IDCI problem sometimes. From another point of view, the operator (e.g. Chunghwa Telecom) may not be able to deploy the overlay coverage over multiple frequencies everywhere due to the consideration of deployment cost and coverage planning complexity. UE may not be able to find out an appropriate operating frequency band to use FDM solution because the whole LTE frequency band on operator are interfered by WiFi. It is useful only if IDCI is not relatively large.

TDM solution

By segmenting the time resource for different radio usage, when one radio is on

17

during a specific period, the other radio should remain silent. This method can totally avoid interference as orthogonal time resources are used. Since the time resources are segmented for different radio usage, the time resources available to the LTE or WiFi radio are reduced. Both LTE and WiFi suffer from throughput loss as the available time slots are limited by the DRX active mode and DRX power saving mode, respectively. We are interested in finding a proper DRX trigger epoch to maximize the total throughput while meeting the individual radio throughput constraints.

The rest of this thesis is organized as follows. In Chapter II, we describe the operating scenarios in which IDCI exists, present the related system model and assumptions. We also show several simulation results to exemplify the serious IDCI problems. In Chapters III and IV, we provide simulation results of SNR estimation and investigate the effectiveness of the DRX-based TDM solution by finding the optimal trigger parameters. In Chapters V, we analyze the WiFi and LTE throughput performance via Markov modeling. We investigate the theoretical WiFi throughputs with DRX and without DRX mechanism. Finally, we apply the fairness-aware FD-PF scheduling scheme [15] to simulate the throughput behaviors and study the impacts of the DRX parameters and UE-eNB distance. Our major results are then summarized in Chapters VI.

Chapter 2

System Model, Assumptions and Problem Formulation

2.1   Scenario and assumptions

A so-called LTE+WiFi offload scenario is considered in the ensuing investigation. We assume that the OFDMA based LTE system operates on LTE band 40 and in TDD mode. The WiFi system complies with the 802.11g standard–an OFDM system operating on the ISM band close to LTE band 40.

How these two networks interact is illustrated in Fig.2.1 where we consider the case where there is only one macrocell base station (BS) and one access point (AP). The LTE system uplinks and downlinks data streams in different (time) subframes (of 1 ms duration) while the WiFi link is active at the same time. By measuring the signal-to-interference-plus-noise ratio (SINR), we shall determine if a DRX-based IDCI solution should be activated.

The following system parameters are needed in subsequent discourse.

1. User mobility:

    The user mobility affects the channel's fading rate which is often classified into fast fading (> 120km/hr) or slow fading (3km/hr, 30km/hr). If the IDCI user moves

fast, the threshold for IDCI decision .

2. LTE and WiFi traffic type:

   The traffic types include Http, poisson, FTP, VoIP, or full buffer.

3. LTE and WiFi average SINR:

   LTE average SINR is related to the distance between eNB and UE, and it will affect LTE average throughput. WiFi average SINR is related to the distance between AP and UE, and it will affect WiFi transmission rate.

4. Different WiFi stations:

   The number of WiFi stations will affect throughput

5. LTE and WiFi operating frequency band:

   The interference will be different based on operating frequency band at LTE and WiFi.

6. LTE and WiFi throughput constraint:

   The DRX parameters must be chosen to ensure that the LTE/WiFi throughput requirements be satisfied.

2.1.1 A LTE and WiFi coexistence model: Operation and Interference

We assume that other WiFi users always have data to transmit and that they always use RTS/CTS mechanism.

We will introduce the procedure of Fig.2.1 and Fig.2.2 as follows. At first, the network will have some data stream to be transmitted to UE. If eNB receives the data stream from network, it will buffer the data stream and start to schedule downlink resources for UE by previous CQI report on DRX active mode, or it will not transmit data when UE operates on power saving mode until the next on-duration timer is activated. UE
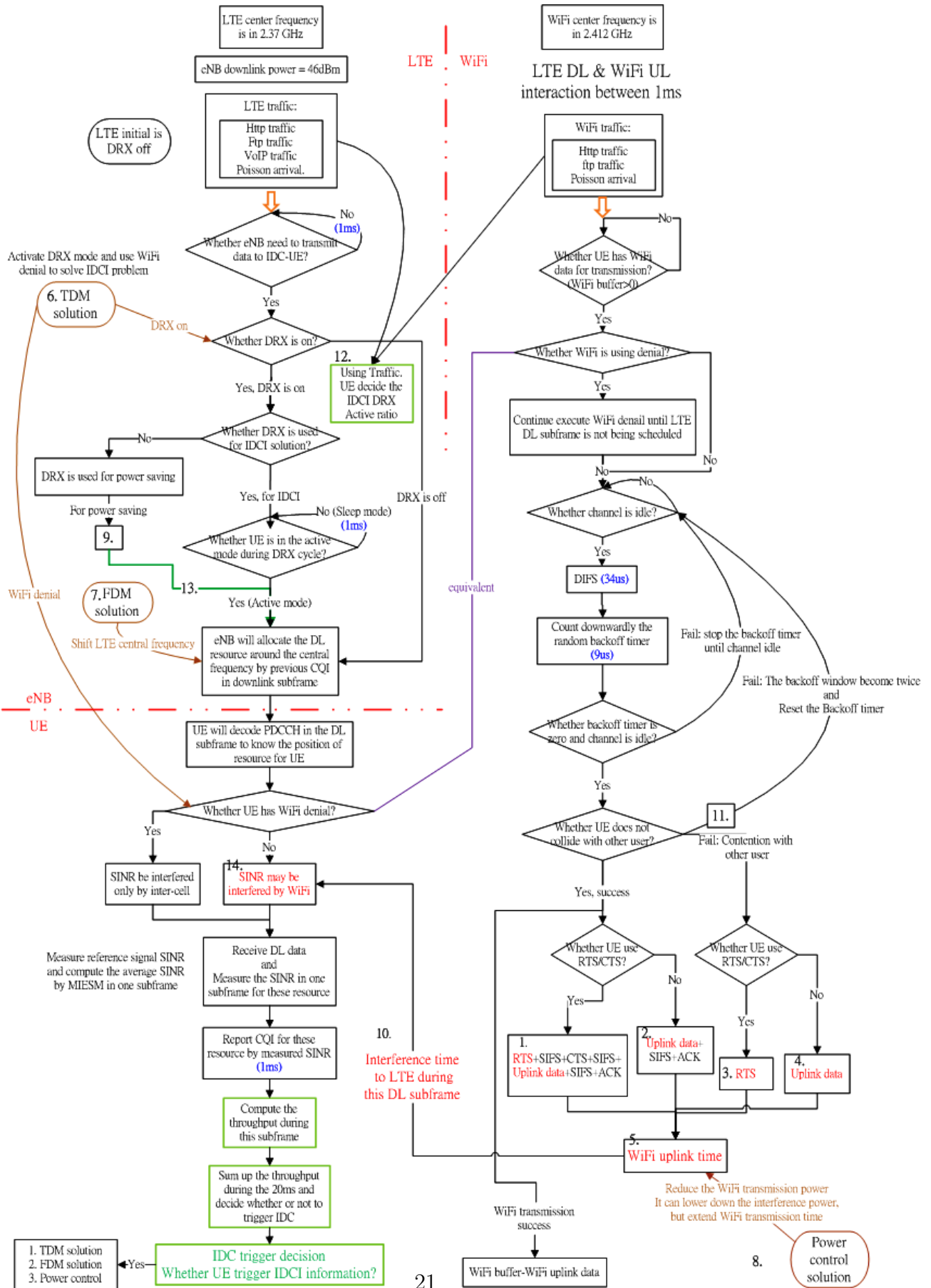
Figure 2.1: Interaction between LTE and WiFi models.
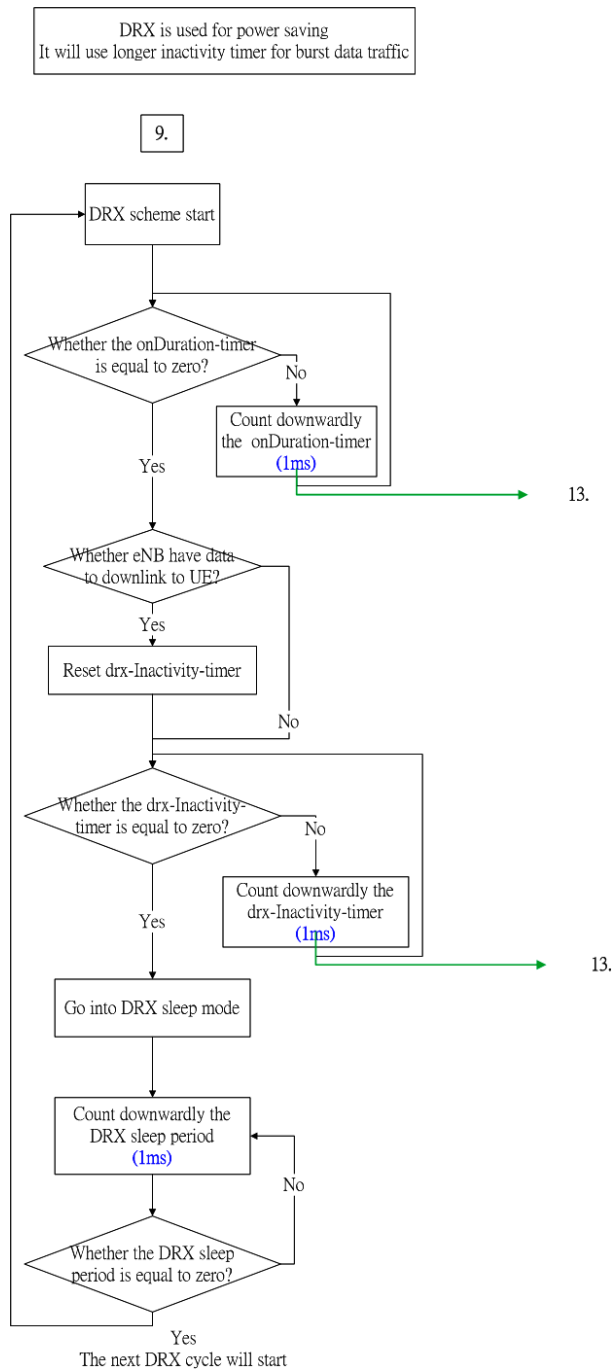
Figure 2.2: DRX procedure.

will decode PDCCH in the downlink subframe to know the position of resource for UE. If UE has WiFi denial, then the LTE downlink subframe will not be interfered by WiFi. However, if UE doesn't use WiFi denial, then LTE SINR may be interfered by WiFi. WiFi uplink signal will be RTS (request to send) and uplink data, they comply with RTS/CTS CSMA-CA scheme. When channel is idle, UE will count down the backoff timer after DIFS time interval(34us) and transmit RTS signal when the backoff timer becomes zero. And if backoff timer of other users also becomes zero, AP will receive RTS signals from different users at the same time. This situation will cause collision, so the AP will not transmit CTS signal, and channel becomes idle. If users don't receive CTS, they will extend backoff timer and reselect the random number from the new backoff timer. The IDC user will measure SINR in every subframe and compute the throughput by SINR mapped to modulation coding scheme for each subframe. At last, UE will average the throughput during measured period and decide whether to trigger IDC solution or not.

Referring to Figs. 2.1 and 2.2, we define the following acronyms:

1. RTS+SIFS+CTS+SIFS+Uplink data+SIFS+ACK: It means that WiFi UE will send RTS to AP when backoff timer is equal to zero, and AP will send CTS after SIFS when AP receives RTS. UE will send uplink data after SIFS when UE receives CTS, and AP will send ACK after SIFS when AP receives uplink data. The period of RTS and Uplink data will interfere with LTE radio.

2. Uplink data+SIFS+ACK: If there is no RTS/CTS scheme, UE will send uplink data directly. Moreover, AP will send ACK after SIFS when AP receives uplink data. Only the period of Uplink data will interfere with LTE radio.

3. RTS: If WiFi UE sends RTS to AP, and meanwhile there are other users sending RTS to AP, it will result in collision. Only the period of RTS will interfere with LTE radio.

4. Uplink data: If WiFi UE sends data to AP, and meanwhile there are other users sending RTS to AP, it will result in collision. Only the period of Uplink data will interfere with LTE radio.

5. WiFi Uplink time: If WiFi is transmitting data, it will be one of the cases which are mentioned above(1, 2, 3 and 4). And red parts of these cases represent the period of WiFi uplink time.

6. TDM solution: For LTE+WiFi case, the TDM solution will be DRX based solution with WiFi denial. Therefore, if the TDM solution is activated, eNB will turn on DRX solution and UE will use WiFi denial to avoid interfering with LTE.

7. FDM solution: eNB will shift LTE central frequency away from ISM band. However, this solution can't be used for some cases. For example, if eNB only has frequency band which is close to ISM band, the interference will be serious even if the resource blocks are allocated away from ISM band. For another example, because FDM solution can't avoid interference completely, WiFi interference will still cause serious effect for UE which is located at cell edge.

8. Power control solution: If LTE is interfered by WiFi, WiFi will decrease transmission power for diminishing the interference to LTE and vice versa. If WiFi lowers its uplink power for PC solution, WiFi may also decrease the link performance between AP and UE, which will result in increasing the WiFi transmission time. It is only used in the case that interference is light because of the limit of maximum power reduction.

9. For DRX in the power saving mode, it has inactivity timer which can extend LTE transmission time. During this inactivity timer, if UE receives the paging signal from PDCCH, UE will reset this inactivity timer and receive the data.

10. Interference time to LTE during this DL subframe: We can observe (5) to get

the period of WiFi uplink time during the DL subframe at present. We need to calculate the period of WiFi interference per subframe to know the WiFi activity property.

11. If the IDC user collides with other users, AP will receive RTS or Uplink data from IDC user and other signal from other users. AP will detect whether collision occurs. If so, it will not transmit CTS or ACK to the IDC user. If the IDC user doesn't receive response from AP after DIFS(DCF inter frame spacing), IDC user will double its backoff timer and contend with other users again.

12. We can use LTE and WiFi traffic to decide the DRX active ratio. Ex. DRX active ratio=active time/DRX cycle=LTE traffic/(LTE+WiFi traffic)

13. When user operates for on-duration timer or Inactivity timer of DRX scheme, it can still receive DL data from eNB, and eNB will allocate the DL resource around the central frequency by previous CQI in downlink subframe.

14. We can calculate SINR by interference time from (10). If interference time is long, the LTE DL subframe will be interfered by WiFi with large probability.

2.2   Problem formulation

2.2.1   A typical IDCI avoidance procedure

Referring to Fig 2.3, we describe an IDCI-avoidance procedure in the following.

1. First, UE will discover the in-device coexistence problem, and it will try to solve it by itself. If the interference becomes too serious for UE to handle this problem, it will need assistance from eNB to deal with the IDCI problem.
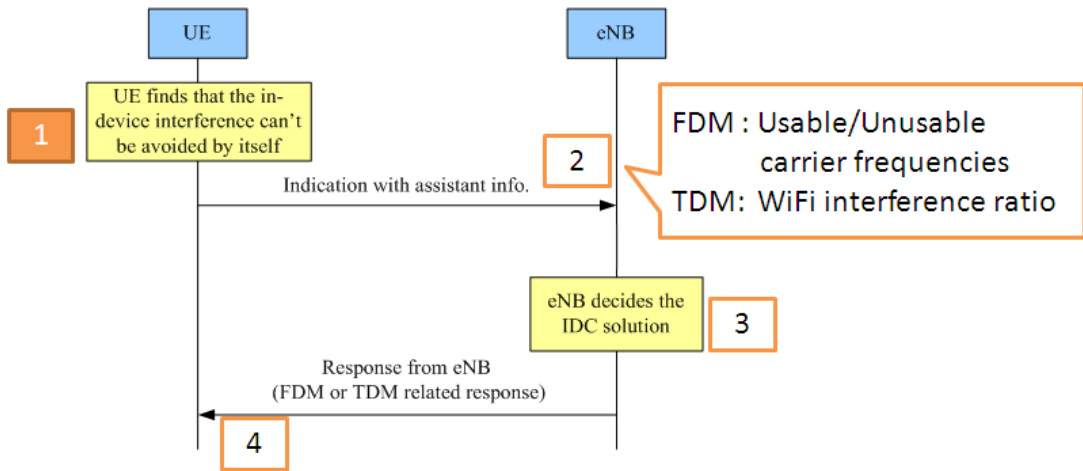
Figure 2.3: A typical IDCI avoidance procedure.

2. After UE wants to trigger IDCI solution and demands eNB for a IDCI solution, UE will send trigger indication to eNB, and this trigger indication will include some suggestible IDCI information to eNB (e.g. power control: the value of maximum power reduction; TDM solution: WiFi uplink activity ratio; FDM solution: usable/unusable carrier frequencies)

3. After eNB receives the indication of IDCI, it will decide an appropriate solution according to different situations (e.g., if usable frequencies are not existed or they are overloding, then eNB will use TDM solution for UE). Finally, eNB configure a specific solution for UE.

4. UE will receive IDC configuration demand and process the IDC solution given by eNB. (e.g. For TDM solution: eNB will configure an appropriate DRX parameters. For FDM solution: eNB will tell UE which frequency band should be used latter)

During the IDCI avoidance procedure, the UE must be denied until this IDC procedure is ended. Otherwise, WiFi will interfere with LTE reception for IDC information

and induce the IDCI procedure failed.

2.2.2 Motivation for IDCI solution trigger study

The in-device interference refers mainly to the adjacent channel interference between WiFi and LTE band 40. If UE can not solve the IDCI problem by itself, it should inform its serving eNB the related IDCI information so that the eNB can determine if an IDCI solution should be activated, i.e., the purpose of IDCI information reporting is to trigger an IDCI solution from the serving eNB. However, TDM solution has drawback mentioned in Section 1.3 because the available transmission time is limited by DRX active mode and DRX power saving mode for LTE and WiFi respectively. Both LTE and WiFi suffer from performance loss. If we activate DRX too early (e.g. sending a trigger message whenever the ISM radio is active), both LTE and WiFi throughput will degrade as a result of DRX-induced transmission time reduction. On the other hand, if we activate DRX too late, LTE DL signal will be severely interfered and cause significant throughput loss. Hence finding an appropriate trigger time is a major design concern.

Chapter 3

Simulation Based TDM Solution–Operation Assumptions

3.1 WiFi operation assumptions

3.1.1 CSMA/CA with RTS/CTS transmission scheme

The IEEE 802.11g standard uses a CSMA/CA (Carrier Sense Multiple Access/Collision Avoidance) protocol for network access and collision avoidance.

▶ **The steps for 802.11 CSMA as follows:**

Step 1: When a station has data to transmit, it will sense the channel. If the channel is idle, the station is allowed to transmit data.

Step 2: When a station is operating at busy mode, the station should wait for transmit until the channel becomes idle.

▶ **The scheme for CA as follows:**

To make sure the basic data frame unit will not be interrupted by other data frames, it use different Inter-Frame Space (IFS) types (e.g. SIFS, PIFS and DIFS). If the IFS is shorter, then the priority will be higher. SIFS is short inter-frame space, it is used for

immediate acknowledge message. PIFS is PCF (Point Coordination Function) IFS, it is used for stations wait the PIFS to transmit data at contention free mode when channel becomes idle, and it is also the WiFi beacon waiting time at DCF scheme. DIFS is DCF (Distributed Coordination Function) IFS, it is used for stations wait the DIFS to transmit data at contention free mode when channel becomes idle. The IFS relationship will be SIFS(16us) < PIFS(25us) < DIFS(34us).

To minimize the probability of collision when the number of users increases, the IEEE 802.11 standard uses binary exponential backoff algorithm to solve this problem.
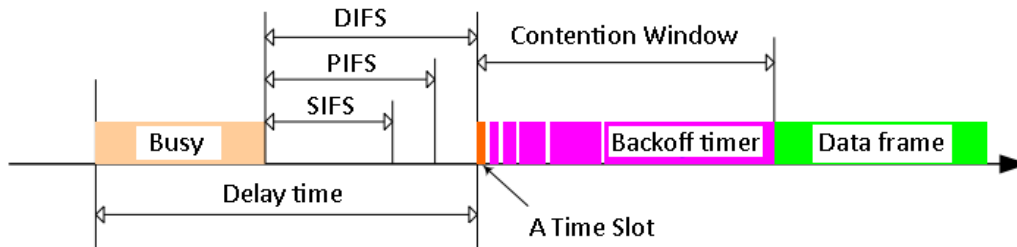
Figure 3.1: DCF with the CSMA/CA protocol.

As can be seen from Fig. 3.1, the contention window size for backoff timer will grow twice every time when collision occurs until it reaches the maximum window size. UE will transmit data after the backoff timer count down to zero and the contention window will be reset to the minimal contention window size if the transmission was successful.

As shown in Fig. 3.2, it can be regarded as a data frame from Fig. 3.1. At this scheme, a UE will transmit RTS (request to send) signal first to avoid contention ,and the target AP will send CTS to the UE after it receives RTS successfully. Next, the UE will transmit data frame and expect to receive the ACK from the AP to finish this data frame transmission. If the packet size greater or equal to 2312 bytes, the RTS threshold, then WiFi will use RTS/CTS transmission scheme.
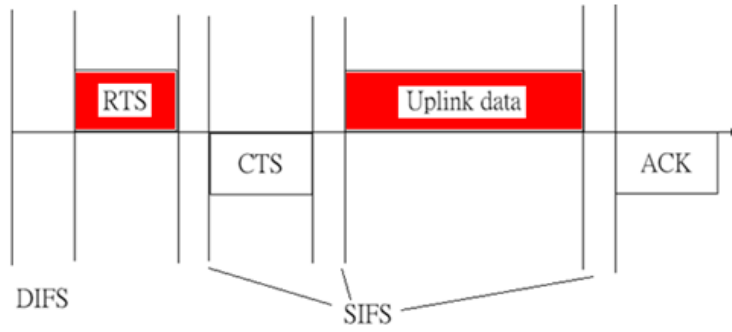
Figure 3.2: Data frame for the RTS/CTS scheme.
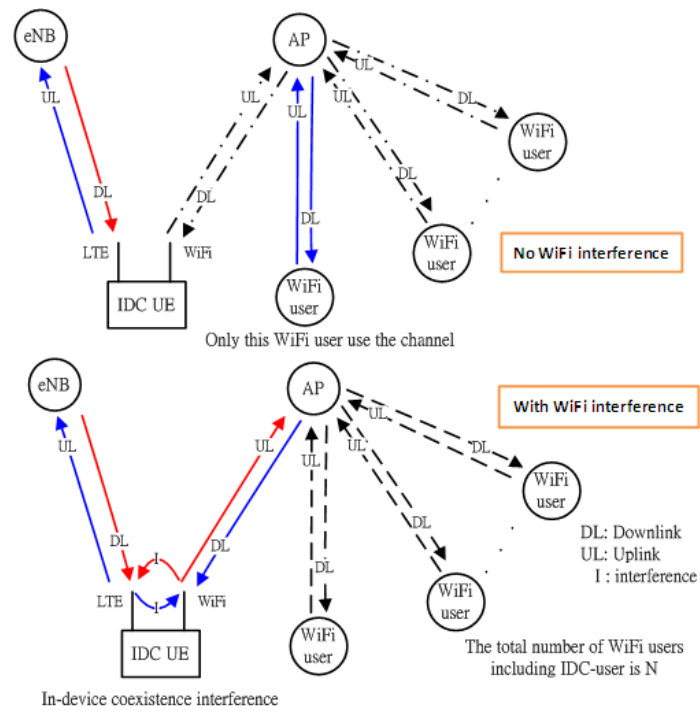
Figure 3.3: IDC user contends with other users.
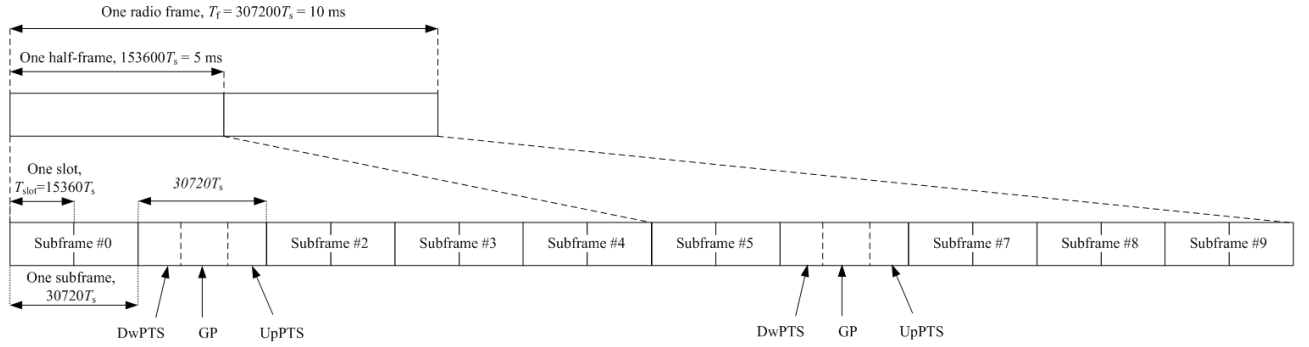
Figure 3.4: TDD frame structure.

3.1.2 Relationship between the number of WiFi users and IDC user

We assume that other WiFi users operate in saturation condition, it means that they always have packet to transmit. We show that how other WiFi users will compete the channel with the IDC WiFi user using CSMA/CA scheme in Fig. 3.3. If the IDC user senses channel to be busy before the backoff timer goes to zero, then it can't transmit WiFi data until the channel becomes idle again and the LTE will not be interfered by WiFi during this period. On the other hand, if the IDC user contend the WiFi channel successfully, then the IDC user's WiFi will transmit data to WiFi AP and thus interferes the LTE DL receiving data.

3.2 LTE frame structure and operation assumptions

Fig. 3.4 presents a TDD frame structure, and one radio frame is 10ms which is composed of ten subframes with the length of 1ms. This scheme needs Guard period when it switches from the downlink to the uplink due to random access synchronous.

As shown in Fig. 3.5, we show the TDD configuration type for 3GPP. Since the downlink traffic usually has larger loading than the uplink one for a UE. The number of

Uplink-downlink configurations

Uplink-downlink configuration	Downlink-to-Uplink Switch-point periodicity	Subframe number									
		0	1	2	3	4	5	6	7	8	9
0	5 ms	D	S	U	U	U	D	S	U	U	U
1	5 ms	D	S	U	U	D	D	S	U	U	D
2	5 ms	D	S	U	D	D	D	S	U	D	D
3	10 ms	D	S	U	U	U	D	D	D	D	D
4	10 ms	D	S	U	U	D	D	D	D	D	D
5	10 ms	D	S	U	D	D	D	D	D	D	D
6	5 ms	D	S	U	U	U	D	S	U	U	D

Figure 3.5: TDD configuration.

downlink subframe should be more than the number of uplink subframe. Here, we set the TDD Uplink-downlink configuration to be 4, where the number of uplink subframe, the number of downlink subframe ,and the number of switch subframe are 2, 7 and 1 respectively.

As can be seen from Fig. 3.6, the resource block can be composed by many downlink resource grid. A grid is called a resource element, and it is a basic unit which distributes over a resource block. Each grid bandwidth contains one subcarrier (15KHz), and its length is one- symbol period (71.4us). Each subcarrier is orthogonal to each other (see Fig. 3.7). A resource block has 12 subcarriers and 7 OFDM symbols, so it includes 84 resource elements. With the knowledge of how many resource blocks is assigned to the UE by the eNB along with the SINR in this subframe, we can calculate the throughput by MCS (Modulation Coding Scheme) level and CQI (Channel quality indicator) table latter.

3.3 LTE downlink SINR

The power spectrum density of thermal noise is -174(dBm/Hz) and if we consider only the inter-cell interference, the average power spectrum density for interference plus noise level will be -164(dBm/Hz) in the cell edge for the rule of thumb. It this work, we assume that an IDC user is located on the urban microcell scenario where the coverage region

Figure 3.6: LTE Resource Block (RB) structure.
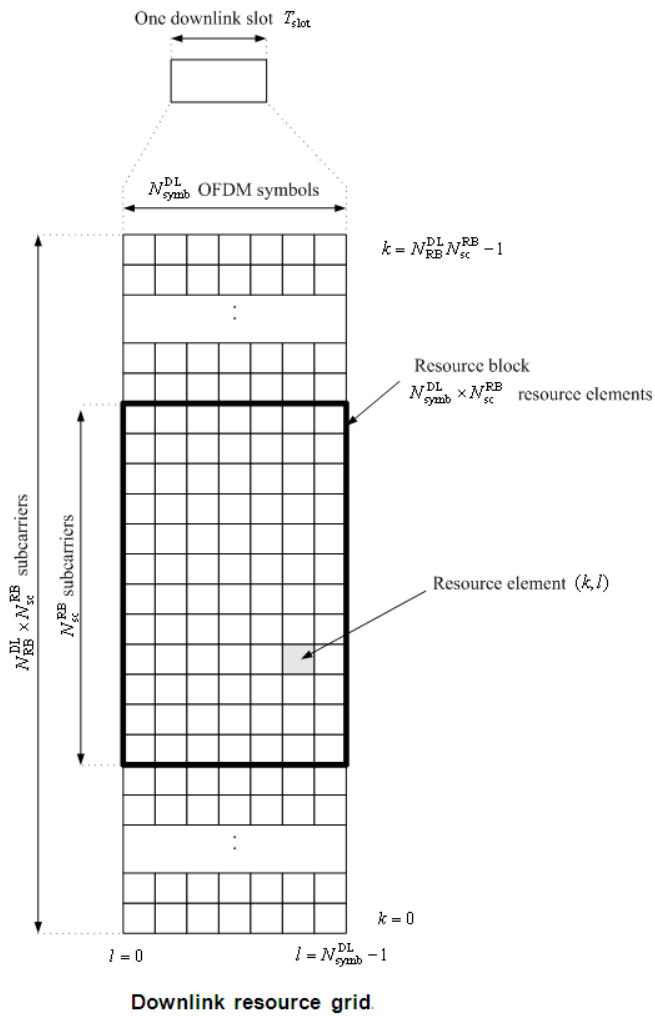
Time slot period	$T_{slot} = 0.5\text{ms}$
Number of downlink symbols	$N_{symb}^{DL} = 7$
Number of subcarriers in a RB	$N_{sc}^{RB} = 12$
Total number of downlink resource block at bandwidth 20MHz	$N_{RB}^{DL} = 100$
resource element at k-th symbol and l-th subcarrier	(k, l)
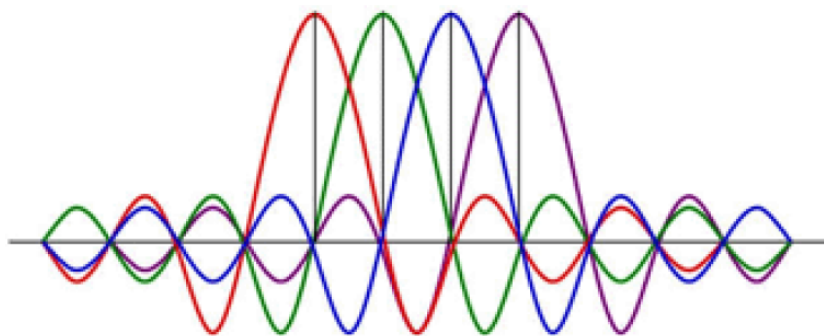
Figure 3.7: OFDM subcarrier spacing.

of the base station is 500 meter. We also assume that the distance between the UE and the eNB is 425 meter which is close to the cell edge. We adopt the pathloss model in 3GPP 25.883, follow the function pathloss(dB) = 34.53+38*$\log_{10}$(the distance between the UE and the eNB). In this case the pathloss will be 134.41(dB). The eNB transmission power is set to be 46dBm and the system bandwidth is 20MHz. The bandwidth for the data transmission will be 18MHz which is smaller than the system bandwidth because it requires a guard band to prevent the adjacent channel interference. As a result, the average power spectrum density is 46(dBm)-10*$\log_{10}$(18MHz)= -26.553(dBm/Hz) and the average SINR calculation considering three informations which are power spectrum density of signal, pathloss and power spectrum density of interference plus noise level. Through the calculation, -26.553(dBm/Hz)-134.41(dB)-(-164(dBm/Hz)), the average SINR is thus to be 3(dB).

In order to investigate SINR performance under IDC interference, we assume that the center frequency for LTE and WiFi are 2370MHz and 2412MHz,respectively. The interference level is -107dBm/Hz. The denominator of SINR is composed of noise power, inter-cell power and in-device interference power. The average power spectrum density of interference will be 10*$\log_{10}(10^{\frac{-164(dBm/Hz)}{10}} + 10^{\frac{-107(dBm/Hz)}{10}})$, which is approximate to -107(dBm/Hz), the power spectrum density of tansmission signal, pathloss and the interference is -26.553(dBm/Hz),-134.41(dB) and -107(dBm/Hz), respectively, the average SINR with IDC interference is -53.96(dB) in this case. Hence, if the in-device interference occurs then SINR will be degrade dramatically and the UE can't get any correct information from the eNB.

3.4 LTE downlink throughput

After a UE measures SINR, the UE will report CQI to the eNB and the eNB will choose a modulation coding scheme according to the CQI reported from UE. SINR will be calculated by the eNB using the above mentioned method and the eNB will
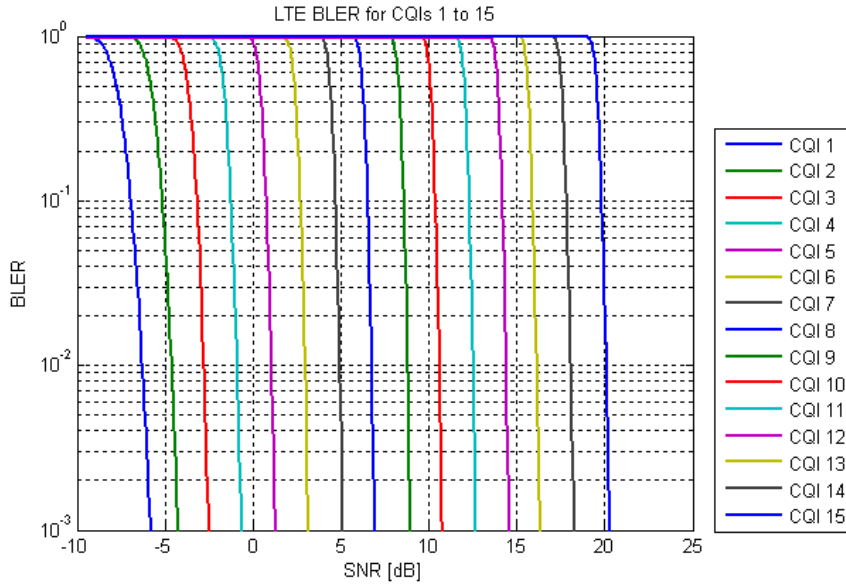
Figure 3.8: SINR versus BLER with different MCS level.

use Fig. 3.8 to find out a proper MCS (modulation coding scheme) level and BLER. In general cases, the block error rate will not be larger than 0.1, so if we want to select a MCS level to maximize the transmission rate, then we should select maximum MCS level with the constraint that BLER is smaller than 0.1. As can be seen from Fig. 3.9, different MCS level will represent different efficiency, and the efficiency is defined by how many bits can a resource element provided. The eNB will allocate some resource blocks to the UE which uses the same MCS level. We assume that the UE will take 10 RBs during a subframe interval, and thus the resource elements that each UE can obtain is 10*12(subcarriers)*7(symbols). So, the transmission bits for the UE will be 10*84*efficiency during a subframe. The efficiency will be different for different subframes and we can obtain the average throughput by averaging over different subframes.

CQI index	modulation	code rate x 1024	efficiency
0	out of range		
1	QPSK	78	0.1523
2	QPSK	120	0.2344
3	QPSK	193	0.3770
4	QPSK	308	0.6016
5	QPSK	449	0.8770
6	QPSK	602	1.1758
7	16QAM	378	1.4766
8	16QAM	490	1.9141
9	16QAM	616	2.4063
10	64QAM	466	2.7305
11	64QAM	567	3.3223
12	64QAM	666	3.9023
13	64QAM	772	4.5234
14	64QAM	873	5.1152
15	64QAM	948	5.5547

Figure 3.9: 4 bit CQI table.

Chapter 4

Appropriate Occasion To Trigger TDM Solution

It is clear that [4] the decision to trigger an IDCI solution depends on the WiFi interference level and the WiFi UL activity (see Fig. 4.1).
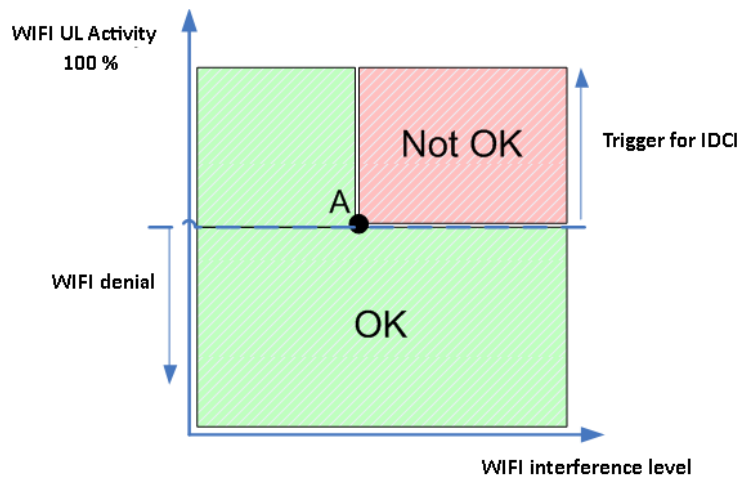
Figure 4.1: IDC indication for LTE DL.

4.1 The effect of WiFi/LTE parameters and WiFi/LTE throughput

1. **WiFi interference level:**

   (a) WiFi/LTE transmission power

   (b) WiFi/LTE operation frequency band

2. **WiFi UL activity:**

   (a) Number of WiFi users

   (b) WiFi traffic type (Full buffer, FTP, http,...)

   (c) WiFi UL transmission rate

   (d) WiFi UL buffer

3. **LTE DL activity:**

   (a) LTE traffic type (Full buffer, FTP, http,...)

   (b) LTE DL transmission rate

   (c) LTE TDD configuration

   (d) LTE DL buffer

4. **DRX parameter:**

   (a) LTE active time/DRX cycle = DRX activity ratio

How do these parameters affect performance(throughput) is the issue we will discuss as follows:
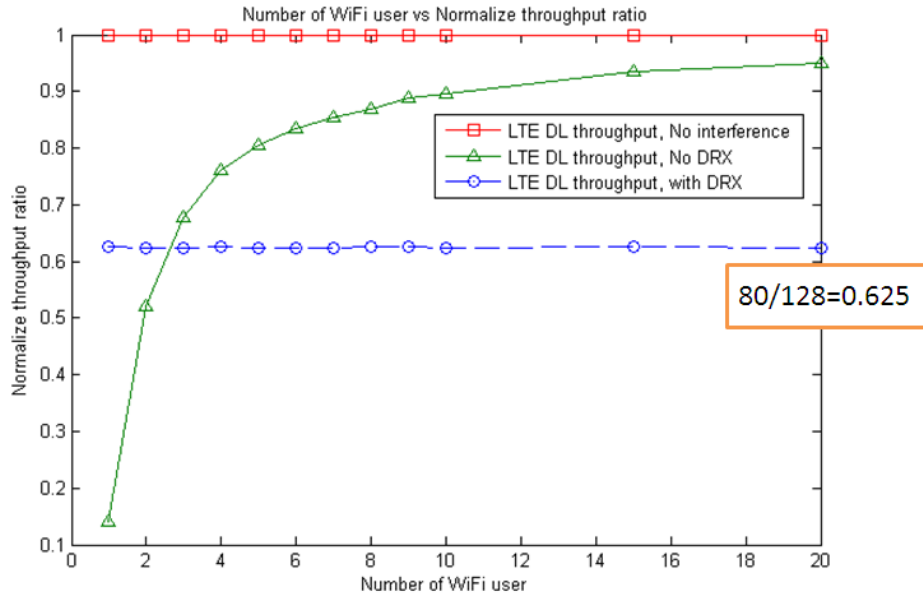
Figure 4.2: Number os WiFi users versus Normalized throughput ratio.

Parameter	value
WiFi power from UE	20dBm
LTE power from eNB	46dBm
LTE center frequency	2370MHz
WiFi center frequency	2412MHz
WiFi interference power per Hz	-107dBm/Hz
Number of RBs for IDC UE	10RBs
WiFi transmission rate	6Mbps
Number of WiFi users	2
DRX parameter	80/128
(active time/DRX cycle)	
LTE traffic type	Full buffer
WiFi traffic type	Full buffer
Distance between UE and eNB	420m
Average SINR no IDCI	3dB
Channel Model	SCM (Spatial Channel model)
	from 3GPP 25.996[5]

Table 4.1: Simulation assumption for LTE and WiFi parameters.

Number of WiFi user
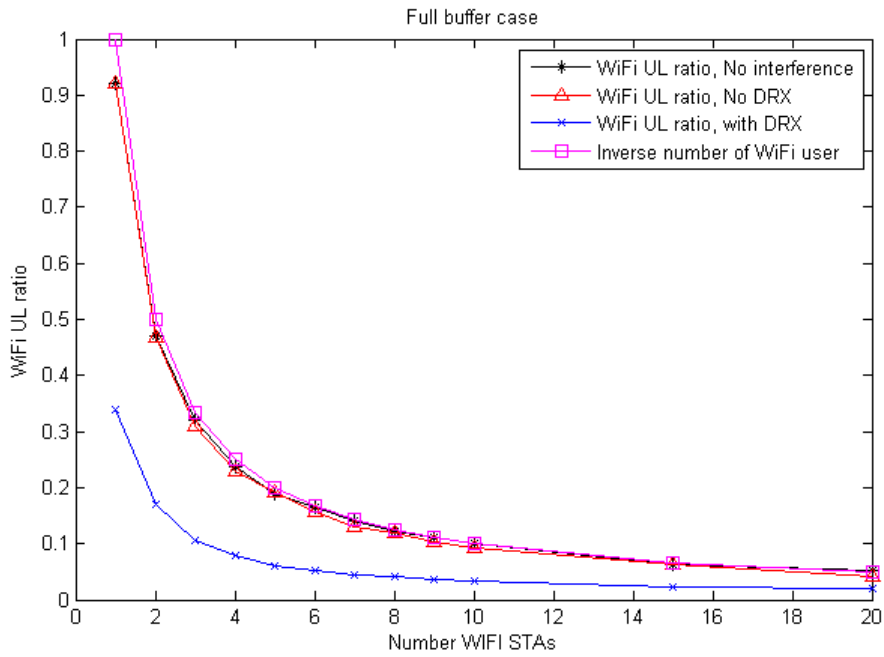
Figure 4.3: Number of WiFi users and WiFi UL activity..
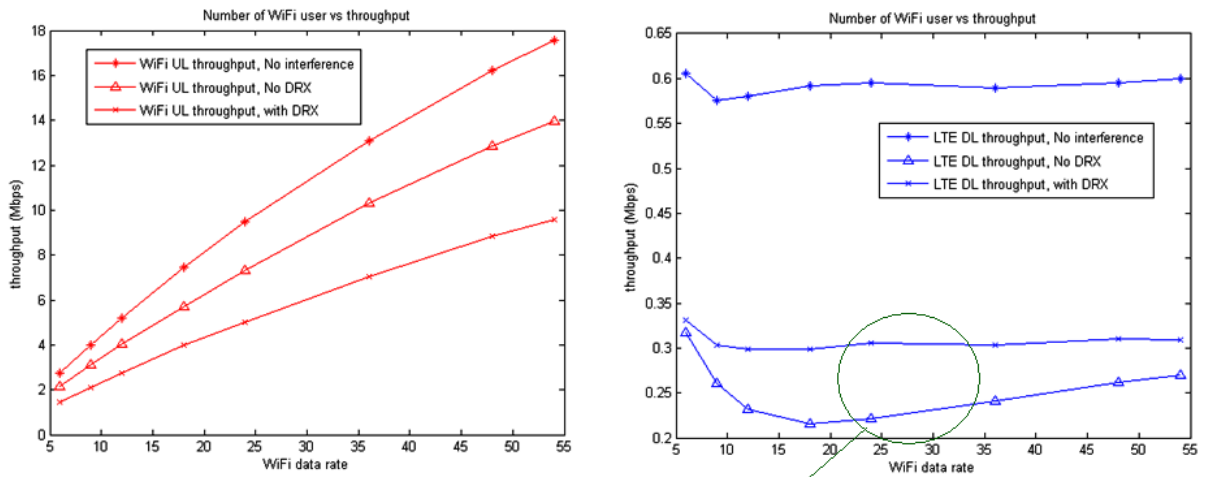
Since WiFi uplinks frequently, LTE will be interfered seriously

Figure 4.4: WiFi transmission rate versus WiFi/LTE throughput (Full buffer case)

As shown in Fig. 4.2, these throughputs are normalized by the throughput without interference. What we mean by no interference implies that both LTE and WiFi operate independently without interfering to each other. The case "without DRX" means LTE and WiFi interfere with each other and both ignore the IDC interference. The case "with DRX" means that UE triggers an IDC solution as soon as WiFi is on and LTE and WiFi will operate on DRX on-duration and off-duration, respectively. We assume that LTE and WiFi are full buffered, i.e., they always have data to transmit. As shown in Fig. 4.2, we find that if the number of WiFi users increases, then LTE DL throughput will increase because the probability of WiFi contention will increase and the WiFi UL ratio will thus decrease. As a result, triggering DRX is not guaranteed to be the best policy with respect to the LTE DL throughput.

From Fig. 4.3, we conclude that WiFi UL activity is influenced by the number of WiFi users, and it is inverse proportional. To explore the number of WiFi users, we can use collision probability of RTS. Before WiFi transmits data, it needs to transmit RTS(request to send) information to AP. In consequence, UE can calculate the collision probability of RTS to analogize the number of WiFi users. In other words, inverse of collision probability of RTS is equal to the number of WiFi users approximately. In Fig. 4.4, we assume that the number of WiFi users is two. Because there are always data in WiFi UL buffer to be transmitted, WiFi UL ratio is still high in no DRX case even if WiFi transmission rate increases.

Fig. 4.5 shows that WiFi UL ratio degrade linearly when WiFi data increases. When WiFi transmission rate increases, the transmission time for one packet will decrease. Because the WiFi contention window size will not change with the transmission rate, it means that WiFi idle time increases when WiFi transmission rate increases. So, the WiFi UL ratio will decrease when WiFi data increases.

In our simulation, we assume that WiFi receives ACK from the AP, with a possibility colliding with LTE UL ACK which results in the reduced probability of the success WiFi
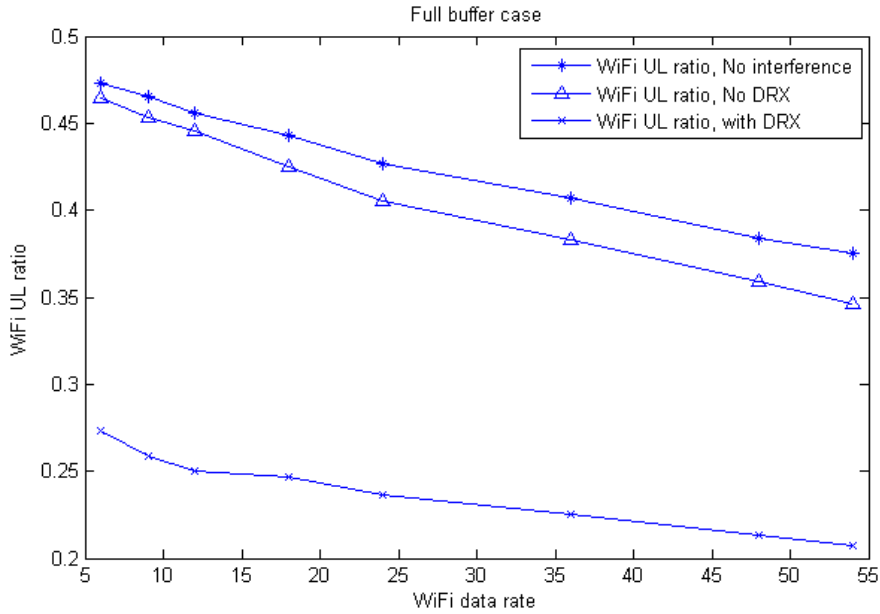
Figure 4.5: WiFi transmission rate versus WiFi UL ratio (Full buffer case)

uplink transmission. Therefore, for the WiFi UL ratio, the performance of the no-DRX case is worse than that of the no-interference case. From the simulation results of Fig. 4.6, we assume that the number of WiFi users is two. Because there are always data in WiFi UL buffer to be transmitted, WiFi UL ratio is still high at no DRX case.

Fig. 4.7 shows that when WiFi transmission rate is large enough, the WiFi activity ratio will degrade fast because the WiFi buffer will be empty sometimes. Compared to no interference and no DRX cases, since no DRX case needs higher data rate to empty the WiFi buffer, WiFi UL ratio will be larger than no interference case.

The results presented in Figs. 4.6 and 4.8 tell us that when WiFi traffic becomes lighter, WiFi throughput will saturate at 5.5 Mbps, which means that WiFi activity ratio for these WiFi transmission rates will become smaller. LTE DL throughput ,no DRX case will increase faster than LTE DL throughput, with DRX case ,because it has more time resources can be used as successful transmission. The WiFi UL ratio with DRX is close to WiFi UL ratio with no interference when WiFi transmission rate is large enough because WiFi traffic is so light; see Fig. 4.9. In this case, even if WiFi only can
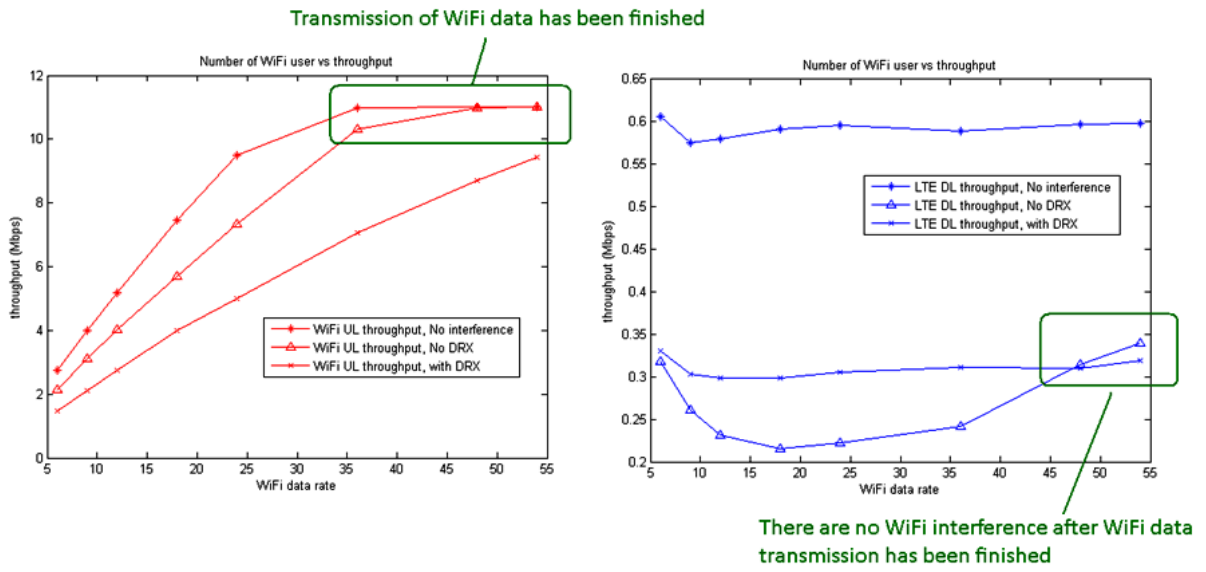
Figure 4.6: WiFi transmission rate versus WiFi/LTE throughput (traffic 11Mbps)
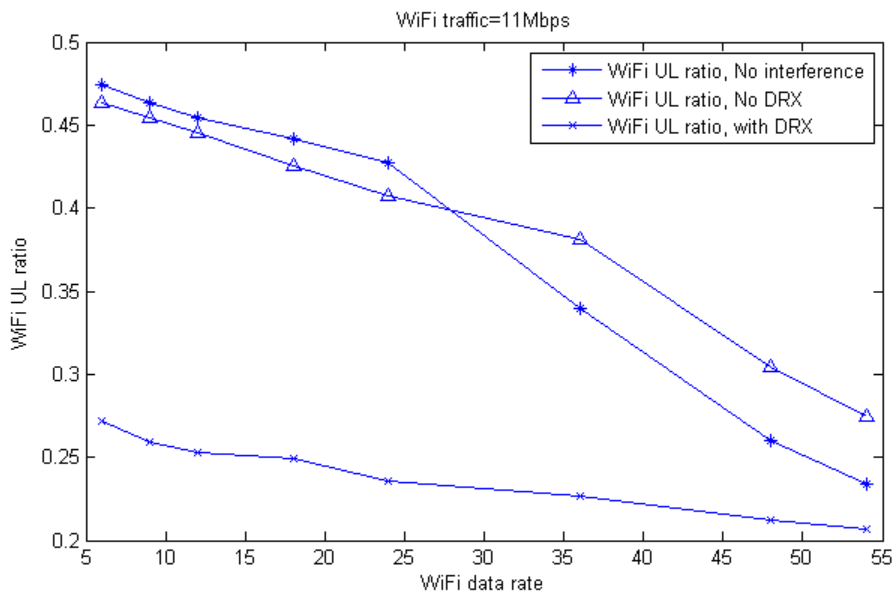
Figure 4.7: WiFi transmission rate and WiFi UL ratio (traffic 11Mbps)
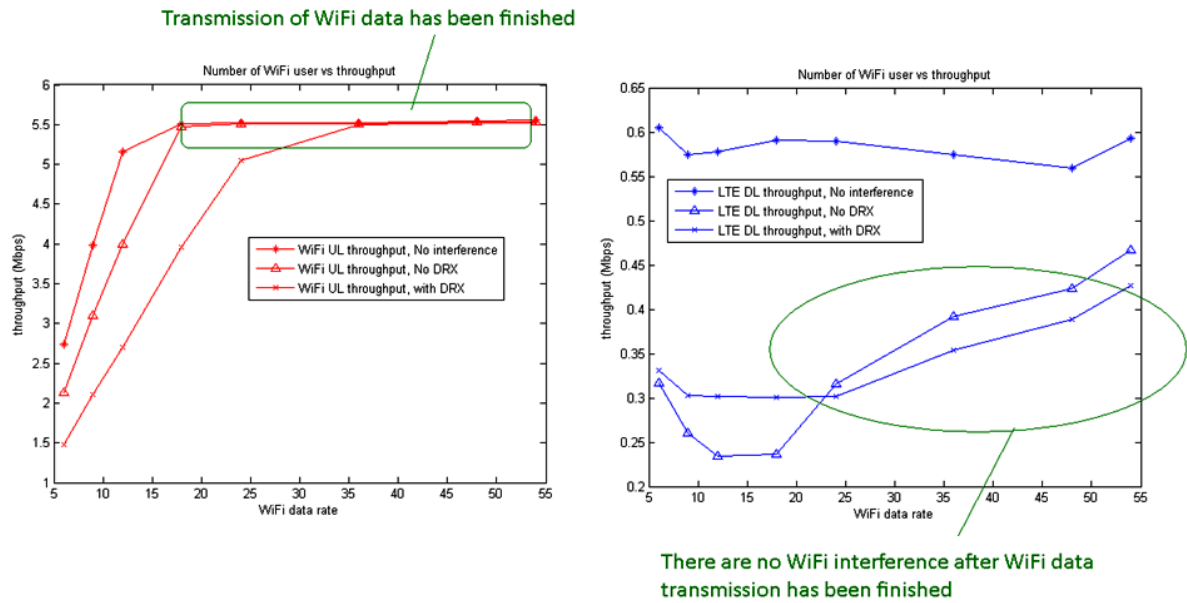
Figure 4.8: WiFi transmission rate versus WiFi/LTE throughput (traffic 5.5Mbps)
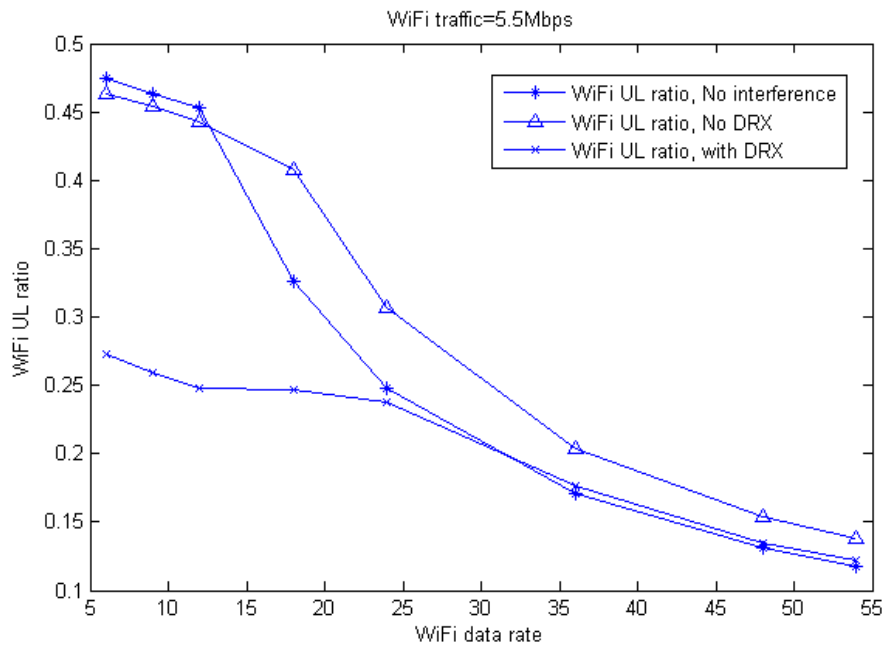
Figure 4.9: WiFi transmission rate and WiFi UL ratio (traffic 5.5Mbps)

transmit data at DRX sleep mode, it is enough to empty the WiFi UL buffer.

WiFi traffic type

The characteristic of different traffic types will affect IDC trigger decision. The traffic load can be light or heavy, and the traffic type can be burst or constant. If WiFi traffic is light, it doesn't need to trigger IDC . Instead, we can use WiFi denial to wait until LTE finishes receiving data. If WiFi traffic is heavy, WiFi UL buffer will have queued data for a long time. It needs to consider whether to activate DRX solution to get a better performance. If WiFi traffic is heavy and burst, the DRX cycle can be chosen to match the burst data inter-arrival time.

WiFi UL buffer

UE can predict how much time it needs to take at least to empty the WiFi UL buffer by the WiFi transmission rate and the number of WiFi users. It is also an important information to decide whether to trigger IDC or not. It may be better not to trigger IDC solution in the case for WiFi buffer remaining small volume data and traffic type being burst traffic, even if WiFi interference power is very high. Because the WiFi buffer is going to being cleared to empty, UE can predict that WiFi will not uplink data after WiFi uplink buffer is empty and LTE can receive data without WiFi interference.

LTE DL activity

If LTE downlink activity ratio is small, maybe we can just use WiFi denial to solve IDC problem.

DRX parameter

In the simulation assumptions, we don't consider DRX with inactivity timer because if LTE always has data needed to be received, then the inactivity timer will extend and thus WiFi has no chance to transmit with DRX power saving mode.

Assuming that the number of WiFi users is two, Fig. 4.10 plots the normalized LTE/WiFi throughput performance. If we increase on-duration timer, LTE DL throughput will increase, but WiFi UL throughput will decrease. If we increase DRX cycle with
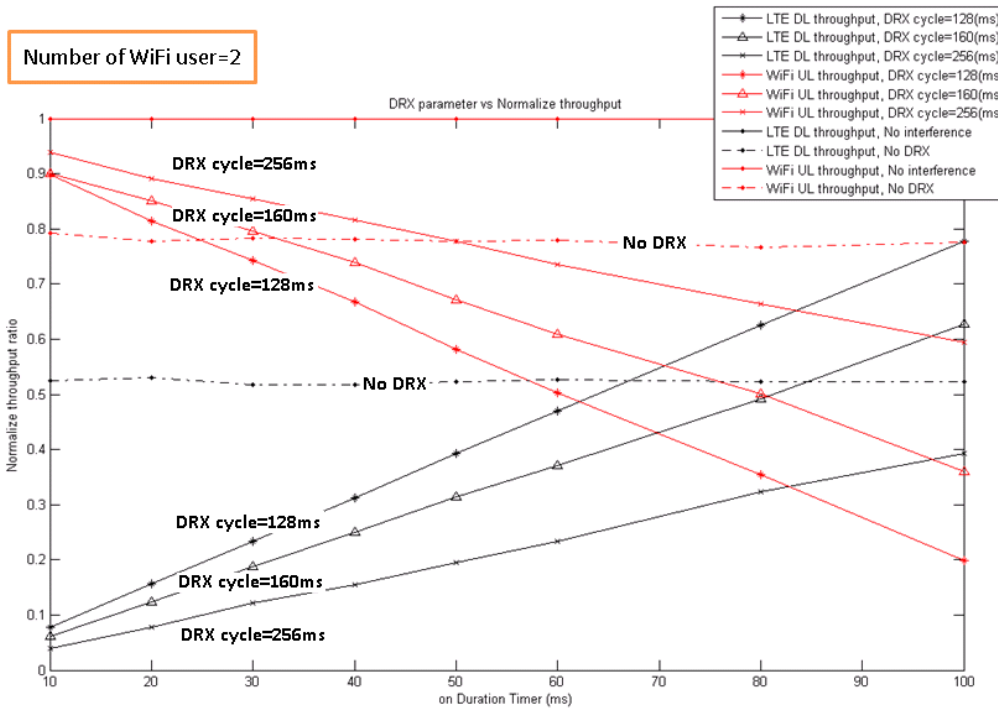
Figure 4.10: Different DRX parameter for normalized throughput

the same on-duration timer, then LTE DL throughput will decrease, but WiFi UL throughput will increase. Compared to the throughput with no DRX, we can find appropriate DRX parameters to match the throughput demand. In Fig. 4.11, the number of WiFi users is three. WiFi UL ratio will decrease when DRX active ratio increases.

Summarizing the above findings, we conclude that if one increases the WiFi transmission rate and the number of WiFi users, then the WiFi UL ratio decreases while LTE DL throughput increases. If one increases the DRX active ratio, the LTE DL throughput increases but the WiFi UL throughput reduces. Obviously, there is a trade off between the LTE and WiFi throughputs.

4.2   Proposed algorithm method

The proposed method is illustrated in Fig. 4.12 when two processing modes are
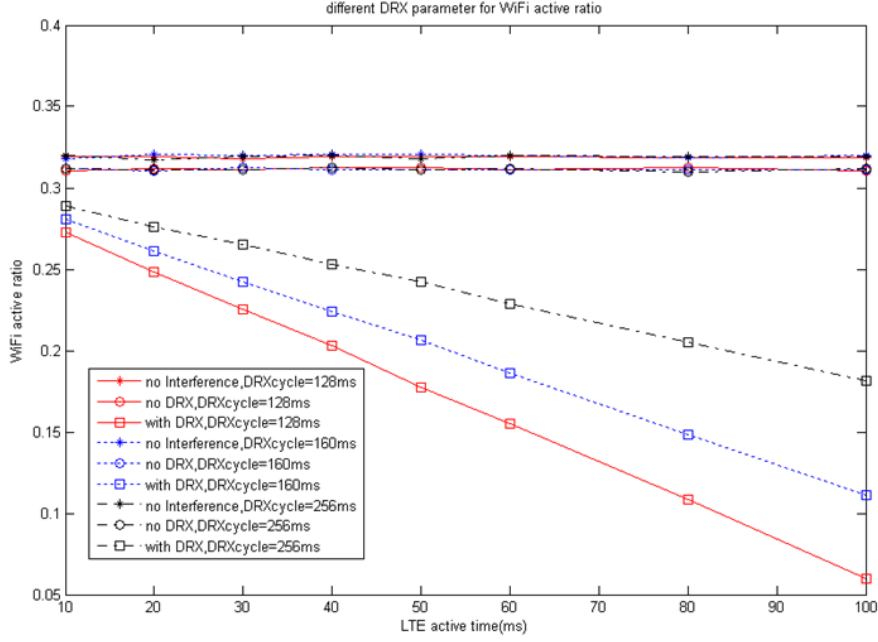
Figure 4.11: WiFi transmission rate and WiFi UL ratio.

introduced. First, we consider that UE operates in no DRX mode and decide when to trigger IDC solution. Second, we consider that UE has operated in DRX mode and decide when to close the DRX mode. The details of our proposed scheme are described as follows:

Initial: assume that UE operates in no DRX mode

Step 1: Set window size

Set an appropriate window size for measurement, ex. Radio link failure timer T310 is 50ms. We set 30ms as the window size.

Step 2: UE measures WiFi active time and LTE SINR during the window size It can judge that whether the interference from WiFi is serious.

Step 3: Decide the DRX active ratio μ

To ensure that the LTE and WiFi will both achieve their respective throughput constraints, the DRX active ratio μ must be carefully chosen. If μ is larger, the LTE DL throughput will become larger, but WiFi UL throughput will become smaller. hence,
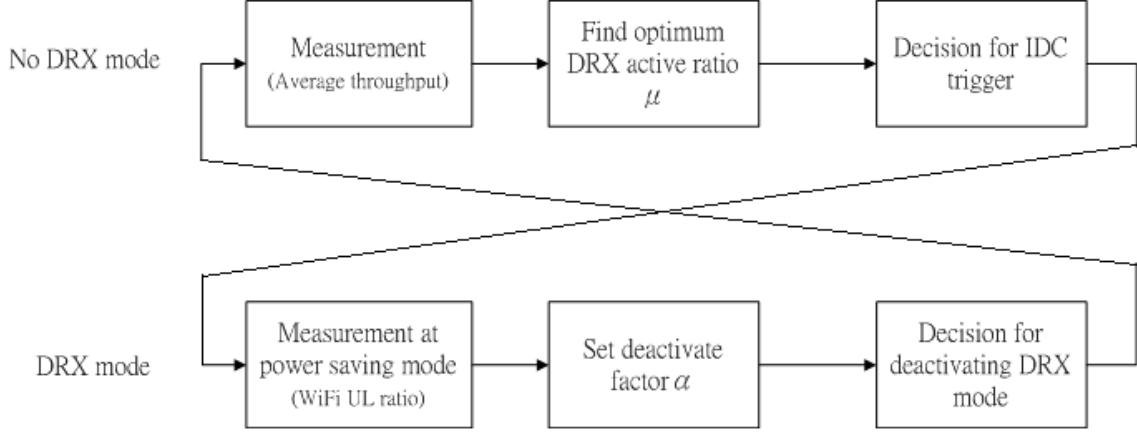
Figure 4.12: Proposed algorithm procedure

the WiFi UL throughput constraint decide the upper bound of μ, and the LTE DL throughput constraint decide the lower bound of μ.

Example 1 WiFi has a constrains of minimum transmission rate of 0.5 Mbps with the average transmission rate of 2 Mbps $\Rightarrow$ 2 Mbps$\times(1-\mu) \geq$0.5 Mbps, μ_{up}=0.75 is the upper bound.

Example 2 LTE's minimum transmission rate = 0.2 Mbps, the average rate = 1 Mbps $\Rightarrow$ 1 Mbps$\times\mu \geq$0.2 Mbps, μ_{low}=0.2 is the lower bound

After these constraints are satisfied, we choose the best DRX active ratio to maximize the throughput with DRX. We can see another example in Fig. 4.13, to comply with the LTE throughput constraint, the DRX parameter can only be chosen from 80/128, 100/160 and 100/128. To comply with the WiFi throughput constraint, the DRX parameter can only be chosen from 80/128 and 100/160. After we meet throughput constraint, we want to find a optimum parameter to maximize LTE DL throughput such that

$$\arg\max_{\mu_{low}\leq\mu\leq\mu_{up}} \text{ total throughput (with DRX)} \Rightarrow \mu_{Optimal} \qquad (4.1)$$

Thus, UE can report TDM solution indication which is included DRX parameter that UE choose to eNB.
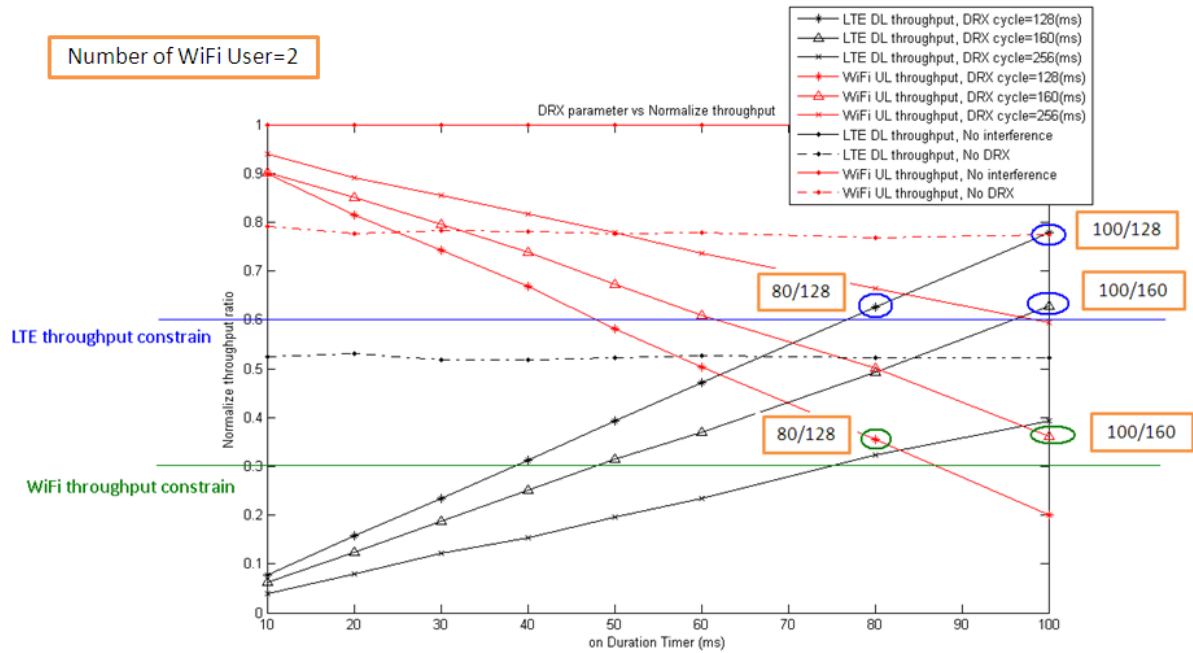
Figure 4.13: Select appropriate parameters

Step 4: Set an active factor β Since the measurement period is finite, the measurement result of the throughput may be lower than the statiscal expectation of throughput. It will result in triggering IDC solution too early and degrading the overall performance. Here, we use an active factor β to avoid switching frequently.

Step 5: Decide whether to trigger the IDC solution or not when DRX scheme is not active

(a)To trigger DRX: The IDC user will average the LTE DL throughput only in the DL subframe which didn't not be interfered by WiFi.

(b)Do not to trigger DRX: The IDC user will average the LTE DL throughput throughout all the DL subframe no matter the interference from WiFi will happen.

To compute the expectation of the throughput for both with DRX case (a) and no DRX case (b) while the window size is given, we need to know which LTE subframe is interfered by WiFi. Classifying the LTE subframes into two groups, one suffers from WiFi interference, and the other isn't interfered by WiFi (see Fig. 4.14). By finding

49

the average throughput for the group which aren't interfered by WiFi, we can know the throughput in on-duration timer after we activate DRX mode. Moreover, we can get expectative throughput, if we activate DRX after considering DRX active ratio. So the throughput after DRX activate is (a)$\cdot\mu$. The average throughput for no DRX case (b) is to average all subframe's throughput no matter whether it is interfered by WiFi. During the given measured period, if (a)$\cdot\mu$ >(b)$\cdot\beta$, $\beta > 1$, then we should trigger IDCI solution. β is an active factor to avoid switching frequently from step 4.
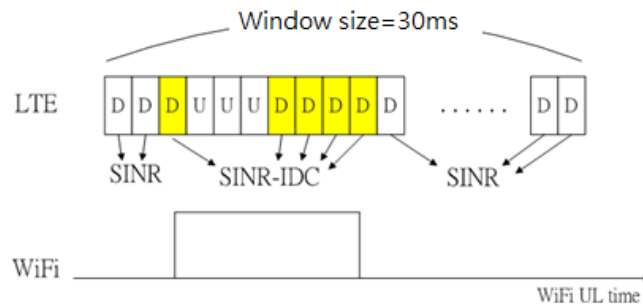
Figure 4.14: Classify the LTE subframes to two groups for without and with WiFi interference

After trigger for IDC : If UE operates at TDM solution DRX mode.

Step1: Measure WiFi UL ratio during power saving mode

WiFi will be denial until DRX power saving mode is starting.

Step 2: Set a deactivate ratio α, $0 < \alpha \leq 1$

Because WiFi UL ratio may change with time, average WiFi UL ratio during limited measured period may be smaller than average WiFi UL ratio during overall simulation time, and it causes deactivating DRX scheme too soon. To avoid deactivate DRX scheme too soon and result in interfere from WiFi seriously, we set a deactivate ratio α.

Step 3: Deactivate DRX

We define the throughput for two situations as follow

(c) The IDC user will average the LTE DL throughput only in the DL subframe in On-duration.

(d) LTE DL throughput constraint

The LTE DL throughput after turning off DRX mode is approach to be $(c) \times (1 -$ WiFi UL ratio) because the interference from WiFi. If we want to turn off the DRX mode, we must ensure that LTE DL throughput will still meet LTE DL throughput constrain, we set $(c) \times (1 - \frac{\text{WiFi UL ratio}}{\alpha}) > (d)$. The former is a expectative throughput after UE deactivate DRX. α is a robust value from step 2.

$\Rightarrow$ WiFi UL ratio $\leq (1 - \frac{(d)}{(c)}) \times \alpha$

If WiFi UL ratio smaller than the threshold then it is time to deactivate DRX.
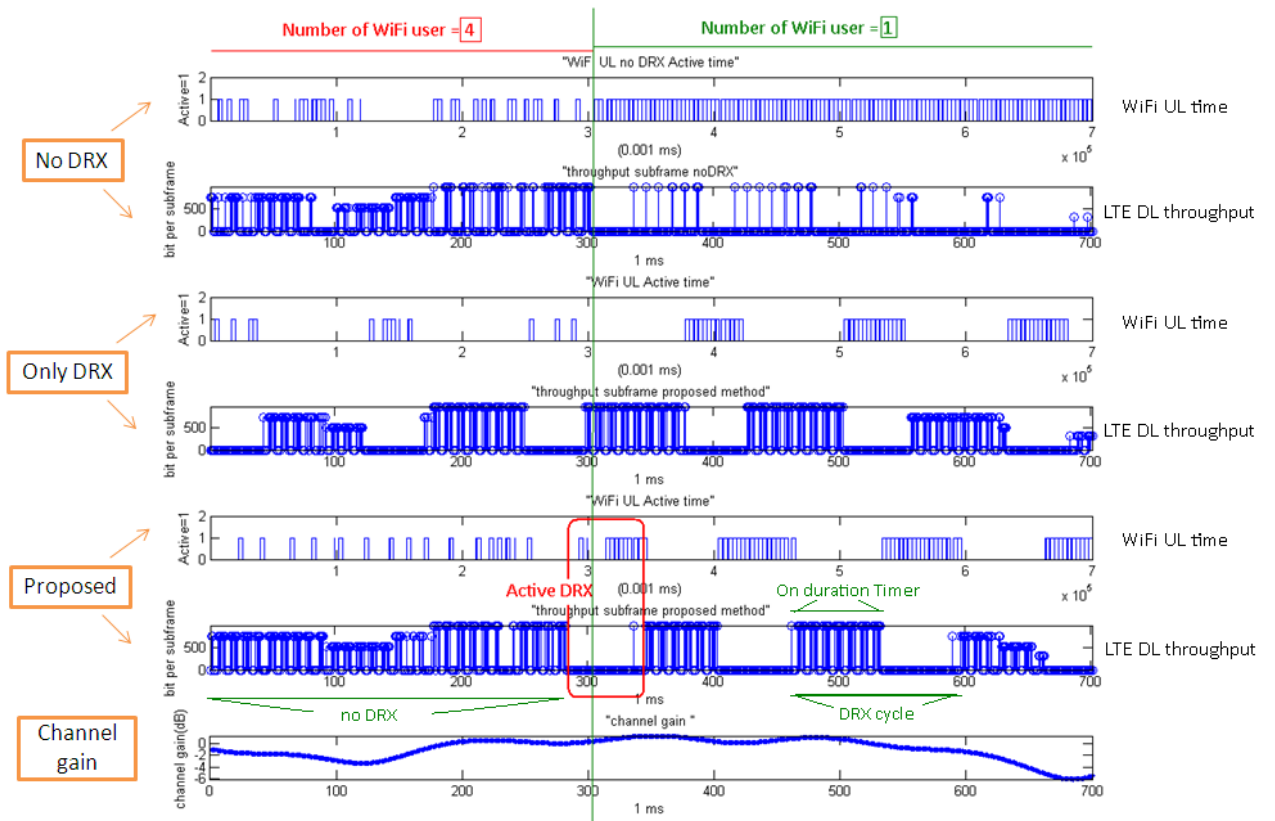
Figure 4.15: WiFi uplink time and LTE DL throughput (no DRX/Only DRX/Proposed)

4.3 Simulation result and summary

51
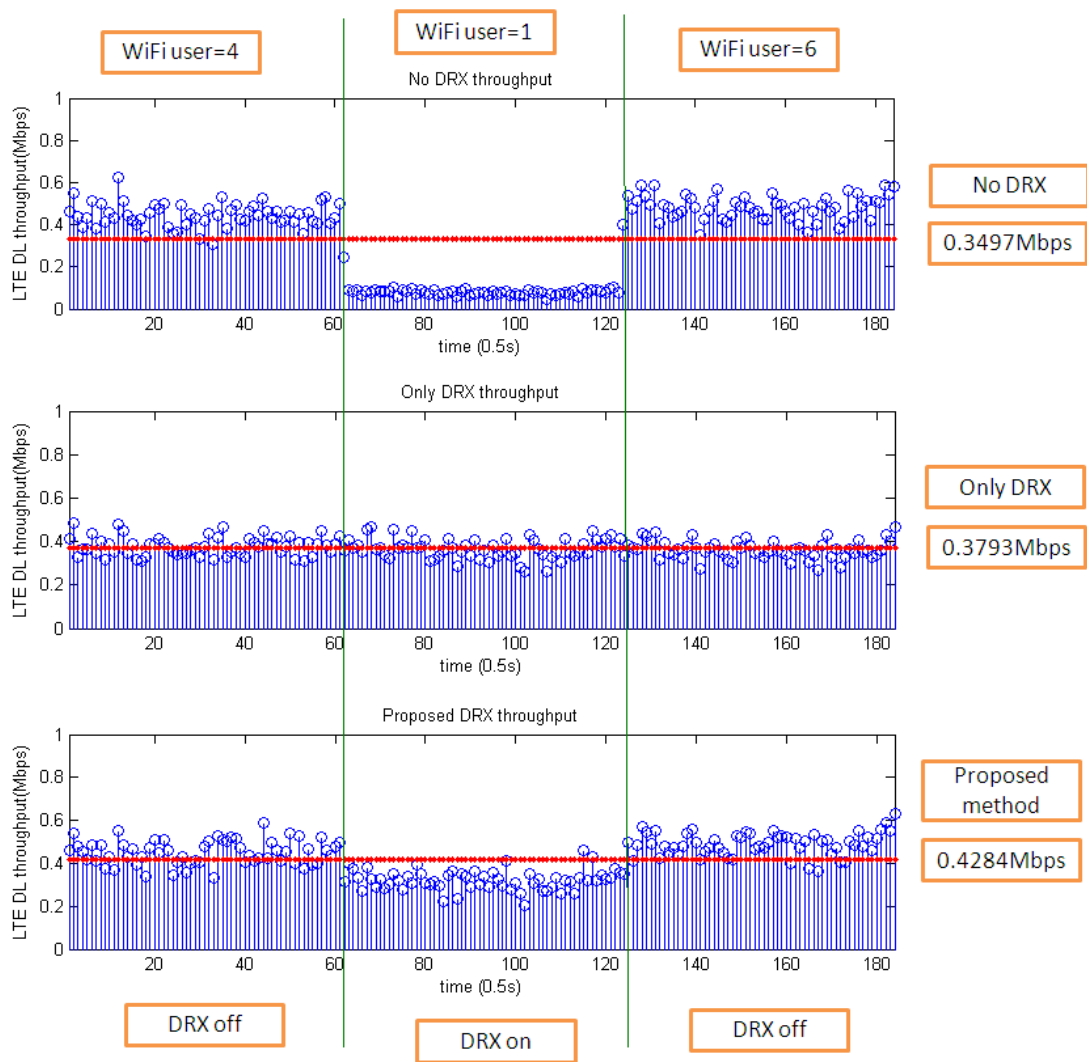
Figure 4.16: Number of WiFi user is time varying versus LTE DL throughput)

In Fig. 4.15, we assume that number of WiFi user is 4 in the first phase so that the WiFi interference is not serious. However, in the second phase the number of WiFi user is reduced to one and the WiFi UL ratio increase causes higher WiFi interference level so it is better to trigger the IDC solution. In Fig. 4.16, the number of WiFi user is still 4 in the first phase where the no-DRX solution has better throughput performance than the one with DRX. In the second phase, the WiFi user number becomes 1 and the throughput performance for no-DRX option deteriorates and becomes worse than the one with DRX. In the third phase, the throughput performance for former option turns
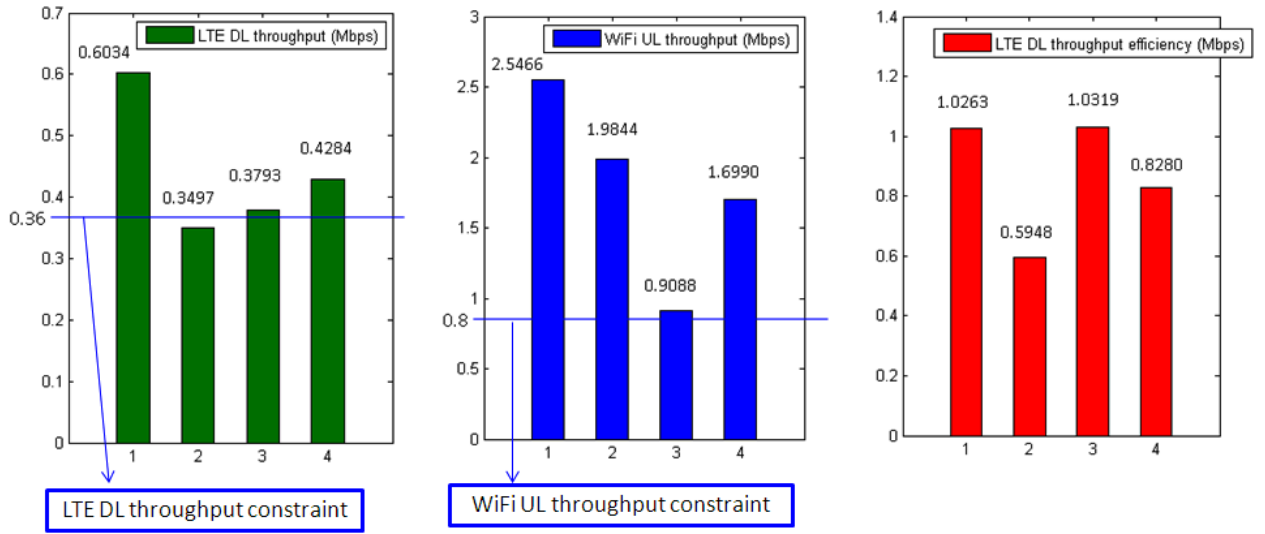
Figure 4.17: Compare with throughput and efficiency

better again. Our method can find out the appropriate time epoches to trigger IDC and deactivate DRX to keep LTE throughput on high level.

From Fig. 4.17, we find that the efficiency, defined as the total transmission bits over scheduling DL subframes, is a decreasing function of the power UE used.

Case 1. No interference: It is the case for LTE WiFi will not interfere to each other

Case 2. No DRX: It is the case for LTE and WiFi will interfere to each other and UE doesn't handle the coexistence interference.

Case 3. Only DRX: It is the case for UE to trigger IDC solution once the WiFi turn on and it will keep operating on DRX mode.

Case 4. Proposed method: UE can use measurement to decide when to trigger or to deactivate DRX scheme to keep the throughput at high level.

Compared to LTE DL throughput, if we select an appropriate DRX parameter, then LTE throughput will be better than no DRX case, our proposed method will be even better than only DRX case.

Compared to WiFi UL throughput, our proposed method will be lower than no DRX case because DRX scheme will limit WiFi UL time. Nevertheless our proposed method

will outperform the only DRX case.

Compared to LTE DL throughput efficiency, only DRX case will have the same efficiency as no interference case and the efficiency of our proposed method can outperform no DRX case.

4.4 SNR and SINR estimations

In this section, we will introduce new SINR estimator to help us decide a more accurate trigger occasion for trigger IDC.

4.4.1 Importance for SINR estimation

▶ **Motivation**

For above work, we assume that SINR is perfectly known. However, if we consider SINR estimation error, it will affect IDC trigger decision. Therefore, we propose an accurate SINR estimator which can degrade possibility of improper trigger for IDC. If UE measures SINR inaccurately, it will report improper CQI and cause performance loss.

▶ **System operating model**

As shown in Fig. 4.18, eNB transmits OFDM symbols including pilot and data to the UE, and UE can use pilots for channel and SINR estimation. The SINR estimation can be improved by decision feedbacks, i.e., after channel estimation, compensation and data detection, we treat decoded data as pilots and re-estimate the SINR. Note that the received frequency domain signal is given by

$$Y_{i,j} = H_{i,j} \cdot X_{i,j} + \sqrt{\sigma^2} \cdot N_{i,j} + I_{i,j} \tag{4.2}$$
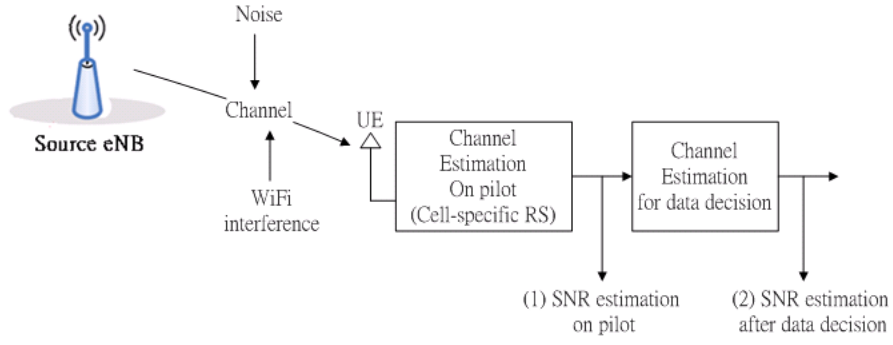
Figure 4.18: Procedure for SINR estimation.
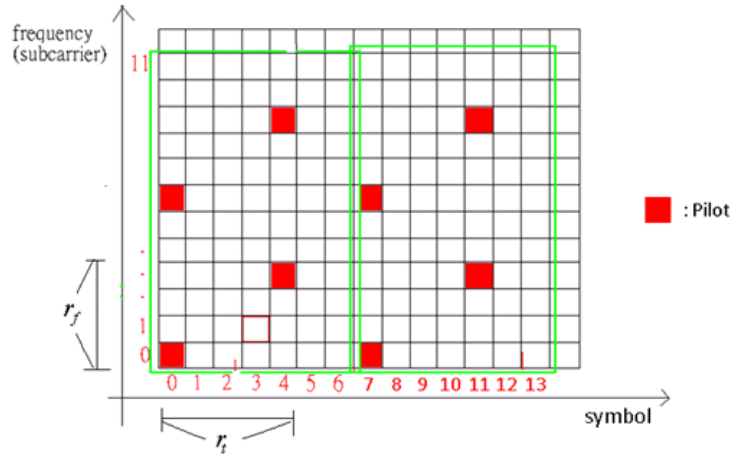
Figure 4.19: Pilot position on resource element.

$i = 0, 1, ..., M - 1$, which is the symbol index; $j = 0, 1, ..., N - 1$, which is the subcarrier index; $X_{i,j}$ is the received signal at i-th OFDM symbol and j-th subcarrier, $X_{i,j} = \{P_{i,j}, D_{i,j}\}$, $P_{i,j} \in \{$pilot set$\}$, $D_{i,j} \in \{$data set$\}$; σ^2 is the noise variance; $N_{i,j}$ is a Gaussian random variable with zero mean and unit variance; $I_{i,j}$ is the interference from inter-cell or WiFi.

Let (i, j) be the pilot positions shown in Fig. 4.19 which include

$$(i,j) \begin{cases} m = 0, r_f, 3r_f, ...(M_0 - 1)r_f \\ n = 0, r_t, 3r_t, ...(N_0 - 1)r_t \end{cases} \bigcup (i,j) \begin{cases} m = 0, 2r_f, 4r_f, ...(M_0 - 2)r_f \\ n = 0, 2r_t, 4r_t, ...(N_0 - 2)r_t \end{cases}$$

where M_0 is the number of subcarriers and N_0 is the number of symbols in the pilot set.

Since WiFi interference pattern is a nonstationary random process, we begin the SINR estimation issue by excluding the WiFi interference first. We will include the WiFi interference later.

4.4.2 Channel estimation

As the fading channel is correlated in both frequency and time domains, we follow the approach of [3] by using a regression model to describe the time-frequency channel response. It has been shown that this approach outperforms conventional least square plus interpolation based method for both channel and SINR estimations.

▶ **Least square channel estimation + linear interpolation**

To estimate channel on pilot set, the observation function will be

$$\min \sum_{i,j \in \{\text{pilot set}\}} |Y_{i,j} - H_{i,j}^{LS} \cdot P_{i,j}|^2 \Rightarrow H_{i,j}^{LS} = \frac{Y_{i,j}}{P_{i,j}} = H_{i,j} + \frac{N_{i,j}}{P_{i,j}} \tag{4.3}$$

$H_{i,j}^{LS}$ is least square channel estimation result at pilot with i-th subcarrier and j-th OFDM symbol. After we get channel estimation result at pilot, we use linear interpolation to get channel estimation of data.

$$H_{c,j}^{LS+Linear} = H_{i,j}^{LS} + \frac{n+1}{C+1} \cdot (H_{i+1,j}^{LS} - H_{i,j}^{LS}), c = 0, 1, .., C-1, \text{ frequency index} \tag{4.4}$$

$$H_{i,k}^{LS+Linear} = H_{i,j}^{LS} + \frac{n+1}{K+1} \cdot (H_{i,j+1}^{LS} - H_{i,j}^{LS}), k = 0, 1, .., K-1, \text{time index} \tag{4.5}$$

We will interpolate frequency domain first and interpolate time domain later.

▶ **Model based channel estimation:**

By using two order regression model, the observation function will be

$$\min \sum_{i,j \in \{\text{pilot set}\}} |Y_{i,j} - \hat{F}_{i,j} \cdot P_{i,j}|^2 \Rightarrow \hat{F}_{m,n} = am^2 + bmn + cn^2 + dm + en + f$$
$$\hat{\mathbf{c}}^H = [a\ b\ c\ d\ e\ f], \ \mathbf{q}_{m,n} = [m^2\ mn\ n^2\ m\ n\ 1]^T \tag{4.6}$$

$\hat{F}_{m,n}$ is a Model based channel estimation result. $\hat{F}_{m,n}$ can be expressed as two order function with variables m-th subcarrier and n-th symbol index. $\hat{\mathbf{c}}$ is the coefficient which needs to be estimated by pilots, and $\mathbf{q}_{m,n}$ is the frequency-time domain indexes vector. After we estimate the coefficient of $\hat{\mathbf{c}}$, we use the position vector $\mathbf{q}_{m,n}$ to get channel value of the data position (m, n). In the objective function (4.6), we do partial differential for (4.6) with $\hat{\mathbf{c}}$.

$$\min \sum_{i,j\in\{\text{pilot set}\}} |Y_{i,j} - \hat{F}_{i,j} \cdot X_{i,j}|^2 \Rightarrow \min \sum_{i,j\in\{\text{pilot set}\}} |Y_{i,j} - \hat{\mathbf{c}}^H \mathbf{q}_{i,j} \cdot X_{i,j}|^2 \qquad (4.7)$$

$$\Rightarrow \frac{\partial \sum_{i,j\in\{\text{pilot set}\}} |Y_{i,j} - \hat{\mathbf{c}}^H \mathbf{q}_{i,j} \cdot X_{i,j}|^2}{\partial \mathbf{c}} = 0 \qquad (4.8)$$

We express numerator as follows

$$|Y_{i,j} - \hat{\mathbf{c}}^H \mathbf{q}_{i,j} \cdot X_{i,j}|^2 = |Y_{i,j}|^2 - \hat{\mathbf{c}}^H \mathbf{q}_{i,j} \cdot X_{i,j} \cdot Y_{i,j}^* - \mathbf{q}_{i,j}^H \hat{\mathbf{c}} \cdot X_{i,j}^* \cdot Y_{i,j}$$
$$+ \mathbf{q}_{i,j}^H \hat{\mathbf{c}} \hat{\mathbf{c}}^H \mathbf{q}_{i,j} |X_{i,j}|^2 \qquad (4.9)$$

Taking derivative of (4.8) with respect to $\hat{\mathbf{c}}$, we obtain

$$\frac{\partial \sum_{i,j\in\{\text{pilot set}\}} |Y_{i,j} - \hat{\mathbf{c}}^H \mathbf{q}_{i,j} \cdot X_{i,j}|^2}{\partial \mathbf{c}}$$
$$= \sum_{i,j\in\{\text{pilot set}\}} -\mathbf{q}_{i,j}^* \cdot X_{i,j}^* \cdot Y_{i,j} + \mathbf{q}_{i,j}^* \hat{\mathbf{c}}^H \mathbf{q}_{i,j} \cdot |X_{i,j}|^2 = 0$$
$$\Rightarrow \sum_{i,j\in\{\text{pilot set}\}} \mathbf{q}_{i,j} \mathbf{q}_{i,j}^T \hat{\mathbf{c}} \cdot |X_{i,j}|^2 = \sum_{i,j\in\{\text{pilot set}\}} \mathbf{q}_{i,j} \cdot X_{i,j} \cdot Y_{i,j}^* \qquad (4.10)$$

$\hat{\mathbf{c}}$ has close form which can be describe as

$$\hat{\mathbf{c}} = \mathbf{P}\mathbf{b}, \ \mathbf{P} = \mathbf{Q}^{-1}, \quad \mathbf{Q} = \sum_{i,j\in\{\text{pilot set}\}} \mathbf{q}_{i,j} \mathbf{q}_{i,j}^T |X_{i,j}|^2, \ \mathbf{b} = \sum_{i,j\in\{\text{pilot set}\}} \mathbf{q}_{i,j} X_{i,j} Y_{i,j}^* \ (4.11)$$

Channel estimation of the data position will be

$$\hat{H}_{m,n} = \hat{F}_{m,n} = \mathbf{q}_{m,n}^T \hat{\mathbf{c}}^* = \mathbf{q}_{m,n}^T \sum_{i,j\in\{\text{pilot set}\}} \mathbf{P}\mathbf{q}_{i,j} \cdot |X_{i,j}|^2 \cdot \hat{H}_{i,j}^{LS} \qquad (4.12)$$
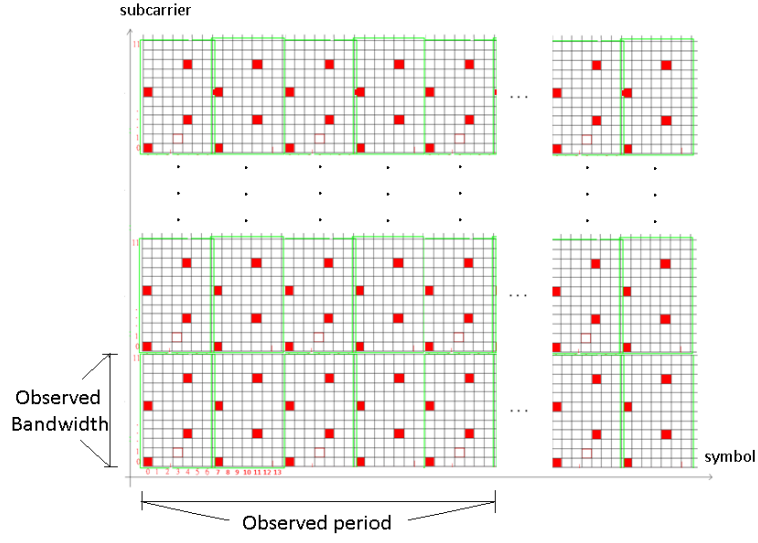
Figure 4.20: observed region.

4.4.3 SNR estimation

Fig. 4.20 shows the pilots distribution over resource blocks with which we calculate SINR for each block in observation window. We define true SINR in the observation window as

$$\frac{\frac{1}{MN} \sum_{i,j \in \{\text{observed region}\}} |H_{i,j} \cdot X_{i,j}|^2}{\sigma^2} \tag{4.13}$$

M is total number of symbols in observed region, N is total number of subcarriers in observed region. i is symbol index which covers from 0 to $M - 1$, j is subcarrier index which covers from 0 to $N - 1$. $X_{i,j} \in \{P_{i,j}, D_{i,j}\}$ $P_{i,j}$ is pilot set in observed region and $D_{i,j}$ is data set in observed region.

We then estimate SINR at pilot positions as follows.

$$\frac{\sum_{i,j \in \{\text{pilot set}\}} |\hat{H}_{i,j} \cdot P_{i,j}|^2}{\sum_{i,j \in \{\text{pilot set}\}} |Y_{i,j} - \hat{H}_{i,j} \cdot P_{i,j}|^2} \tag{4.14}$$

$\hat{H}_{i,j}$ is the channel estimation value at pilot position $\{i, j\}$, $Y_{i,j}$ is the receive signal on ith symbol and jth subcarrier.

58

The initial SINR estimate can be improved by decision feedbacks.

$$\frac{\sum_{i,j\in\{\text{observed region}\}} |\hat{H}_{i,j} \cdot \hat{X}_{i,j}|^2}{\sum_{i,j\in\{\text{observed region}\}} |Y_{i,j} - \hat{H}_{i,j} \cdot \hat{X}_{i,j}|^2} \tag{4.15}$$

$\hat{X}_{i,j} = \{P_{i,j}, \hat{D}_{i,j}\}$, $P_{i,j}$ is the pilot set which already known and $D_{i,j}$ is the decision data set after channel estimation interpolation.

After calculating for the same block size but different observed regions, we take average of the SNRs in different windows and simulate the performance as follows.

4.4.4 Numerical examples

Parameter	value
Simulation time	140ms
Total system bandwidth	20MHz(100RBs)
Block size for time period	2.5ms(5RBs)
Coherence time	3.8ms
Block size for frequency bandwidth	180kHz(1RBs)
Coherence bandwidth	500kHz
LTE center frequency	2.39GHz
UE velocity	30km/hr

Table 4.2: Simulation assumption.

From the simulation result of Fig. 4.21, the channel gain is varying with different symbol time on the same subcarrier. As shown in Fig. 4.22, we assume that the channel gain is varying with different symbols and subcarriers. We notice that the variation of LS+linear interpolation will be serious, but that model based channel estimation will be smooth and much close to the real channel.

Fig. 4.23 shows SNR vs BER curves for different channel estimation methods. The curve from model based channel estimation is always more close to curve of perfect channel than LS estimation method. The advantage of model based method is obvious when user operates at high SNR. The channel estimation error will dominate the bit error rather than noise.

SNR=35dB ,UE Velocity=30 km/hr ,LTE center frequency=2.39GHz
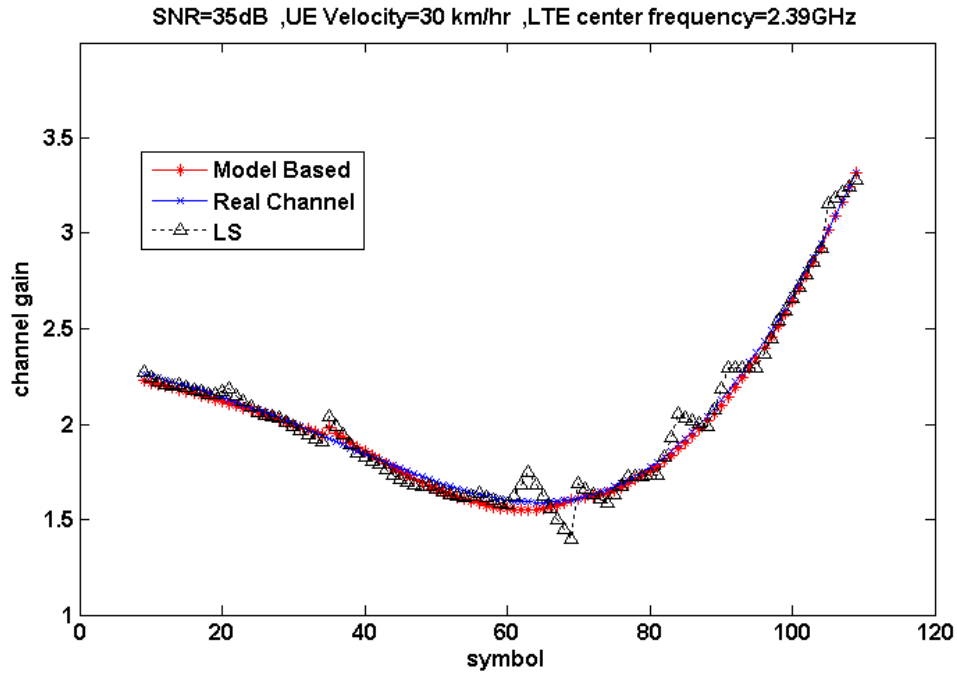
Figure 4.21: Channel gain for different symbols.

The model based channel estimation after data decision (Data Aided(DA)-ModelBased method) will be the most accurate method to estimate SNR which is investigated in Fig. 4.24. Only using pilot to estimate SNR (Only Pilot (OP)-ModelBased) will induce over-estimated SNR. Although the pilot position will provide better channel estimation result, noise variance calculation will be underestimated because the number of samples is not enough. The LS channel estimation (DA-LS) will be underestimate seriously when SNR is high. When SNR is high, and the noise variance is low, the channel estimation error will dominate the accuracy of SNR estimation. In that way, it will overestimate the noise variance and make the SNR estimation result lower than the real SNR. When interference becomes serious, and SNR is low, the estimation of SNR will be close to 0dB, but real SNR may be smaller than 0 dB. The accuracy of SNR estimation will be limited by noise because the channel estimation error will contribute to both the signal power and noise power measurement.
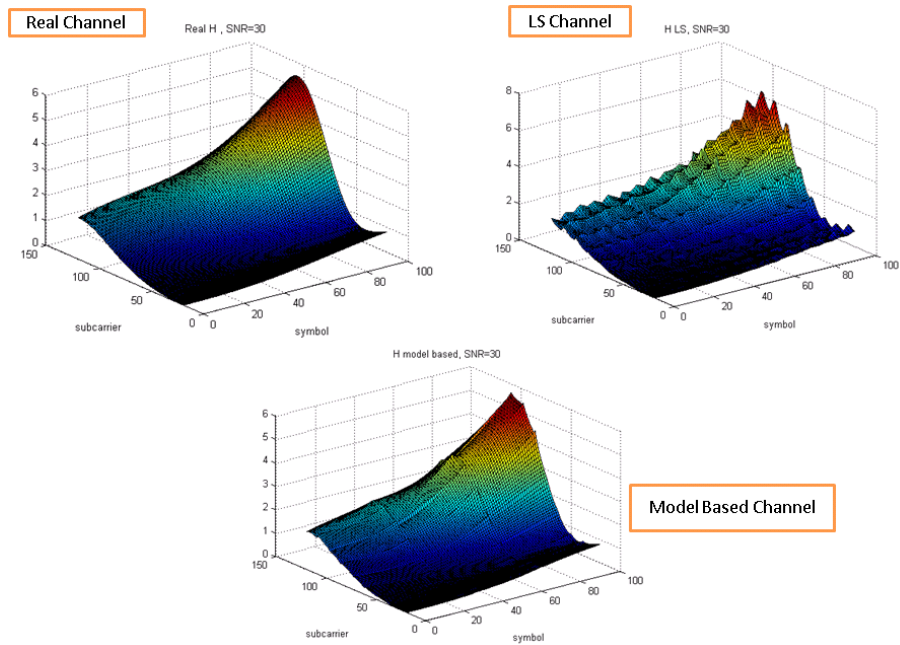
Figure 4.22: Channel estimation over frequency and time domain.
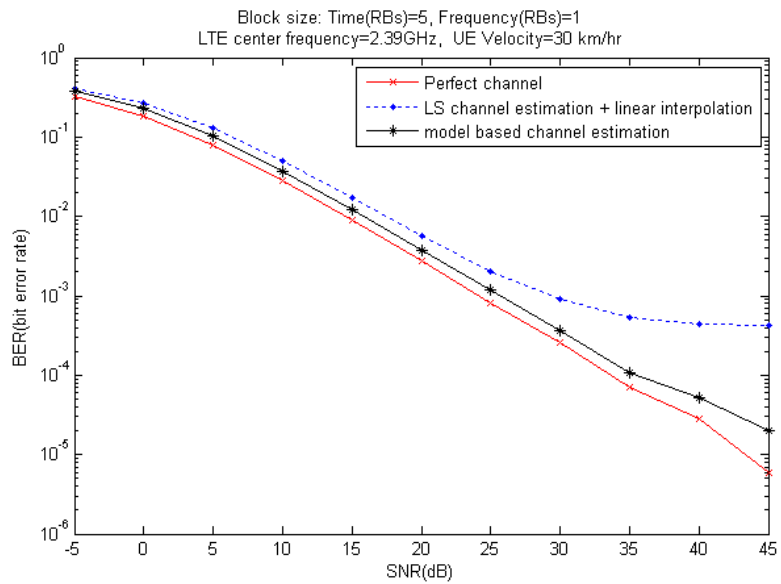
Figure 4.23: SNR vs BER for different channel estimation method at UE velocity of 30km/hr.
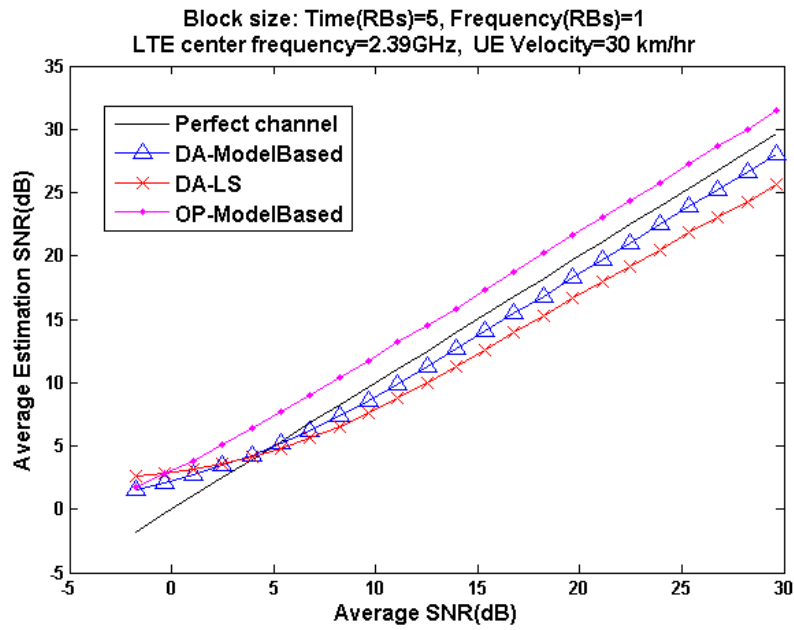
Figure 4.24: Compare different SNR estimation method with real SNR at UE velocity of 30km/hr.
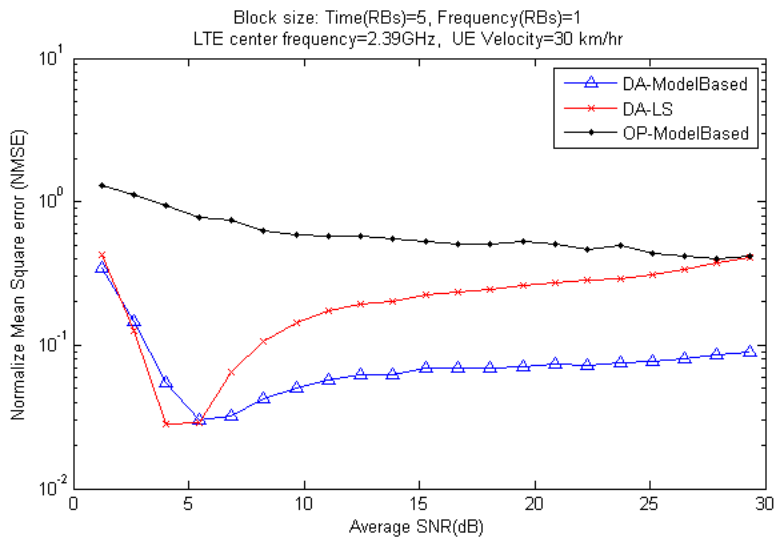
Figure 4.25: Compare NMSE for different SNR estimation method at UE velocity of 30km/hr.
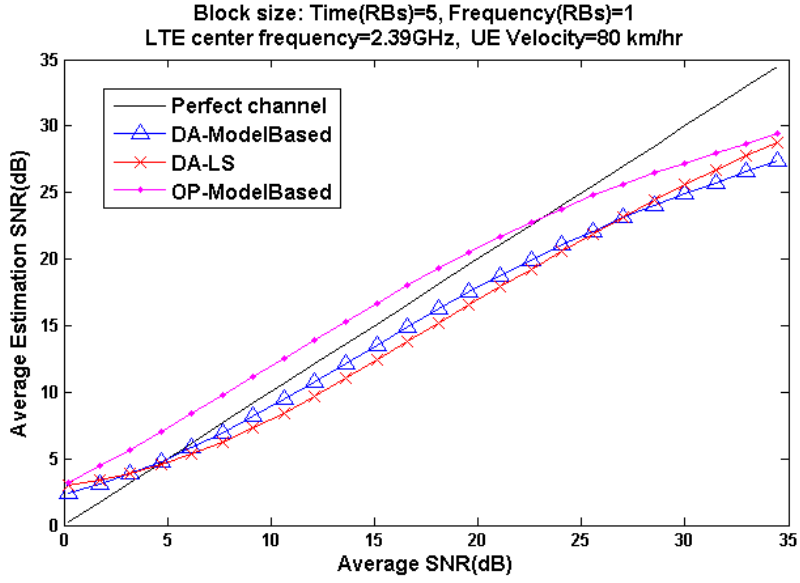
Figure 4.26: Compare different SNR estimation method with real SNR at UE velocity of 80km/hr.

Fig. 4.25 depicts the normalized mean square error performance for different SNR estimation methods when UE velocity = 30km/hr. The MSE for DA-LS and OP-ModelBased both will decrease when SNR is smaller than 5dB, and increase when SNR is larger than 5dB. When SNR is high then the noise variance will be low, the channel estimation error will dominate the accuracy of SNR estimation. Because channel estimation in Model based method is more accurate than in LS method, the NMSE will be much less in Model based method. The OP-ModelBased method always get higher SNR result, so the NMSE will be larger than other two methods.

Fig. 4.26 indicates that the model based channel estimator is unreliable because the channel varies fast, and two order regression model is not good enough to chase the channel variation when the block size is 2.5ms in time and 180kHz in frequency. The dopper shift will be $D_s = \frac{f_c \cdot v}{c} = \frac{2.39GHz \cdot 80km/hr \cdot 10/36}{3 \times 10^8 m/s} = 177Hz$. The coherence time will be $\frac{1}{4 \times D_s} = 1.412ms$ which is smaller than the block size in time. Hence, the SNR estimation will be inaccurate specially on high SNR because of channel estimation error.

63
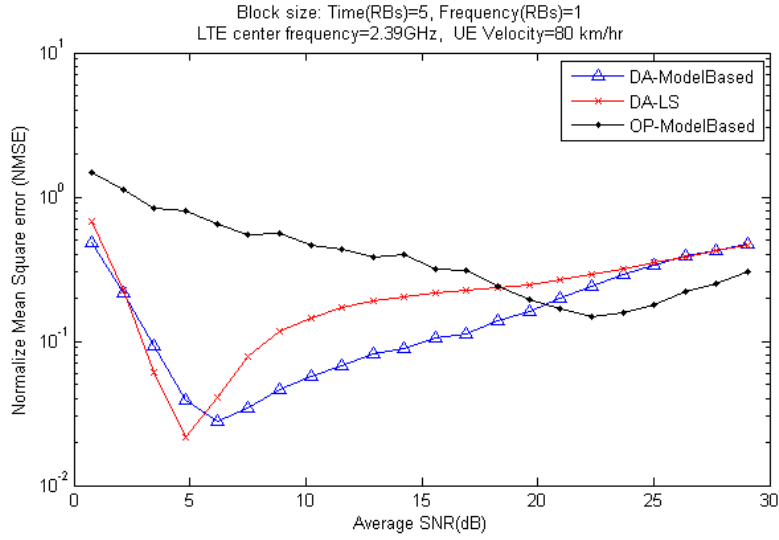
Figure 4.27: Compare NMSE for different SNR estimation method at UE velocity of 80km/hr.

The mean square error performance for different SNR estimation methods when UE velocity = 80 km/hr is plotted in Fig. 4.27. Most of the property is approach to Fig. 4.25, but the NMSE increase fast than UE at slow speed because two order regression model is not good enough to chase the channel variation. The OP-ModelBased method will be more precise than other two methods when SNR is high because channel estimation is accurate at pilot. And average SNR at pilot will close to real SNR in enough block size at UE high speed because the small number of time slot will obtain enough statistic property.

From Fig. 4.28, we find that the UE velocity is too fast for the model based channel estimator to have decent performance. We can adjust the block size in time which is 2ms (4RBs) to be smaller. The SNR estimation accuracy will be better than DA-LS. Fig. 4.29 shows that as the block size in time is small, DA-ModelBased method will be able to track the channel variation, the NMSE will improve. But the NMSE of OP-ModelBased method will become larger than in Fig. 4.27 because the number of time slot is not enough to obtain real SNR statistic property.
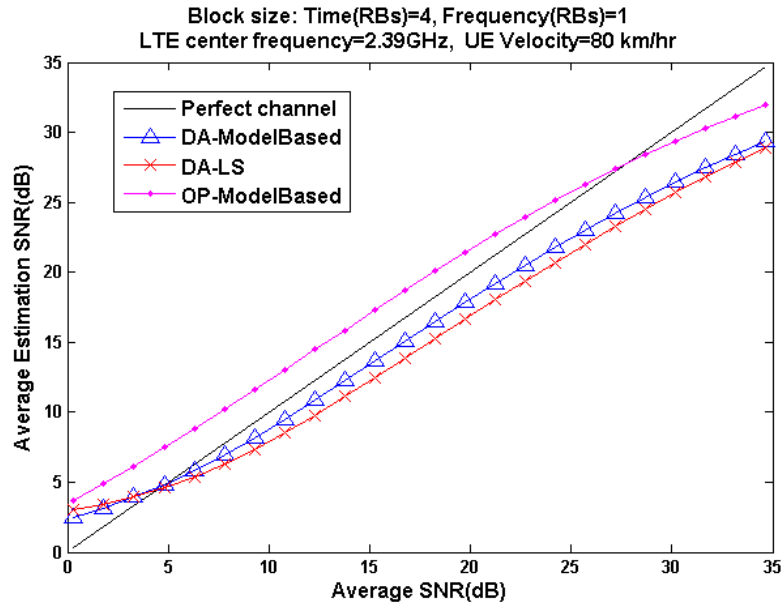
Figure 4.28: Compare different SNR estimation method with real SNR at UE velocity of 80km/hr and block size of time is 4(RBs).
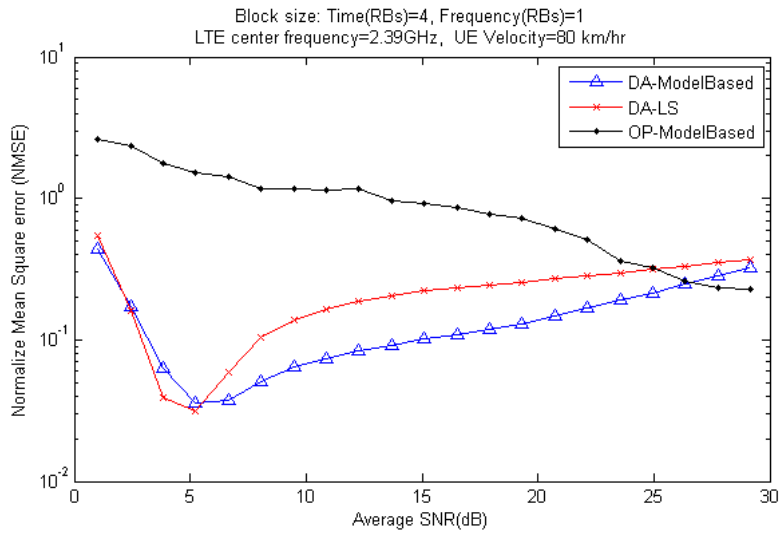
Figure 4.29: Compare NMSE for different SNR estimation method at UE velocity of 80km/hr and block size of time is 4(RBs).

The above simulation results indicate that the accuracy of SNR estimation for the regression model based approach of [3] is usually better than conventional least square (LS) based channel estimator.

Chapter 5

LTE/WiFi Throughput Analysis

An IDCI user will experience WiFi/LTE throughput degradation once the DRX mode is activated to solve IDCI. In this chapter, we analyze WiFi/LTE throughput without DRX and then discuss WiFi/LTE throughput when DRX scheme is on. Finally, we find the DRX parameters to fit the LTE/WiFi throughput demand from user after DRX scheme is on.

5.1 WiFi throughput analysis

5.1.1 Introduction of WiFi protocal

For IEEE 802.11 network based structure, access point (AP) is the point coordinated center and network synchronization is coordinated by AP. Each WiFi user have a timing synchronization function (TSF) counter which has a resolution of 1 us. Each WiFi user has to align its clock with the AP's TSF counter. The time point of TSF is positioned on the timestamp of beacon from AP, which is transmitted with a period of 102.4 ms so that WiFi users can keep synchronous with the AP. When a WiFi user receives the beacon, it takes the time point of TSF from the timestamp and calculate the offset to calibrate the time point of AP. The offset represents the time needed for the beacon waveform to

travel from AP to the WiFi user. The operation of synchronization is illustrated in Fig. 5.1.
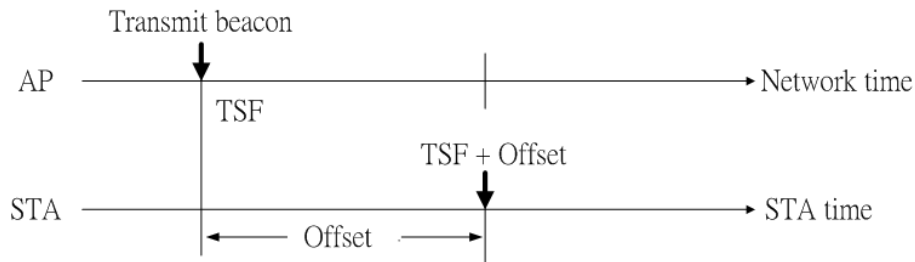
Figure 5.1: Based structure for time sychronization.

In Fig. 5.2, we show the CSMA/CA scheme in which a WiFi user is allowed to transmit whenever the channel become idle. A user must wait for a Inter Frame Space (IFS) before transmitting. IFS can be classified into Short IFS (SIFS), PCF IFS (PIFS) and DCF IFS (DIFS), respectively. The SIFS is the smallest time space and goes with highest priority signals such as ACK, RTS and CTS. The PIFS is invoked when the user operates on Point Coordinated Function (PCF) scheme, the contention-free scheme for the AP to polls different WiFi users. PIFS is shorter than DIFS and beacon also uses this inter frame space. The DIFS is used in conjunction with the Distributed Coordinated Function (DCF) scheme. DCF is a contention scheme that allows an user to contend when channel become idle.

Even with DIFS, a transmit packet may collide with other contending packets. To reduce the collision probability WLAN uses a collision avoidance (CA) scheme which requires an user to select a random backoff time described by a random binary exponential distribution. The probability that multiple users select the same backoff time is much smaller than simultaneous retransmissions. To further guarantee minimum collision, 802.11 adopts the RTS/CTS scheme which enforces an user to transmit Request to send (RTS) to AP and inform other WiFi users about the occupied time in the form of Network Allocation Vector (NAV). Other users will not sense the channel during this

time interval. The position of NAV in a data frame is shown in the Fig. 5.3. When AP successfully receives a RTS it sends a message called clear to send (CTS) to this user and inform other WiFi users near AP about the time interval specified by NAV. The user then start to transmit a packet after receiving CTS and no other transmission is permitted until NAV is over. The AP will transmit ACK after it receives the data packet successfully.
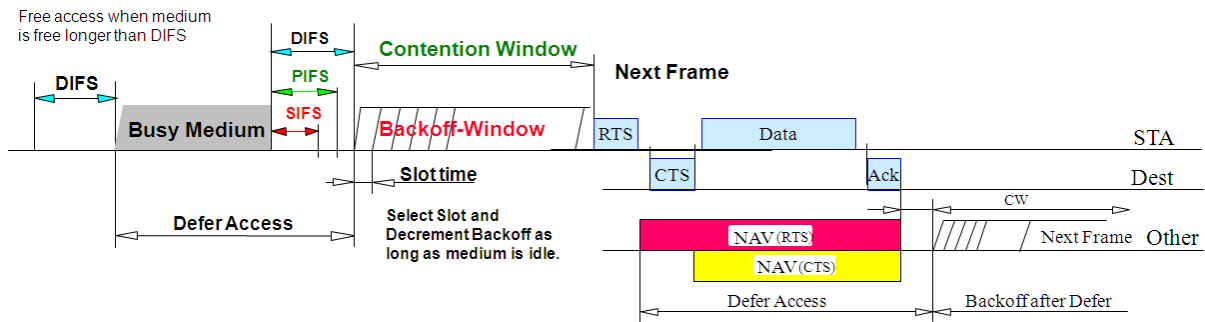
Figure 5.2: Procedure of WiFi signal transmission.
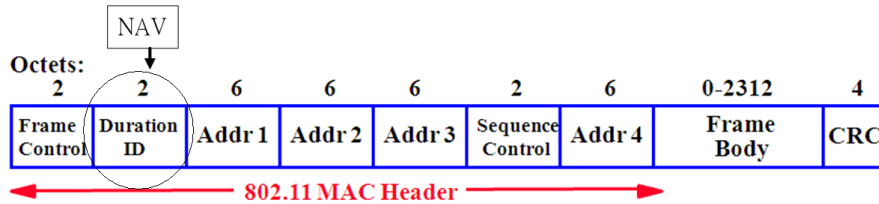
Figure 5.3: The position of NAV in a data frame.

5.1.2 Introduction of WiFi system throughput analysis

In [14], the author formulates the WiFi backoff model to a semi-Markov chain and derive the system throughput using the model chain model. In the thesis, we will introduce analysis from reference [14] first and discuss single user throughput in the WiFi network for different number of users. After we formulate the formulation of single WiFi user throughput, we will compare the math formulation result and real WiFi network model throughput and the results will close to each other.

69
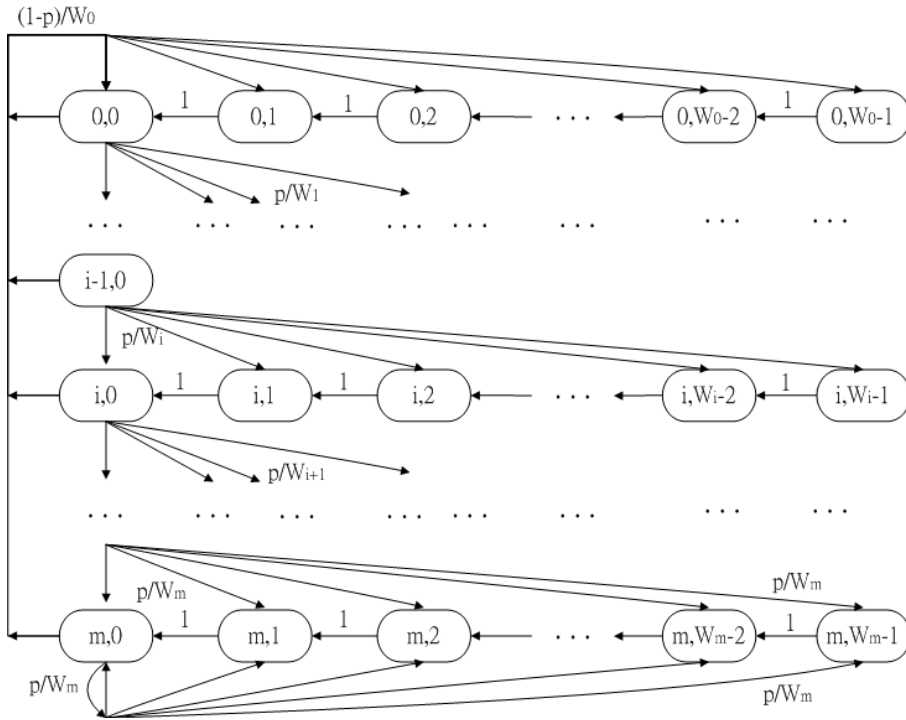
Figure 5.4: Markov Chain model for the backoff window size.

The state transition diagram is shown as Fig. 5.4. Each state is bidimensional process $\{s(t), b(t)\}$. $b(t)$ is the stochastic process representing the backoff time counter for a given WiFi user. A discrete and integer time scale is adopted: t and $t+1$ correspond to beginning of two consecutive slot times, and the backoff time counter of each station decrements at the beginning of each slot time. $s(t)$ is the stochastic process representing the backoff stage $(0, ..., m)$ of the WiFi user at time t. m is maximum backoff stage. Let $CW_{min} = W$ which is the minimum contention window size, and the contention window size will be $W_i = 2^i W$, where $i \in (0, m)$ is backoff stage. The maximum contention window size will be $CW_{max} = 2^m W$. Regardless of the number of retransmissions suffered, each packet collides with constant and independent probability p, and the assumption will accurate as long as W and n get larger, n is number of WiFi user in the WiFi network. p is conditional collision probability, it is probability of a collision seen by a packet being transmitted on the channel after the backoff timer count to zero. Once

independent is assumed, the p is supposed to be a constant value, and the bidimensional process $\{s(t), b(t)\}$ will be discrete Markov chain.

The one-step transition probability in Fig. 5.4 is

$$
\begin{cases}
P\{i, k | i, k+1\} = 1, & k \in (0, W_i - 2) \quad i \in (0, m); \\
P\{0, k | i, 0\} = (1-p)/W_0, & k \in (0, W_0 - 1) \quad i \in (0, m); \\
P\{i, k | i-1, 0\} = p/W_i, & k \in (0, W_i - 1) \quad i \in (1, m); \\
P\{m, k | m, 0\} = p/W_m, & k \in (0, W_m - 1).
\end{cases} \tag{5.1}
$$

First equation shows that backoff timer decrement when backoff timer still not goes to zero. Second equation shows that a packet transmit successfully after backoff timer goes to zero and the state goes to 0 stage. Third equation shows that a packet transmits failed after backoff timer goes to zero and the state goes to next stage. Fourth equation shows that a packet transmit failed after backoff timer goes to zero and it will still stay in m stage because it has operated on maximum backoff stage.

Using transition probability equation and the property for summation of all state probabilities is equal to one. We can calculate state probability respectively

$$
b_{i,k} = \frac{W_i - k}{W_i} b_{i,0} \ i \in (0, m), \ k \in (0, W_i - 1) \tag{5.2}
$$

$$
1 = \sum_{i=0}^{m} \sum_{k=0}^{W_i - 1} b_{i,k} = \frac{b_{0,0}}{2} [W(\sum_{i=0}^{m-1} (2p)^i + \frac{(2p)^m}{1-p}) + \frac{1}{1-p}] \tag{5.3}
$$

$$
b_{0,0} = \frac{2(1-2p)(1-p)}{(1-2p)(W+1) + pW(1-(2p)^m)} \tag{5.4}
$$

Let τ be the probability that a WiFi user transmits in a randomly chosen time slot. The transmission occurs once the backoff timer counter is equal to zero, so the τ can be expressed as

$$
\tau = \sum_{i=0}^{m} b_{i,0} = \frac{b_{0,0}}{1-p} = \frac{2(1-2p)}{(1-2p)(W+1) + pW(1-(2p)^m)} \tag{5.5}
$$

At steady state, each remaining WiFi user transmits a packet with probability τ. Let n be the total number of WiFi users, at least one of the $n-1$ remaining WiFi users

71

transmit in a time slot when a transmitted packet encounters a collision. This yields

$$p = 1 - (1 - \tau)^{n-1} \tag{5.6}$$

The collision probability p and the transmission probability τ can be calculated by combining equation (5.5) and equation (5.6).

Let S be the normalized system throughput, defined as the fraction of time the channel is used to successfully transmit payload bits. To get S, we need to analyze the probability what will happen in a randomly chosen slot time. Let P_{tr} be the probability that there is at least one WiFi user transmitting in considered slot time

$$P_{tr} = 1 - (1 - \tau)^n \tag{5.7}$$

$(1 - \tau)^n$ means the probability that all of WiFi users didn't transmit at this time slot, so P_{tr} is transmission probability in WiFi network. Let P_s be the probability of successful transmission conditional on transmission occurring on the channel.

$$P_s = \frac{n\tau(1 - \tau)^{n-1}}{P_{tr}} = \frac{n\tau(1 - \tau)^{n-1}}{1 - (1 - \tau)^n} \tag{5.8}$$

The normalized system throughput S can be express as

$$S = \frac{E[\text{payload information transmitted in a slot time}]}{E[\text{length of a slot time}]} = \frac{P_s P_{tr} E[P]}{(1 - P_{tr})\sigma + P_{tr} P_s T_s + P_{tr}(1 - P_s)T_c} \tag{5.9}$$

where $E[P]$ is average payload size. σ is the duration of an empty slot time, T_s is the average time the channel is sensed busy because of a successful transmission, and T_c is the average time the channel is sensed busy by each WiFi user during a collision. In this thesis, we let all packets have the same fixed size, E[P]=P(Payload: 3000 bits), so the T_s and T_c are also constant as Fig. 5.5 and Fig. 5.6

5.1.3 WiFi throughput analysis for single user

To compute WiFi throughput for single user, we will analyze transmission time for a packet first. A payload size divides by expectation of transmission time for a packet

72
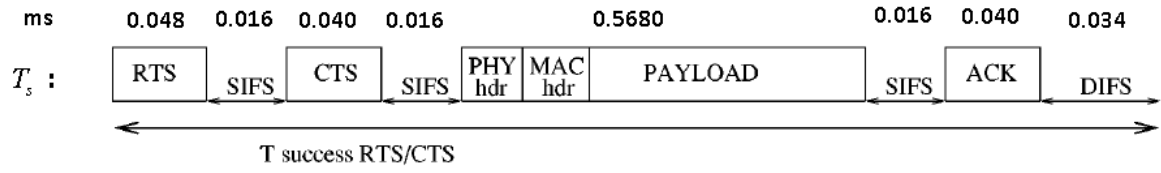
Figure 5.5: T_s, duration for transmitting a packet successfully .
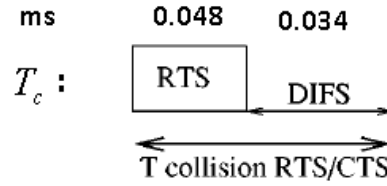
Figure 5.6: T_c, duration for transmitting a packet fail.

can obtain the throughput for single user. We will compare math formulation and real scenario simulation, the result will close to each other.

In Fig. 5.7, we show the route for states that the WiFi user will undergo during a packet successful transmission. It assumes that this WiFi user get the random number X_0 at 0 stage first, and the collision occurs the random value of backoff timer will be X_1 at 1 stage. The WiFi user keeps collision until i stage, and it will go back to 0 stage when the user transmits packet successfully.

When the backoff timer counter is not equal to zero (see Fig. 5.8), the backoff timer will keep count down, and the state transition time interval will be a random variable. Because the backoff timer will be fixed when it senses the channel is busy, which means the other WiFi user is occupying the channel. So, the backoff timer will keep counting down until the channel becomes idle. The random variable of transition time interval will include $T_s + \sigma$, $T_c + \sigma$ and σ which have probability P_s, P_c and P_σ as equation (5.11).

The backoff timer counter will fixed until one of other WiFi users transmit successfully for case 1 in Fig. 5.9. Sometimes, the WiFi user transmits successfully and the random number it choose from contention window is exact equal to zero and it will

73
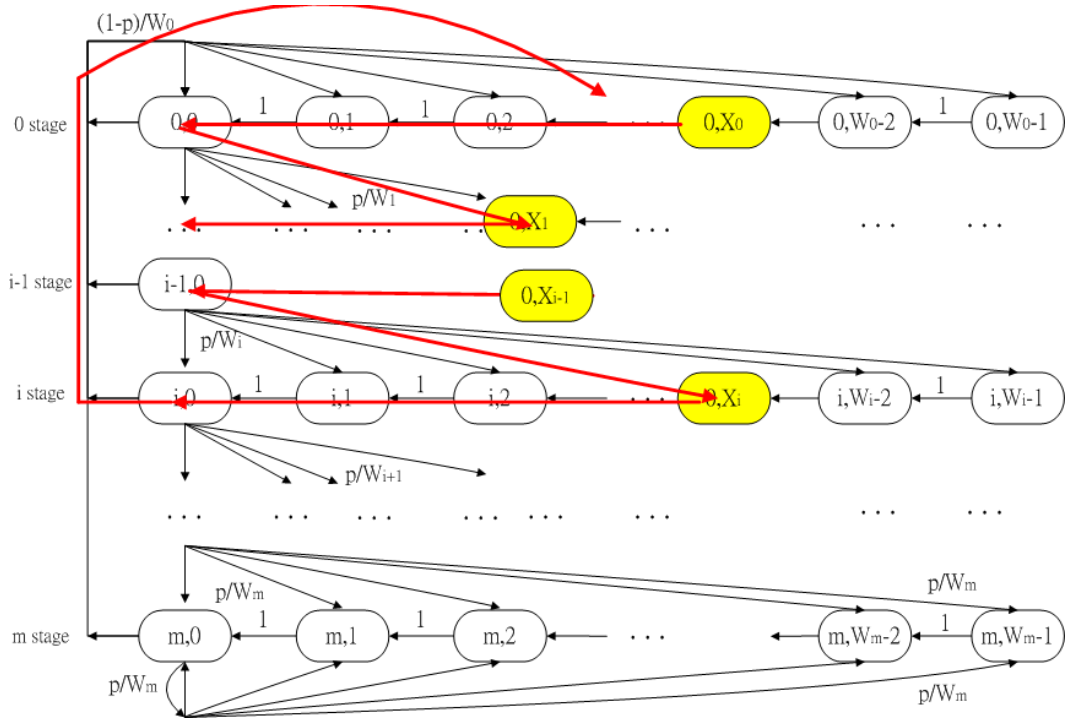
Figure 5.7: The route of a packet successful transmission on Markov Chain model for the backoff window.

transmit a packet successfully because the backoff timer counter from other WiFi users will not count down because the channel becomes busy again for case 2 in Fig. 5.9. For the case 3 in Fig. 5.9, there are more than one WiFi users transmit signal to AP at the same time, so the backoff timer counter will fixed until channel becomes idle again, it needs to take T_c to let channel becomes idle and counter down a clock takes time σ . For the case 4 in Fig. 5.9, it shows that no one occupy the WiFi channel because the backoff timer counter of all WiFi users are still not equal to zero. The transition time

$$k \in (0, W_i - 2) , i \in (0, m)$$
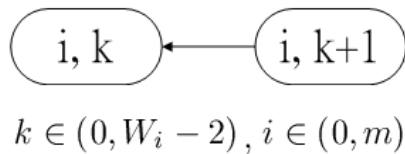
Figure 5.8: State transition when the backoff timer counter is not equal to zero.

74

We can use Fig. 5.9 to explain the all situations of transition time interval.

PDF: $\boxed{P_s \cdot \delta(t - (T_s + \sigma))} + \boxed{P_s \cdot (\frac{1}{W}) \cdot \delta(t - (2T_s + \sigma))} + \boxed{P_s \cdot (\frac{1}{W})^2 \cdot \delta(t - (3T_s + \sigma))} + \cdots + \boxed{P_\sigma \cdot \delta(t - \sigma)} + \boxed{P_c \cdot \delta(t - (T_c + \sigma))}$

$= \sum_{k=1}^{\infty} P_s \cdot (\frac{1}{W})^{k-1} \cdot \delta(t - (kT_s + \sigma)) + P_c \cdot \delta(t - (T_c + \sigma)) + P_\sigma \cdot \delta(t - \sigma)$

Figure 5.9: Random variable of transition time interval.

75

interval will be one time slot of backoff timer counter.

We can calculate the average time $E[T_{Backoff}]$ for state transition when the backoff timer counter is not equal to zero as follows

$$
\begin{aligned}
E[T_{Backoff}] &= P_c(T_c + \sigma) + P_\sigma \sigma + P_s T_s + P_s \frac{1}{W}(2T_s + \sigma) + P_s(\frac{1}{W})^2(3T_s + \sigma) + \cdots \\
&= P_c T_c + \left[P_c + P_\sigma + P_s(\frac{W}{W-1}) \right] \sigma + (\frac{W}{W-1})^2 T_s \quad\quad (5.10)
\end{aligned}
$$

$$
\begin{aligned}
P_s &= (n-1) \cdot \tau \cdot (1-\tau)^{n-2}, \quad \text{is successful probability for one time} \\
P_s&(\frac{W}{W-1})^2 \quad \text{is all the possibilities of success} \\
P_\sigma &= (1-\tau)^{n-1} \quad \text{is idle probability} \qu\quad\quad\quad\quad\quad\quad\quad (5.11) \\
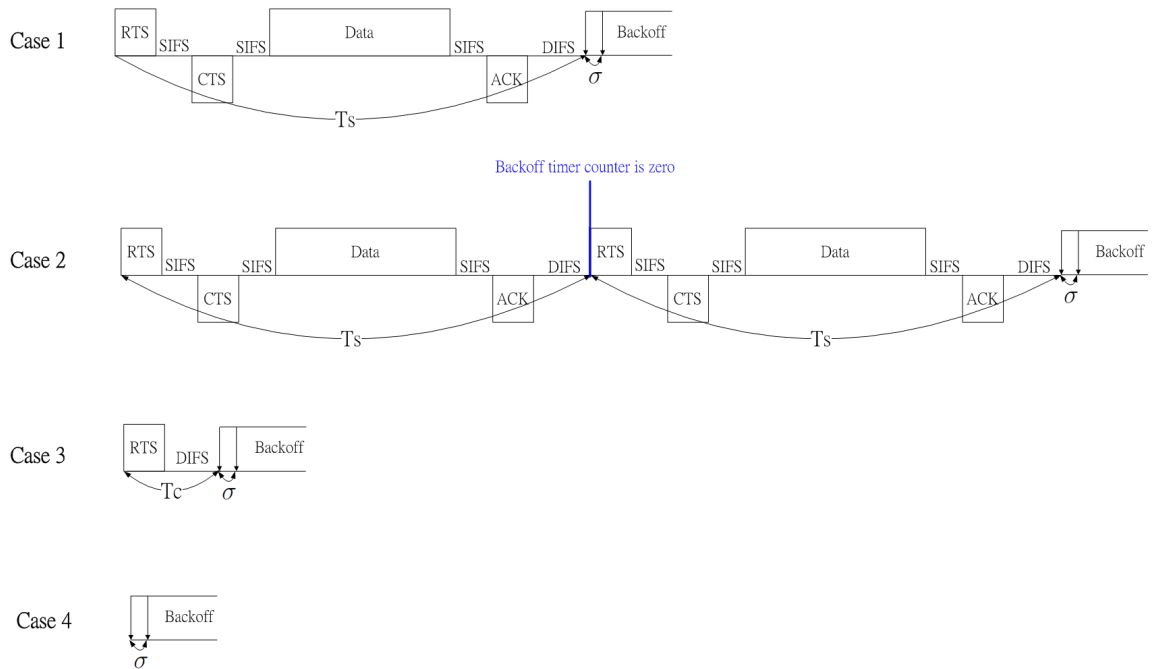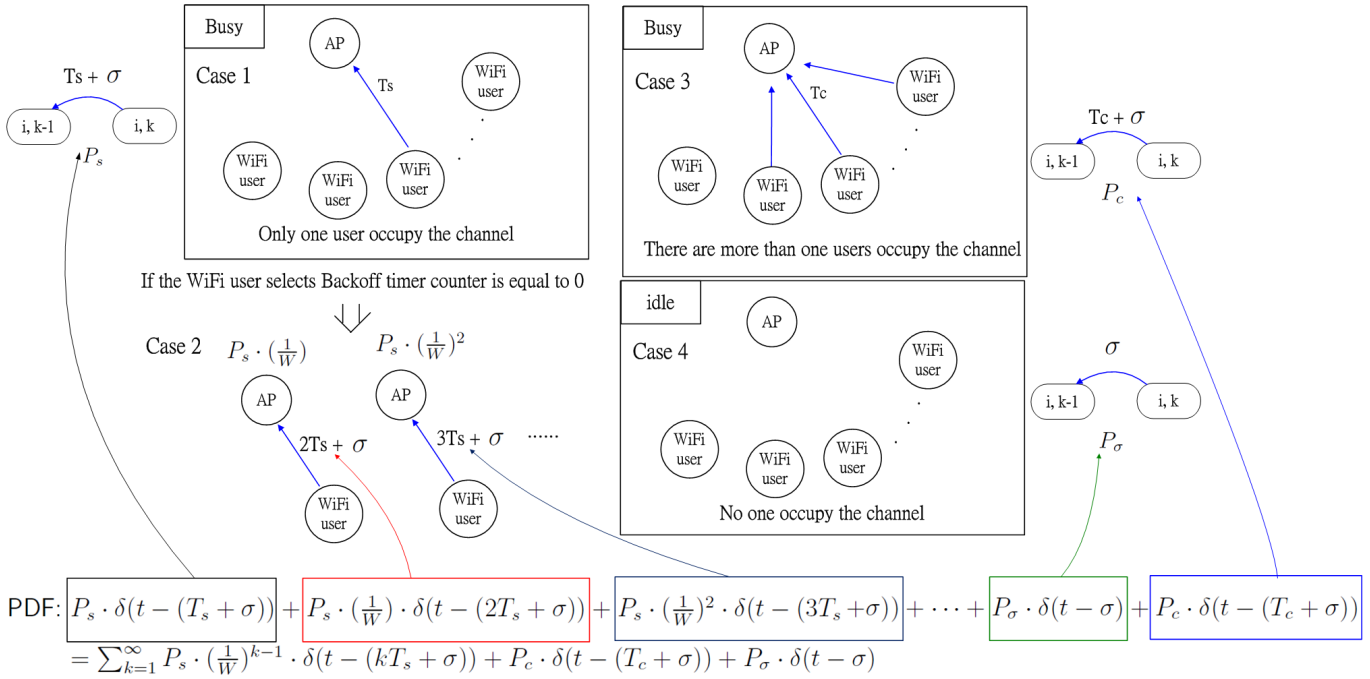P_c &= 1 - P_s(\frac{W}{W-1})^2 - P_\sigma \quad \text{is collision probability}
\end{aligned}
$$

$\frac{1}{W}$ is the probability that WiFi user choose zero to initial backoff timer counter from the contention window. After a packet transmits successfully once with probability P_s, the WiFi user will select for zero continuously with probability $(\frac{1}{W})^{k-1}$, and the transition time interval will take $kT_s + \sigma$. By summing up the expectation value, we can get $E[T_{Backoff}]$ the average time interval for state transition.

Next, we will analyze the probability density function (PDF) of transmission time for a packet. From Fig. 5.7, we know that user will undergo many transition time interval, and each of the transition interval when the counter isn't equal to zero is a random variable which we assume that they are i.i.d (identity and independent) to each other. And the random variable of total transmission time for a packet will be derived by summing up all of transition time interval. Because the PDF from summation of many random variable will be a huge work to do convolution, we use laplace transform to calculate PDF and it replace convolution with multiple which reduce the complexity of analysis.

For $E[T_{Backoff}]$, the time domain expression and its Laplace transform will be

$$\sum_{k=1}^{\infty} P_s \cdot (\frac{1}{W})^{k-1} \cdot \delta(t - (kT_s + \sigma)) + P_c \cdot \delta(t - (T_c + \sigma)) + P_\sigma \cdot \delta(t - \sigma)$$

$$\Rightarrow F(s) = \sum_{k=1}^{\infty} P_s \cdot (\frac{1}{W})^{k-1} \cdot e^{-s(kT_s+\sigma)} + P_c \cdot e^{-s(T_c+\sigma)} + P_\sigma \cdot e^{-s\sigma} \qquad (5.12)$$

$F(s)$ is Laplace transform from $E[T_{Backoff}]$ in time domain.

Here, we consider that the PDF Laplace transform for a packet transmission collide i times and access successfully, $\Phi(A, (i, 0))$, $(i, 0)$ means i stage and backoff timer counter is zero.

$$\Phi(A, (i, 0)) = \sum_{X_0} \Phi(A, (i, 0)|(0, X_0)) \cdot P(0, X_0) \qquad (5.13)$$

$P(0, X_0)$ is the probability that X_0 is chose, X_0 is the value of backoff timer counter. $\Phi(A, (i, 0)|(0, X_0))$ is the PDF Laplace transform for a packet transmission from state $(0, X_0)$ to state $(i, 0)$ and access successfully.

The equation 5.13 can be express as follows

$$\Phi(A, (i, 0)) = \sum_{X_i} \Phi(A, (i, 0)|(i, X_i)) \cdot P((i, X_i)|F, (i - 1, 0)) \cdot \Phi(F, (i - 1, 0)) \quad (5.14)$$

$\Phi(A, (i, 0)|(i, X_i))$ means the Laplace transform for a packet transmit successfully from state (i, X_i) to $(i, 0)$, X_i is the backoff timer counter value in i-th stage. $\Phi((i, X_i)|F, (i - 1, 0))$ means WiFi user transmission fail at $i - 1$ stage and it selects new counter value X_i at i stage. $\Phi(F, (i - 1, 0))$ means Laplace expression for transmission fail at $i - 1$ stage and it will be related to expression of next stage as follows

$$\Phi(F, (i, 0)) = \sum_{X_i} \Phi(F, (i, 0)|(i, X_i)) \cdot P((i, X_i)|F, (i - 1, 0)) \cdot \Phi(F, (i - 1, 0)) \quad (5.15)$$

When the collision times surpass m, the Laplace transform can be expressed as

$$\Phi(A, (i, 0)) = \sum_{X_i} \Phi(A, (m, 0)_i|(m, X_i)) \cdot P((m, X_i)|F, (m, 0)_{i-1}) \cdot \Phi(F, (m, 0)_{i-1}) \ (5.16)$$

The state $(m, 0)_i$ means user has occurred collision $i(i > m)$ times and operates at m stage. To summarize the Laplace transform formulation, we can get

$$\Phi(A,(i,0)) = \begin{cases} \sum_{X_0} \Phi(A,(1,0)|(0,X_0)) \cdot P(0,X_0) & \text{for} \quad i = 0 \\ \sum_{X_i} \Phi(A,(i,0)|(i,X_i)) \cdot P((i,X_i)|F,(i-1,0)) \cdot \Phi(F,(i-1,0)) & \text{for} \quad i \le m \\ \sum_{X_i} \Phi(A,(m,0)_i|(m,X_i)) \cdot P((m,X_i)|F,(m,0)_{i-1}) \cdot \Phi(F,(m,0)_{i-1}) & \text{for} \quad i > m \end{cases} \quad (5.17)$$

$$\Phi(F,(i,0)) = \begin{cases} \sum_{X_0} \Phi(F,(1,0)|(0,X_0)) \cdot P(0,X_0) & \text{for} \quad i = 0 \\ \sum_{X_i} \Phi(F,(i,0)|(i,X_i)) \cdot P((i,X_i)|F,(i-1,0)) \cdot \Phi(F,(i-1,0)) & \text{for} \quad i \le m \\ \sum_{X_i} \Phi(F,(m,0)_i|(m,X_i)) \cdot P((m,X_i)|F,(m,0)_{i-1}) \cdot \Phi(F,(m,0)_{i-1}) & \text{for} \quad i > m \end{cases} \quad (5.18)$$

The expression for each item can be

$$\begin{cases} X_0 = 0,1,\cdots,W & \text{for} \quad i = 0 \\ X_i = 0,1,\cdots,W \cdot 2^i - 1 & \text{for} \quad i \le m \\ X_i = 0,1,\cdots,W \cdot 2^m - 1 & \text{for} \quad i > m \end{cases} \quad (5.19)$$

$$\begin{cases} P(0,X_0) = \frac{1}{W} & \text{for} \quad i = 0 \\ P((i,X_i)|F,(i-1,0)) = \frac{1}{W \cdot 2^i} & \text{for} \quad i \le m \\ P((m,X_i)|F,(m,0)_{i-1}) = \frac{1}{W \cdot 2^m} & \text{for} \quad i > m \end{cases} \quad (5.20)$$

$$\begin{cases} \Phi(A,(0,0)|(0,X_0)) = (1-p)F(s)^{X_0} e^{-sT_s} & \text{for} \quad i = 0 \\ \Phi(A,(i,0)|(i,X_i)) = (1-p)F(s)^{X_i} e^{-sT_s} & \text{for} \quad i \le m \\ \Phi(A,(m,0)_i|(m,X_i)) = (1-p)F(s)^{X_i} e^{-sT_s} & \text{for} \quad i > m \end{cases} \quad (5.21)$$

$$\begin{cases} \Phi(F,(0,0)|(0,X_0)) = pF(s)^{X_0} e^{-sT_c} & \text{for} \quad i = 0 \\ \Phi(F,(i,0)|(i,X_i)) = pF(s)^{X_i} e^{-sT_c} & \text{for} \quad i \le m \\ \Phi(F,(m,0)_i|(m,X_i)) = pF(s)^{X_i} e^{-sT_c} & \text{for} \quad i > m \end{cases} \quad (5.22)$$

The equation 5.19 shows the range of backoff timer counter on different collision times. The equation 5.20 provide the probability that the value selected by next stage. The equation 5.21 and 5.22 are Laplace expression on different collision times. For eq 5.21, $F(s)^{X_i}$ is Laplace expression for state transition X_i times. $(1-p)$ is the probability for successful transmission. e^{-sT_s} is the time interval user will across successful transmission.

To get the Laplace formulation for transmitting a packet, we replace equation 5.18∼5.22

to 5.17 and we can obtain

$$\Phi(A,(i,0)) = \sum_{X_i} \Phi(A,(i,0)|(i,X_i)) \cdot P((i,X_i)|F,(i-1,0)) \cdot \Phi(F,(i-1,0))$$

$$= \sum_{X_i} \Phi(A,(i,0)|(i,X_i)) \cdot P((i,X_i)|F,(i-1,0)) \cdot$$

$$\left(\sum_{X_{i-1}} \Phi(F,(i-1,0)|(i-1,X_{i-1})) \cdot P((i-1,X_{i-1})|F,(i-2,0)) \cdot \Phi(F,(i-2,0)) \right)$$

$$= \sum_{X_i} \Phi(A,(i,0)|(i,X_i)) \cdot P((i,X_i)|F,(i-1,0)) \cdot \qquad (5.23)$$

$$\sum_{X_{i-1}=0}^{W \cdot 2^{i-1}-1} \cdots \sum_{X_0=0}^{W-1} \prod_{k=1}^{i-1} \Phi(F,(k,0)|(k,X_k)) \prod_{k=1}^{i-1} P((k,X_k)|F,(k-1,0)) \Phi(F,(0,0))$$

The Laplace transform expression for collision i times

$$\Phi(A,(i,0)) = \sum_{X_0=0}^{W-1} \cdots \sum_{X_i=0}^{W \cdot 2^i-1} F(s)^{X_0+X_1+\cdots+X_i} \cdot \frac{p^i(1-p)}{W^{i+1} \cdot 2^{\frac{i(i+1)}{2}}} e^{-s(iT_c+T_s)} \qquad \text{for} \quad i \leq m \;\; (5.24)$$

$$\Phi(A,(i,0)) = \sum_{X_0=0}^{W-1} \cdots \sum_{X_i=0}^{W \cdot 2^i-1} F(s)^{X_0+X_1+\cdots+X_i} \cdot \frac{p^i(1-p)}{W^{i+1} \cdot (2^m)^{(i-m)} 2^{\frac{m(m+1)}{2}}} e^{-s(iT_c+T_s)} \quad \text{for} \quad i > m \;\; (5.25)$$

Let $L(s)$ be the Laplace transform function for a packet transmission time which includes all collision possibilities.

$$L(s) = \sum_{i=0}^{\infty} \Phi(A,(i,0))$$

$$= \sum_{i=0}^{m-1} \sum_{X_0=0}^{W-1} \cdots \sum_{X_i=0}^{W \cdot 2^i-1} F(s)^{X_0+X_1+\cdots+X_i} \cdot \frac{p^i(1-p)}{W^{i+1} \cdot 2^{\frac{i(i+1)}{2}}} e^{-s(iT_c+T_s)}$$

$$+ \sum_{i=m}^{\infty} \sum_{X_0=0}^{W-1} \cdots \sum_{X_i=0}^{W \cdot 2^i-1} F(s)^{X_0+X_1+\cdots+X_i} \cdot \frac{p^i(1-p)}{W^{i+1} \cdot (2^m)^{(i-m)} 2^{\frac{m(m+1)}{2}}} e^{-s(iT_c+T_s)} \;(5.26)$$

Let $l(t)$ be the PDF of transmission time interval

$$
\mathcal{L}^{-1}[L(s)] = \sum_{i=0}^{m-1}\sum_{X_0=0}^{W-1}\cdots\sum_{X_i=0}^{W\cdot 2^i-1}\sum_{\substack{(n_s+n_c+n_\sigma)\\=X_0+X_1+\cdots+X_i}} C_{n_c}^{X_0+\cdots+X_i}C_{n_\sigma}^{X_0+\cdots+X_i-n_c}C_{n_s}^{n_s}P_c^{n_c}P_\sigma^{n_\sigma}
$$

$$
\sum_{\substack{n_s=n_{s_1}+\\\cdots+n_{s_k}+\cdots}} C_{n_{s_1}}^{n_s}C_{n_{s_2}}^{n_s-n_{s_1}}\cdots C_{n_{s_k}}^{n_s-\sum_{g=1}^{k-1}n_{sg}}\cdots(P_s)^{n_{s_1}}\left(P_s\frac{1}{W}\right)^{n_{s_2}}\cdots\left[P_s(\frac{1}{W})^{k-1}\right]^{n_{s_k}}\cdots
$$

$$
\left\{\frac{p^i(1-p)}{W^{i+1}\cdot 2^{\frac{i(i+1)}{2}}}\cdot\delta\left(t-\left[(\sum_{k=1}^{\infty}n_{s_k}\cdot k+1)T_s+(n_c+i)T_c+(X_0+X_1+\cdots+X_i)\sigma\right]\right)\right\}
$$

$$
+\sum_{i=m}^{\infty}\sum_{X_0=0}^{W-1}\cdots\sum_{X_i=0}^{W\cdot 2^i-1}\sum_{\substack{(n_s+n_c+n_\sigma)\\=X_0+X_1+\cdots+X_i}} C_{n_c}^{X_0+\cdots+X_i}C_{n_\sigma}^{X_0+\cdots+X_i-n_c}C_{n_s}^{n_s}P_c^{n_c}P_\sigma^{n_\sigma} \quad (5.27)
$$

$$
\sum_{\substack{n_s=n_{s_1}+\\\cdots+n_{s_k}+\cdots}} C_{n_{s_1}}^{n_s}C_{n_{s_2}}^{n_s-n_{s_1}}\cdots C_{n_{s_k}}^{n_s-\sum_{g=1}^{k-1}n_{sg}}\cdots(P_s)^{n_{s_1}}\left(P_s\frac{1}{W}\right)^{n_{s_2}}\cdots\left[P_s(\frac{1}{W})^{k-1}\right]^{n_{s_k}}\cdots
$$

$$
\left\{\frac{p^i(1-p)}{W^{i+1}(2^m)^{(i-m)}2^{\frac{m(m+1)}{2}}}\cdot\delta\left(t-\left[(\sum_{k=1}^{\infty}n_{s_k}\cdot k+1)T_s+(n_c+i)T_c+(X_0+X_1+\cdots+X_i)\sigma\right]\right)\right\}
$$

To get further statistic, we derive first order moment and second order moment from Laplace transform to obtain mean and variance for a packet transmission time interval. The first order moment will be as follows

$$
-\frac{\partial L(s)}{\partial s}\Big|_{s=0} = \left(\sum_{i=0}^{m-1}\frac{p^i(1-p)}{W^{i+1}\cdot 2^{\frac{i(i+1)}{2}}}+\sum_{i=m}^{\infty}\frac{p^i(1-p)}{W^{i+1}\cdot(2^m)^{(i-m)}2^{\frac{m(m+1)}{2}}}\right)
$$

$$
\sum_{X_0=0}^{W-1}\cdots\sum_{X_i=0}^{W\cdot 2^i-1}\{(X_0+X_1+\cdots+X_i)F(s)^{X_0+X_1+\cdots+X_i-1}\left[-F(s)\right]'e^{-s(iT_c+T_s)} \quad (5.28)
$$

$$
+ F(s)^{X_0+X_1+\cdots+X_i}\left[+(iT_c+T_s)\right]e^{-s(iT_c+T_s)}\Big|_{s=0}\}
$$

The items from (5.28) can be express as

$$
\{(X_0+X_1+\cdots+X_i)F(s)^{X_0+X_1+\cdots+X_i-1}\left[-F(s)\right]'e^{-s(iT_c+T_s)}+
$$

$$
F(s)^{X_0+X_1+\cdots+X_i}\left[+(iT_c+T_s)\right]e^{-s(iT_c+T_s)}\}\Big|_{s=0} = \left\{[\sum_{k=0}^{i}X_k][E[T_{Backoff}]]+[iT_c+T_s]\right\}
$$

$$
[-F(s)]'\Big|_{s=0} = E[T_{Backoff}] = \left[P_cT_c+\left[P_c+P_\sigma+P_s(\frac{W}{W-1})\right]\sigma+(\frac{W}{W-1})^2T_s\right], \quad F(s)\Big|_{s=0}=1
$$

$$\text{Mean} = \sum_{i=0}^{m-1} \frac{\sum_{X_i=0}^{W \cdot 2^i - 1} \sum_{X_{i-1}=0}^{W \cdot 2^{i-1} - 1} \cdots \sum_{X_0=0}^{W-1} \left[\sum_{k=0}^{i} X_k \right]}{W^{i+1} \cdot 2^{\frac{i(i+1)}{2}}} p^i (1-p) E[T_{Backoff}]$$

$$+ \sum_{i=m}^{\infty} \frac{\sum_{X_i=0}^{W \cdot 2^i - 1} \sum_{X_{i-1}=0}^{W \cdot 2^{i-1} - 1} \cdots \sum_{X_0=0}^{W-1} \left[\sum_{k=0}^{i} X_k \right]}{W^{i+1} \cdot (2^m)^{(i-m)} 2^{\frac{m(m+1)}{2}}} p^i (1-p) E[T_{Backoff}]$$

$$+ \sum_{i=0}^{m-1} \frac{\sum_{X_i=0}^{W \cdot 2^i - 1} \sum_{X_{i-1}=0}^{W \cdot 2^{i-1} - 1} \cdots \sum_{X_0=0}^{W-1} 1}{W^{i+1} \cdot 2^{\frac{i(i+1)}{2}}} p^i (1-p)[iT_c + T_s]$$

$$+ \sum_{i=m}^{\infty} \frac{\sum_{X_i=0}^{W \cdot 2^i - 1} \sum_{X_{i-1}=0}^{W \cdot 2^{i-1} - 1} \cdots \sum_{X_0=0}^{W-1} 1}{W^{i+1} \cdot (2^m)^{(i-m)} 2^{\frac{m(m+1)}{2}}} p^i (1-p)[iT_c + T_s]$$

$$= \sum_{i=0}^{m-1} \left[\frac{W-1}{2} + \frac{W \cdot 2 - 1}{2} + \cdots + \frac{W \cdot 2^i - 1}{2} \right] E[T_{Backoff}] p^i (1-p)$$

$$+ \sum_{i=m}^{\infty} \left[\frac{W-1}{2} + \frac{W \cdot 2 - 1}{2} + \cdots + \frac{W \cdot 2^m - 1}{2} + (i-m)\frac{W \cdot 2^m - 1}{2} \right] E[T_{Backoff}] p^i (1-p)$$

$$+ \sum_{i=0}^{\infty} [iT_c + T_s] p^i (1-p)$$

$$= \sum_{i=0}^{m-1} \left[\sum_{k=0}^{i} \frac{W \cdot 2^k - 1}{2} \right] p^i (1-p) E[T_{Backoff}] + \sum_{i=0}^{\infty} i p^i T_c (1-p) + \sum_{i=0}^{\infty} p^i T_s (1-p)$$

$$\sum_{n=0}^{\infty} \left[\sum_{k=0}^{m} \frac{W \cdot 2^k - 1}{2} + n \cdot \frac{W \cdot 2^m - 1}{2} \right] p^{m+n} (1-p) E[T_{Backoff}]$$

$$= \sum_{i=0}^{m-1} \left[\frac{W(2^{i+1} - 1) - (i+1)}{2} \right] p^i (1-p) E[T_{Backoff}] + \frac{p}{(1-p)^2} T_c (1-p) + \frac{T_s}{(1-p)}(1-p)$$

$$+ \sum_{n=0}^{\infty} \left[\frac{W(2^{m+1} - 1) - (m+1)}{2} + \frac{(W \cdot 2^m - 1)n}{2} \right] p^n \cdot p^m (1-p) E[T_{Backoff}]$$

$$= \frac{1}{2} \left\{ W \left(2\frac{1 - (2p)^m}{1 - 2p} - \frac{1 - p^m}{1 - p} \right) - \frac{p[-mp^{m-1}(1-p) + (1 - p^m)]}{(1-p)^2} - \frac{1 - p^m}{1 - p} \right\} (1-p) E[T_{Backoff}]$$

$$+ \left[\frac{W(2^{m+1} - 1) - (m+1)}{2} + \frac{(W \cdot 2^m - 1)p}{2(1-p)} \right] p^m E[T_{Backoff}] + \frac{p}{1 - p} T_c + T_s \quad (5.30)$$

The Laplace transform for first order and second order moment will be

$$L(s) = \int_0^{\infty} l(t) e^{-st} dt, \quad \frac{\partial^2 L(s)}{\partial s^2}\Big|_{s=0} = \int_0^{\infty} t^2 \cdot l(t) dt, \quad \frac{\partial L(s)}{\partial s}\Big|_{s=0} = \int_0^{\infty} -t \cdot l(t) dt \quad (5.31)$$

Since equation 5.30, the variance for transmission time interval can be

$$Variance = \int_0^\infty t^2 \cdot l(t)dt - \left[\int_0^\infty t \cdot l(t)dt\right]^2 = \left[\frac{\partial^2 L(s)}{\partial s^2}\right]|_{s=0} - \left[\frac{\partial L(s)}{\partial s}\right]^2|_{s=0} \quad (5.32)$$

The $L(s)$ second order differentiation will be

$$\left[\frac{\partial^2 L(s)}{\partial s^2}\right]|_{s=0} = \left(\sum_{i=0}^{m-1}\frac{p^i(1-p)}{W^{i+1}\cdot 2^{\frac{i(i+1)}{2}}} + \sum_{i=m}^\infty \frac{p^i(1-p)}{W^{i+1}\cdot (2^m)^{(i-m)}2^{\frac{m(m+1)}{2}}}\right)\sum_{X_0=0}^{W-1}\cdots\sum_{X_i=0}^{W\cdot 2^i-1}$$

$$\left[\frac{\partial}{\partial s}\left(\left(\sum_{k=0}^i X_k\right)F(s)^{\sum_{k=0}^i X_k-1}\left[F(s)\right]' e^{-s(iT_c+T_s)} + F(s)^{\sum_{k=0}^i X_k}[-(iT_c+T_s)]e^{-s(iT_c+T_s)}\right)\right]$$

$$= \left(\sum_{i=0}^{m-1}\frac{p^i(1-p)}{W^{i+1}\cdot 2^{\frac{i(i+1)}{2}}} + \sum_{i=m}^\infty \frac{p^i(1-p)}{W^{i+1}\cdot (2^m)^{(i-m)}2^{\frac{m(m+1)}{2}}}\right)\cdot\sum_{X_0=0}^{W-1}\cdots\sum_{X_i=0}^{W\cdot 2^i-1} \quad (5.33)$$

$$\{(\sum_{k=0}^i X_k)(\sum_{k=0}^i X_k-1)F(s)^{\sum_{k=0}^i X_k-2}([F(s)]')^2 e^{-s(iT_c+T_s)} + (\sum_{k=0}^i X_k)F(s)^{\sum_{k=0}^i X_k-1}\left[F(s)\right]'' e^{-s(iT_c+T_s)}$$

$$+2\cdot(\sum_{k=0}^i X_k)F(s)^{\sum_{k=0}^i X_k-1}\left[F(s)\right]'[-(iT_c+T_s)]e^{-s(iT_c+T_s)} + F(s)^{\sum_{k=0}^i X_k}[-(iT_c+T_s)]^2 e^{-s(iT_c+T_s)}\}$$

The $[F(s)]''|_{s=0}$ can be express as

$$[F(s)]''|_{s=0} = \frac{\partial^2\left(\sum_{k=1}^\infty P_s\cdot(\frac{1}{W})^{k-1}\cdot e^{-s(kT_s+\sigma)} + P_c\cdot e^{-s(T_c+\sigma)} + P_\sigma\cdot e^{-s\sigma}\right)}{\partial s^2}$$

$$= P_s\sum_{k=1}^\infty(kT_s+\sigma)^2(\frac{1}{W})^{k-1} + P_cT_c + \sigma^2 + P_\sigma T_\sigma{}^2$$

$$= (P_s+P_c+P_\sigma)\sigma^2 + P_c\cdot 2T_c\cdot\sigma + P_s(\frac{W}{W-1})^2 2T_s\cdot\sigma + P_sT_s{}^2\frac{1+\frac{1}{W}}{(1-\frac{1}{W})^3} + P_cT_c{}^2 \quad (5.34)$$

By substituting (5.34) and (5.29) for (5.33), (5.33) can be express as

$$
\left[\frac{\partial^2 L(s)}{\partial s^2}\right]\Big|_{s=0} = \left(\sum_{i=0}^{m-1}\frac{p^i(1-p)}{W^{i+1}\cdot 2^{\frac{i(i+1)}{2}}} + \sum_{i=m}^{\infty}\frac{p^i(1-p)}{W^{i+1}\cdot(2^m)^{(i-m)}2^{\frac{m(m+1)}{2}}}\right)\cdot\sum_{X_0=0}^{W-1}\cdots\sum_{X_i=0}^{W\cdot 2^i-1}
$$

$$
\{(\sum_{k=0}^{i}X_k)(\sum_{k=0}^{i}X_k - 1)\left(E[T_{Backoff}]\right)^2 + (\sum_{k=0}^{i}X_k)\left[P_sT_s^{2}\frac{1+\frac{1}{W}}{(1-\frac{1}{W})^3} + P_cT_c^{2} + P_\sigma T_\sigma^{2}\right]
$$

$$
+2\cdot(\sum_{k=0}^{i}X_k)\left[E[T_{Backoff}]\right](iT_c + T_s) + (iT_c + T_s)^2\}
$$

$$
= \left(\sum_{i=0}^{m-1}\frac{\sum_{X_0=0}^{W-1}\cdots\sum_{X_i=0}^{W\cdot 2^i-1}\left(\sum_{k=0}^{i}X_k\right)^2}{W^{i+1}\cdot 2^{\frac{i(i+1)}{2}}}p^i + \sum_{i=m}^{\infty}\frac{\sum_{X_0=0}^{W-1}\cdots\sum_{X_i=0}^{W\cdot 2^i-1}\left(\sum_{k=0}^{i}X_k\right)^2}{W^{i+1}\cdot(2^m)^{(i-m)}2^{\frac{m(m+1)}{2}}}p^i\right)(1-p)\cdot
$$

$$
(E[T_{Backoff}])^2 + \sum_{i=0}^{m-1}\frac{\sum_{X_0=0}^{W-1}\cdots\sum_{X_i=0}^{W\cdot 2^i-1}\left(\sum_{k=0}^{i}X_k\right)}{W^{i+1}\cdot 2^{\frac{i(i+1)}{2}}}p^i\{2(iT_c + T_s)E[T_{Backoff}] + V_0\}(1-p)
$$

$$
+\sum_{i=m}^{\infty}\frac{\sum_{X_0=0}^{W-1}\cdots\sum_{X_i=0}^{W\cdot 2^i-1}\left(\sum_{k=0}^{i}X_k\right)}{W^{i+1}\cdot(2^m)^{i-m}\cdot 2^{\frac{m(m+1)}{2}}}p^i\{2(iT_c + T_s)E[T_{Backoff}] + V_0\}(1-p)
$$

$$
+\left(\sum_{i=0}^{m-1}\frac{\sum_{X_0=0}^{W-1}\cdots\sum_{X_i=0}^{W\cdot 2^i-1}1}{W^{i+1}\cdot 2^{\frac{i(i+1)}{2}}} + \sum_{i=m}^{\infty}\frac{\sum_{X_0=0}^{W-1}\cdots\sum_{X_i=0}^{W\cdot 2^i-1}1}{W^{i+1}\cdot(2^m)^{i-m}\cdot 2^{\frac{m(m+1)}{2}}}\right)(iT_c + T_s)^2p^i(1-p) \qquad (5.35)
$$

$$
= Var_1 + Var_2 + Var_3 + Var_4
$$

where V_0 is $\left[(P_s + P_c + P_\sigma)\sigma^2 + P_c\cdot 2T_c\cdot\sigma + P_s(\frac{W}{W-1})^2 2T_s\cdot\sigma + P_sT_s^{2}\frac{1+\frac{1}{W}}{(1-\frac{1}{W})^3} + P_cT_c^{2}\right] - (E[T_{Backoff}])^2$ The variance is composed of Var_1, Var_2, Var_3 and Var_4, which are expressed as follows (5.36) to (5.39)

$$
Var_1 = \left(\sum_{i=0}^{m-1}\frac{\sum_{X_0=0}^{W-1}\cdots\sum_{X_i=0}^{W\cdot 2^i-1}\left(\sum_{k=0}^{i}X_k\right)^2}{W^{i+1}\cdot 2^{\frac{i(i+1)}{2}}}p^i + \sum_{i=m}^{\infty}\frac{\sum_{X_0=0}^{W-1}\cdots\sum_{X_i=0}^{W\cdot 2^i-1}\left(\sum_{k=0}^{i}X_k\right)^2}{W^{i+1}\cdot(2^m)^{(i-m)}2^{\frac{m(m+1)}{2}}}p^i\right)
$$

$$
(1-p)\cdot(E[T_{Backoff}])^2
$$

where $\left(\sum_{k=0}^{i} X_k\right)^2 = \sum_{k=0}^{i} X_k{}^2 + 2\sum_{k=0}^{i-1}\sum_{r=k+1}^{i} X_k X_r$

$$
Var_1 = \Big\{ \sum_{i=0}^{m-1}\sum_{k=0}^{i} \frac{\sum_{X_0=0}^{W-1}\cdots\sum_{X_i=0}^{W\cdot2^i-1}(X_k)^2}{W^{i+1}\cdot 2^{\frac{i(i+1)}{2}}}p^i + \sum_{i=1}^{m-1}\sum_{k=0}^{i-1}\sum_{r=k+1}^{i}\frac{\sum_{X_0=0}^{W-1}\cdots\sum_{X_i=0}^{W\cdot2^i-1}2X_k X_r}{W^{i+1}\cdot 2^{\frac{i(i+1)}{2}}}p^i
$$

$$
+\sum_{i=m}^{\infty}\Big[\sum_{k=0}^{i}\frac{\sum_{X_0=0}^{W-1}\cdots\sum_{X_m=0}^{W\cdot2^m-1}\sum_{X_{m+1}=0}^{W\cdot2^m-1}\cdots\sum_{X_i=0}^{W\cdot2^m-1}(X_k)^2}{W^{i+1}\cdot(2^m)^{i-m}\cdot 2^{\frac{m(m+1)}{2}}}
$$

$$
+\sum_{k=0}^{i-1}\sum_{r=k+1}^{i}\frac{\sum_{X_0=0}^{W-1}\cdots\sum_{X_m=0}^{W\cdot2^m-1}\sum_{X_{m+1}=0}^{W\cdot2^m-1}\cdots\sum_{X_i=0}^{W\cdot2^m-1}2X_k X_r}{W^{i+1}\cdot(2^m)^{i-m}\cdot 2^{\frac{m(m+1)}{2}}}\Big] \Big\}p^i(1-p)\cdot E[T_{Backoff}]
$$

$$
= \Big\{ \sum_{i=0}^{m-1}\sum_{k=0}^{i}\frac{\sum_{X_k=0}^{W\cdot2^k-1}X_k{}^2}{W\cdot 2^k}p^i + 2\sum_{i=1}^{m-1}\sum_{k=0}^{i-1}\sum_{r=k+1}^{i}\frac{\sum_{X_k=0}^{W\cdot2^k-1}\sum_{X_r=0}^{W\cdot2^r-1}X_k X_r}{W\cdot2^k\cdot W\cdot2^r}p^i + \sum_{i=m}^{\infty}\Big[\sum_{k=0}^{m}\frac{\sum_{X_k=0}^{W\cdot2^k-1}X_k{}^2}{W\cdot2^k}
$$

$$
+(i-m)\frac{\sum_{X=0}^{W\cdot2^m-1}X^2}{W\cdot2^m} + \sum_{k=0}^{m-1}\sum_{r=k+1}^{m}\frac{\sum_{X_k=0}^{W\cdot2^k-1}\sum_{X_r=0}^{W\cdot2^r-1}2X_k X_r}{W\cdot2^k\cdot W\cdot2^r} + \sum_{k=0}^{m}\sum_{r=m+1}^{i}\frac{\sum_{X_k=0}^{W\cdot2^k-1}\sum_{X_r=0}^{W\cdot2^m-1}2X_k X_r}{W\cdot2^k\cdot W\cdot2^m}
$$

$$
+\sum_{k=m+1}^{i-1}\sum_{r=k+1}^{i}\frac{\sum_{X_k=0}^{W\cdot2^m-1}\sum_{X_r=0}^{W\cdot2^m-1}2X_k X_r}{W\cdot2^m\cdot W\cdot2^m}\Big]p^i \Big\}(1-p)E[T_{Backoff}]
$$

$$
= \Big\{ \sum_{i=0}^{m-1}\sum_{k=0}^{i}\frac{(W\cdot2^k-1)(W\cdot2^k)(W\cdot2^{k+1}-1)}{6\cdot(W\cdot2^k)}p^i + \sum_{i=1}^{m-1}\sum_{k=0}^{i-1}\sum_{r=k+1}^{i}\frac{\frac{W\cdot2^k(W\cdot2^k-1)}{2}\cdot\frac{W\cdot2^r(W\cdot2^r-1)}{2}}{W\cdot2^k\cdot W\cdot2^r}p^i
$$

$$
+\sum_{i=m}^{\infty}\frac{1}{6}\Big[2W^2\frac{4^{m+1}-1}{4-1}-3W\frac{2^{m+1}-1}{2-1}+(m+1)+(i-m)(W\cdot2^m)(W\cdot2^{m+1}-1)\Big]p^i
$$

$$
+\sum_{i=m}^{\infty}\Big[\sum_{k=0}^{m-1}\sum_{r=k+1}^{m}\frac{(W\cdot2^k-1)(W\cdot2^r-1)}{2}\Big]p^i + \sum_{i=m+1}^{\infty}\Big[\sum_{k=0}^{m}\sum_{r=m+1}^{i}\frac{(W\cdot2^k-1)(W\cdot2^m-1)}{2}\Big]p^i
$$

$$
+\sum_{i=m+2}^{\infty}\Big[\sum_{k=m+1}^{i-1}\sum_{r=k+1}^{i}\frac{(W\cdot2^m-1)^2}{2}\Big]p^i \Big\}(1-p)E[T_{Backoff}]
$$

$$
= \Big\{ \sum_{i=0}^{m-1}\frac{1}{6}\sum_{k=0}^{i}[W^2\cdot2^{2k+1}-W\cdot2^k-W\cdot2^{k+1}+1]p^i
$$

$$
+\sum_{i=1}^{m-1}\frac{1}{2}\sum_{k=0}^{i-1}\sum_{r=k+1}^{i}\Big[W^2\cdot2^k\cdot2^r-W\cdot2^k-W\cdot2^r+1\Big]p^i
$$

$$
+\sum_{i=m}^{\infty}\frac{1}{6}\Big\{2W^2\Big[\frac{4^{m+1}-1}{3}+4^m(i-m)\Big]-3W\big[2^{m+1}-1+2^m(i-m)\big]+(i+1)\Big\}p^i
$$

$$
+\sum_{i=m}^{\infty}\Big[\sum_{k=0}^{m-1}\frac{W\cdot2^k-1}{2}\big(W\cdot(2^{m+1}-2^{k+1})-(m-k)\big)\Big]p^i + \sum_{i=m}^{\infty}\sum_{k=0}^{m}(W\cdot2^k-1)
$$

$$
\cdot\frac{(W\cdot2^m-1)(i-m)}{2}p^i + \sum_{i=m+2}^{\infty}\sum_{k=m+1}^{i-1}\frac{(W\cdot2^m-1)^2}{2}(i-k)p^i \Big\}(1-p)E[T_{Backoff}] \qquad (5.36)
$$

$$Var_1 = \{ \quad \sum_{i=0}^{m-1} \frac{1}{6} \left[2W^2 \frac{4^{i+1}-1}{3} - 3W(2^{i+1}-1) + (i+1) \right] p^i$$

$$+ \sum_{i=0}^{m-1} \left[W^2(4^i - 2^i - \frac{4^i-1}{3}) + \frac{W \cdot i}{2} - W \cdot i \cdot 2^i + \frac{i(i+1)}{4} \right] p^i$$

$$+ \sum_{i=m}^{\infty} \left[W(2^{m+1}-1) - (m+1) \right] \frac{(W \cdot 2^m - 1)(i-m)}{2} p^i$$

$$+ \sum_{i=m+2}^{\infty} \frac{(W \cdot 2^m - 1)^2}{2} \left[\frac{(i-1-m)(i-m)}{2} \right] p^i \quad \} (1-p) E[T_{Backoff}]$$

$$= \{ \quad \frac{1}{6} \cdot \left[\quad 2W^2 \left(\frac{4\frac{1-(4p)^m}{1-4p} - \frac{1-p^m}{1-p}}{3} + \left(\frac{4^{m+1}-1}{3} \right) \frac{p^m}{1-p} + 2^{2m} \frac{p^{m+1}}{(1-p)^2} \right) \right.$$

$$\left. -3W \left(2\frac{1-(2p)^m}{1-2p} + 2^m \frac{p^{m+1}}{(1-p)^2} + (2^{m+1}p^m - 1)\frac{1}{1-p} \right) + \frac{1}{(1-p)^2} \quad \right]$$

$$+ W^2 \left(\frac{1-(4p)^m}{1-4p} 4p - \frac{1-(2p)^m}{1-2p} 2p \right) - \frac{W^2}{3} \left(\frac{1-(4p)^m}{1-4p} 4p - \frac{1-p^m}{1-p} p \right)$$

$$+ \frac{W}{2} \left[p \cdot \frac{1-(m+1)p^m + mp^{m+1}}{(1-p)^2} \right] - W \left[2p\frac{1-(m+1)(2p)^m + m(2p)^{m+1}}{(1-2p)^2} \right]$$

$$+ \frac{-m(m+1)p^{m+3} + 2m(m+2)p^{m+2} - (m+1)(m+2)p^{m+1} + 2p}{4(1-p)^3}$$

$$+ \left[W(2^{m+1}-1) - (m+1) \right] \frac{W \cdot 2^m - 1}{2} \frac{p^{m+1}}{(1-p)^2} + \frac{(W \cdot 2^m - 1)^2 p^{m+2}}{2(1-p)^3} \qquad (5.37)$$

$$+ \left[W^2(2^{2m} - 2^m - \frac{4^m-1}{3}) + \frac{W \cdot m}{2} - W \cdot m \cdot 2^m + \frac{m(m+1)}{4} \right] \frac{p^{m+1}}{1-p} \quad \} (1-p) E[T_{Backoff}]$$

The Var_2 from (5.35) can be expressed as

$$Var_2 = \sum_{i=0}^{m-1} \frac{\sum_{X_0=0}^{W-1} \cdots \sum_{X_i=0}^{W \cdot 2^i - 1} \left(\sum_{k=0}^{i} X_k \right)}{W^{i+1} \cdot 2^{\frac{i(i+1)}{2}}} p^i \left\{ 2(iT_c + T_s)E[T_{Backoff}] + V_0 \right\} (1-p)$$

$$= \sum_{i=0}^{m-1} \sum_{k=0}^{i} \frac{W \cdot 2^k - 1}{2} p^i \left\{ 2(iT_c + T_s)E[T_{Backoff}] + V_0 \right\} (1-p)$$

$$= \sum_{i=0}^{m-1} \left[\frac{W(2^{i+1} - 1) - (i+1)}{2} \right] \cdot i \cdot p^i \cdot (2T_c \cdot E[T_{Backoff}]) \cdot (1-p)$$

$$+ \sum_{i=0}^{m-1} \left[\frac{W(2^{i+1} - 1) - (i+1)}{2} \right] \cdot p^i \cdot (2T_s \cdot E[T_{Backoff}] + V_0) \cdot (1-p)$$

$$= \left\{ \frac{W}{2} \left(4p \cdot \frac{(m-1)(2p)^m - m(2p)^{m-1} + 1}{(1-2p)^2} - \frac{(m-1)p^{m+1} - mp^m + p}{(1-p)^2} \right) \right. \tag{5.38}$$

$$\left. - \frac{1}{2} \left(\frac{-m(m-1)p^{m+2} + 2(m+1)(m-1)p^{m+1} - (m+1)mp^m + 2p}{(1-p)^3} \right) \right\} (2T_c \cdot E[T_{Backoff}])(1-p)$$

$$+ \left\{ \frac{W}{2} \left(2\frac{1 - (2p)^m}{1 - 2p} - \frac{1 - p^m}{1 - p} \right) - \frac{1}{2} \left(\frac{1 - mp^{m-1} + (m-1)p^m}{(1-p)^2} \right) \right\} (2T_s \cdot E[T_{Backoff}] + V_0)(1-p)$$

The Var_3 from (5.35) can be expressed as

$$Var_3 = \sum_{i=m}^{\infty} \frac{\sum_{X_0=0}^{W-1} \cdots \sum_{X_i=0}^{W \cdot 2^i - 1} \left(\sum_{k=0}^{i} X_k \right)}{W^{i+1} \cdot (2^m)^{i-m} \cdot 2^{\frac{m(m+1)}{2}}} p^i \left\{ 2(iT_c + T_s)E[T_{Backoff}] + V_0 \right\} (1-p)$$

$$= \sum_{i=m}^{\infty} \left(\sum_{k=0}^{m} \frac{W \cdot 2^k - 1}{2} + \sum_{k=m+1}^{i} \frac{W \cdot 2^k - 1}{2} \right) p^i \left\{ 2(iT_c + T_s)E[T_{Backoff}] + V_0 \right\} (1-p)$$

$$= \sum_{i=m}^{\infty} \left[\frac{W(2^{m+1} - 1) - (m+1)}{2} + \frac{W \cdot 2^m - 1}{2}(i - m) \right] \cdot i \cdot p^i \cdot (2T_c \cdot E[T_{Backoff}]) \cdot (1-p)$$

$$+ \sum_{i=m}^{\infty} \left[\frac{W(2^{m+1} - 1) - (m+1)}{2} + \frac{W \cdot 2^m - 1}{2}(i - m) \right] \cdot p^i \cdot (2T_s \cdot E[T_{Backoff}] + V_0) \cdot (1-p)$$

$$= \left\{ \frac{W(2^{m+1} - 1) - (m+1)}{2} \cdot \frac{mp^m(1-p) + p^{m+1}}{(1-p)^2} + \frac{W \cdot 2^m - 1}{2} \cdot \right.$$

$$\left[\frac{m(m-1)p^{m+1} - 2(m+1)(m-1)p^m + (m+1)mp^{m-1}}{(1-p)^3} - (m+1)\frac{mp^m - (m-1)p^{m+1}}{(1-p)^2} \right] \right\} \cdot$$

$$(2T_c \cdot E[T_{Backoff}])(1-p) \tag{5.39}$$

$$+ \left[\frac{W(2^{m+1} - 1) - (m+1)}{2} \frac{p^m}{1-p} + \frac{W \cdot 2^m - 1}{2} \frac{p^{m+1}}{(1-p)^2} \right] (2T_s \cdot E[T_{Backoff}] + V_0)(1-p)$$

The Var_4 from (5.35) can be expressed as

$$
\left(\sum_{i=0}^{m-1} \frac{\sum_{X_0=0}^{W-1} \cdots \sum_{X_i=0}^{W \cdot 2^i - 1} 1}{W^{i+1} \cdot 2^{\frac{i(i+1)}{2}}} + \sum_{i=m}^{\infty} \frac{\sum_{X_0=0}^{W-1} \cdots \sum_{X_i=0}^{W \cdot 2^i - 1} 1}{W^{i+1} \cdot (2^m)^{i-m} \cdot 2^{\frac{m(m+1)}{2}}} \right) (iT_c + T_s)^2 p^i (1-p)
$$

$$
= \sum_{i=0}^{\infty} (iT_c + T_s)^2 p^i (1-p) = \sum_{i=0}^{\infty} (i^2 \cdot T_c^2 \cdot p^i + 2i \cdot T_c \cdot T_s \cdot p^i + T_s^2 \cdot p^i)(1-p)
$$

$$
= \left(T_c^2 p^2 \left(\frac{2}{(1-p)^3} + \frac{1}{p(1-p)^2} \right) + 2T_c T_s \frac{p}{(1-p)^2} + \frac{T_s^2}{1-p} \right)(1-p)
$$

$$
= T_c^2 \left(\frac{2p^2}{(1-p)^2} + \frac{p}{(1-p)} \right) + 2T_c T_s \frac{p}{1-p} + T_s^2 \tag{5.40}
$$

To compute variance, we combine (5.30),(5.37), (5.38), (5.39) and (5.40) and get

$$Variance = (var_1 + var_2 + var_3 + var_4) - (mean)^2$$

$$= \{ \ \frac{1}{6} \cdot [\ 2W^2 \left(\frac{4\frac{1-(4p)^m}{1-4p} - \frac{1-p^m}{1-p}}{3} + \left(\frac{4^{m+1}-1}{3} \right) \frac{p^m}{1-p} + 2^{2m} \frac{p^{m+1}}{(1-p)^2} \right)$$

$$-3W \left(2\frac{1-(2p)^m}{1-2p} + 2^m \frac{p^{m+1}}{(1-p)^2} + (2^{m+1}p^m - 1)\frac{1}{1-p} \right) + \frac{1}{(1-p)^2} \ ]$$

$$+W^2 \left(\frac{1-(4p)^m}{1-4p}4p - \frac{1-(2p)^m}{1-2p}2p \right) - \frac{W^2}{3} \left(\frac{1-(4p)^m}{1-4p}4p - \frac{1-p^m}{1-p}p \right)$$

$$+\frac{W}{2} \left[p \cdot \frac{1-(m+1)p^m + mp^{m+1}}{(1-p)^2} \right] - W \left[2p\frac{1-(m+1)(2p)^m + m(2p)^{m+1}}{(1-2p)^2} \right]$$

$$+\frac{-m(m+1)p^{m+3} + 2m(m+2)p^{m+2} - (m+1)(m+2)p^{m+1} + 2p}{4(1-p)^3}$$

$$+ \left[W(2^{m+1}-1) - (m+1) \right] \frac{W \cdot 2^m - 1}{2} \frac{p^{m+1}}{(1-p)^2} + \frac{(W \cdot 2^m - 1)^2 p^{m+2}}{2(1-p)^3}$$

$$+ \left[W^2(2^{2m} - 2^m - \frac{4^m - 1}{3}) + \frac{W \cdot m}{2} - W \cdot m \cdot 2^m + \frac{m(m+1)}{4} \right] \frac{p^{m+1}}{1-p} \ \}(1-p)E[T_{Backoff}]$$

$$+\{ \ \frac{W}{2} \left(4p \cdot \frac{(m-1)(2p)^m - m(2p)^{m-1} + 1}{(1-2p)^2} - \frac{(m-1)p^{m+1} - mp^m + p}{(1-p)^2} \right)$$

$$-\frac{1}{2} \left(\frac{-m(m-1)p^{m+2} + 2(m+1)(m-1)p^{m+1} - (m+1)mp^m + 2p}{(1-p)^3} \right) \ \}(2T_c \cdot E[T_{Backoff}])(1-p)$$

$$+\left\{ \frac{W}{2} \left(2\frac{1-(2p)^m}{1-2p} - \frac{1-p^m}{1-p} \right) - \frac{1}{2} \left(\frac{1 - mp^{m-1} + (m-1)p^m}{(1-p)^2} \right) \right\} (2T_s \cdot E[T_{Backoff}] + V_0)(1-p)$$

$$+\{ \ \frac{W(2^{m+1}-1) - (m+1)}{2} \cdot \frac{mp^m(1-p) + p^{m+1}}{(1-p)^2} + \frac{W \cdot 2^m - 1}{2} \cdot$$

$$[\frac{m(m-1)p^{m+1} - 2(m+1)(m-1)p^m + (m+1)mp^{m-1}}{(1-p)^3} - (m+1)\frac{mp^m - (m-1)p^{m+1}}{(1-p)^2} \ ] \ \} \cdot$$

$$(2T_c \cdot E[T_{Backoff}])(1-p) \hfill (5.41)$$

$$+\left[\frac{W(2^{m+1}-1) - (m+1)}{2} \frac{p^m}{1-p} + \frac{W \cdot 2^m - 1}{2} \frac{p^{m+1}}{(1-p)^2} \right] (2T_s \cdot E[T_{Backoff}] + V_0)(1-p)$$

$$+T_c{}^2 \left(\frac{2p^2}{(1-p)^2} + \frac{p}{(1-p)} \right) + 2T_cT_s\frac{p}{1-p} + T_s{}^2$$

$$-\{ \ \frac{1}{2} \left\{ W \left(2\frac{1-(2p)^m}{1-2p} - \frac{1-p^m}{1-p} \right) - \frac{p\left[-mp^{m-1}(1-p) + (1-p^m)\right]}{(1-p)^2} - \frac{1-p^m}{1-p} \right\} (1-p)$$

$$\cdot E[T_{Backoff}] + \left[\frac{W(2^{m+1}-1) - (m+1)}{2} + \frac{(W \cdot 2^m - 1)p}{2(1-p)} \right] p^m E[T_{Backoff}] + \frac{p}{1-p}T_c + T_s \ \}^2$$

5.1.4 Simulation result

In this thesis, we use CSMA/CA with RTS/CTS scheme to simulate WiFi throughput for IDCI user. This IDCI user behaves like other WiFi users, it will get random variable from contention window first, and then execute the backoff procedure. If anyone else counter is equal to zero, all of WiFi users must fix backoff timer counter themselves until channel become idle again. If the collision occurs, these WiFi users who transmit failed will increase their contention window unless it has been maximum window size. When the IDCI user transmits successfully, we will accumulate the packet size until the end of total simulation time and we use total bits which IDCI user transmits successfully divides by total simulation time to get WiFi average throughput from simulation and compare simulation with mathematic. We also gather data from a packet transmission interval by simulation and compare the statistic from simulation and from mathematic.

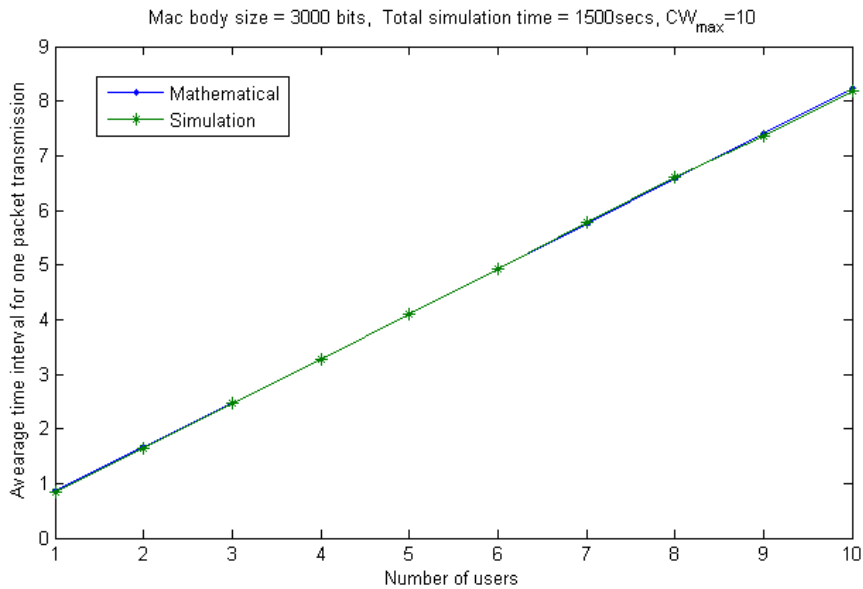Let's compare the mean between the theoretical result from (5.30) and the simulation one:

Figure 5.10: Mean of transmission time for a packet with different number of users, CW_{max}=10.
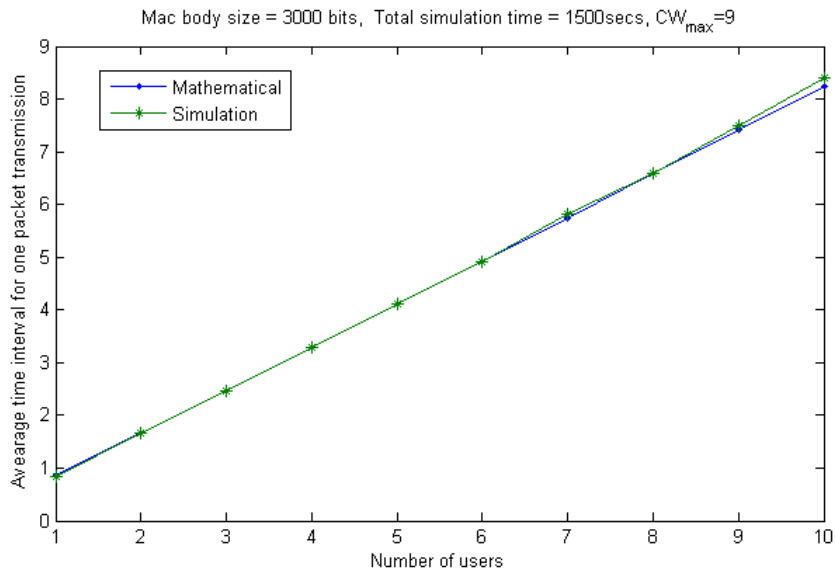
Figure 5.11: Mean of transmission time for a packet with different number of users, CW_{max}=9.
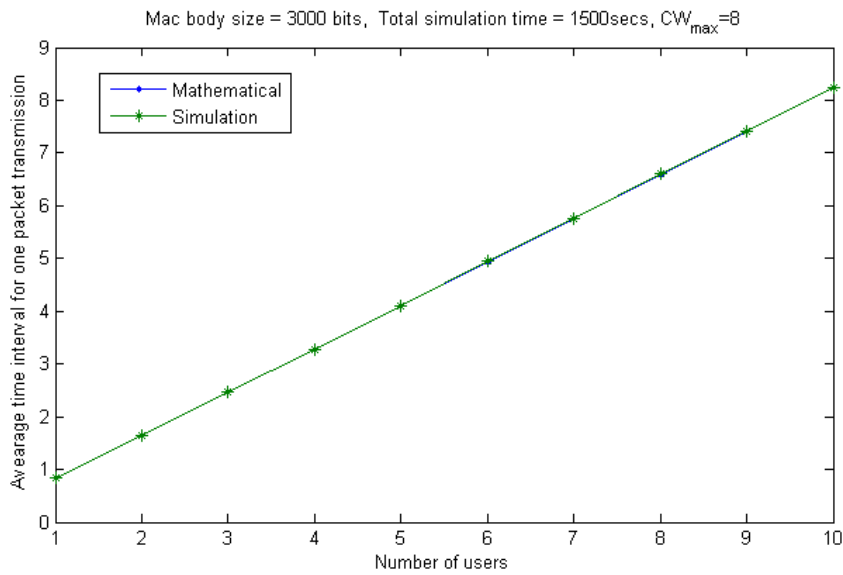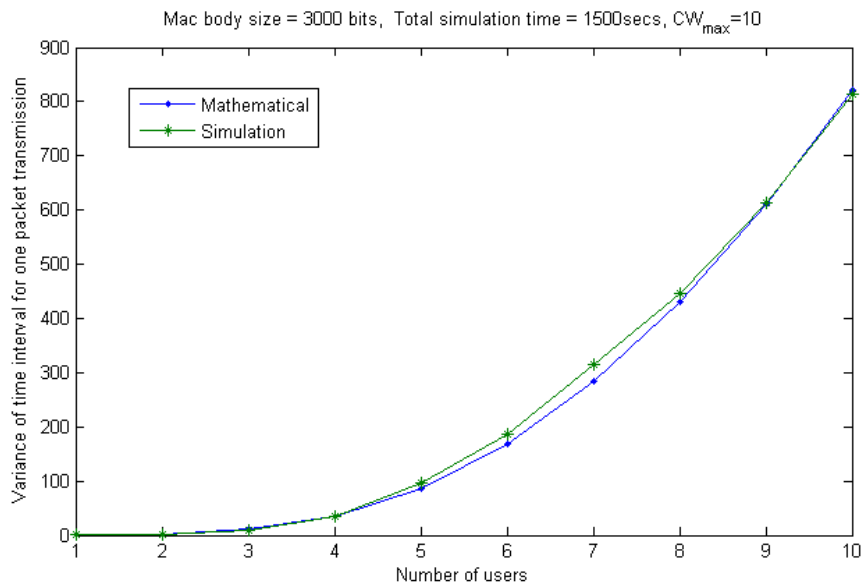

Figure 5.12: Mean of transmission time for a packet with different number of users, CW_{max}=8.

In Fig. 5.10, 5.11 and 5.12, we show the mean comparison in different maximum contention window size, $W2^{CW_{max}}$. These figure describe that mean of transmission time for a packet with different number of users, if we increase the number of users then the mean will also increase. The more number of users will induces higher probability of collision, so the time for a user to transmit a packet is also larger. We can discover that theoretical results are close to simulation results.

Let's compare the variance between the theoretical result from (5.41) and the simulation one:

Figure 5.13: Variance of transmission time for a packet with different number of users, CW_{max}=10.

In Fig. 5.13, 5.14 and 5.15, we show the mean comparison in different maximum contention window size, $W2^{CW_{max}}$. These figure describe that variance of transmission time for a packet with different number of users, the variance will increase more obviously than mean when the number of users is increasing especially in larger contention window size. If the contention window size is large, the WiFi user transmission time for a packet will also be large. Although the collision probability will descend when contention window size is large, the value contribute to variance is still huge so the figure in higher
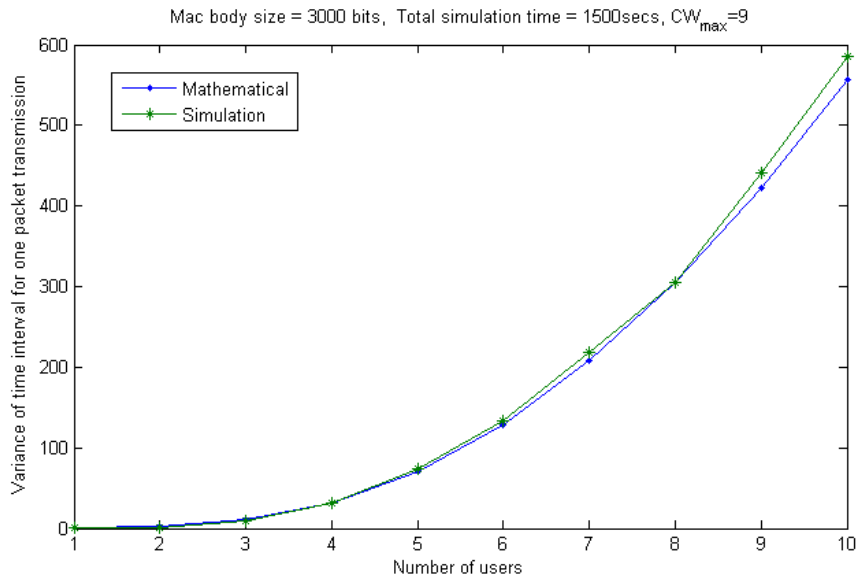
Figure 5.14: Variance of transmission time for a packet with different number of users, CW_{max}=9.
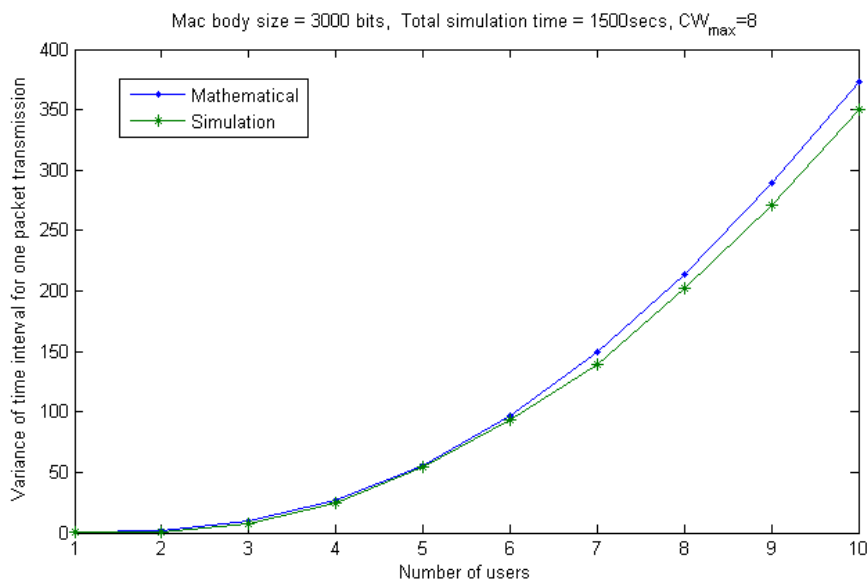

Figure 5.15: Variance of transmission time for a packet with different number of users, CW_{max}=8.

CW_{max} has higher variance value. We can discover that theoretical results are close to simulation results.

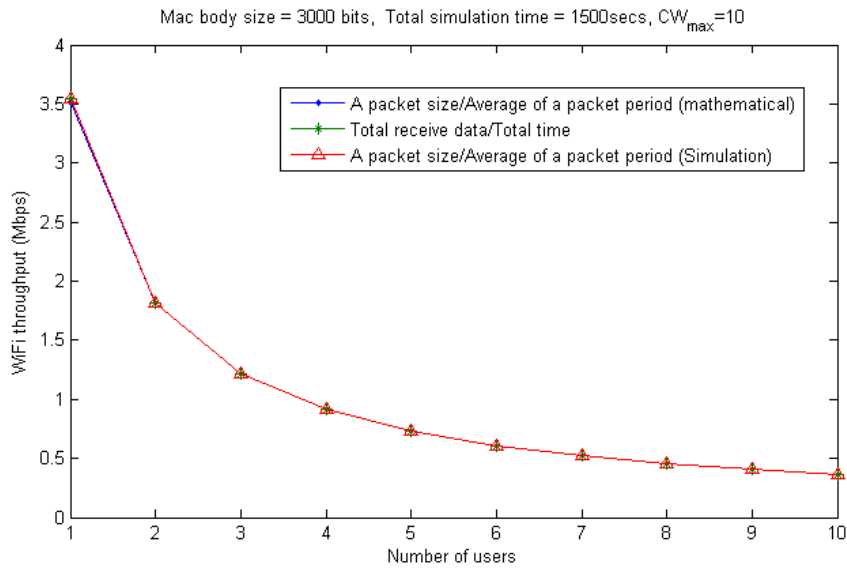Let's compare the throughput between the theoretical result and the simulation one:

Figure 5.16: WiFi throughput for derivation and simulation, CW_{max}=10.

In Fig. 5.16, 5.17 and 5.18, we show the WiFi throughput compare between theoretical results and the simulation results. The WiFi throughput will decrease when the number of users increases because more of users will compete with the channel resource. We compare with three cases, one is the mathematical derivation which is computed by one packet size divide into average transmission time for a packet, and another is the simulation way which accumulates packet size from all of transmission and then divide into total simulation time, the last one is like mathematical derivation but its average transmission time is computed by simulation. We can discover that theoretical results are close to simulation results.
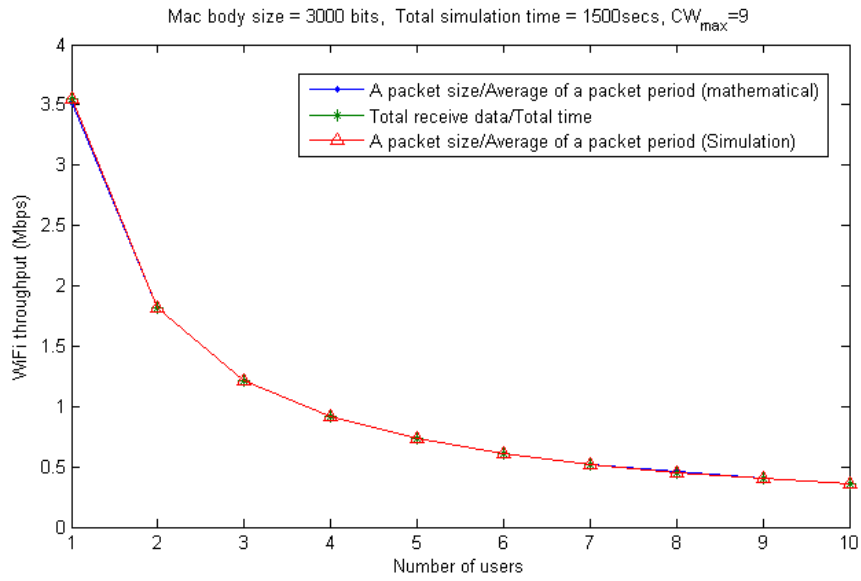
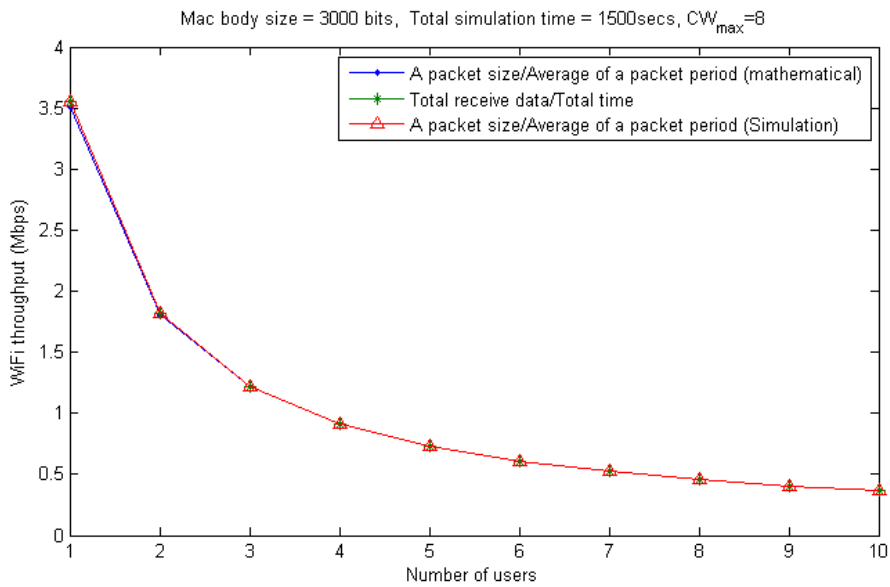Figure 5.17: WiFi throughput for derivation and simulation, CW_{max}=9.

Figure 5.18: WiFi throughput for derivation and simulation, CW_{max}=8.

5.2 WiFi throughput analysis with DRX

When DRX scheme is activated, the IDC user will deny WiFi transmission on DRX On-duration and it can only be allowed to transmit WiFi signal on DRX Off-duration. We assume that most of time IDC user will transmit packet with fixed packet size(3000bits) to AP, but the transmitted packet size will become smaller when the start time for WiFi transmission is close to next DRX On-duration because WiFi can't transmit data at DRX On-duration. We assume that WiFi will transmit a packet which is exact in front of the next DRX On-duration if the IDC user contends channel successfully and we use the remaining time for WiFi of IDC user to get maximum packet size it can transmit during this period. We assume that if WiFi backoff timer counter is not equal to zero when IDC user operates on DRX On-duration, WiFi will fix the backoff timer until the situation becomes DRX Off-duration. This is because that IDC user needs to distinguish the channel busy comes from LTE signal transmission or other WiFi user transmission, it will increase complexity of process. The another reason is that if WiFi keeps running backoff timer, it will increase probability of collision because the backoff timer always go to zero when DRX On-duration is large enough, and WiFi will transmit signal immediately once after the end of DRX On-duration no matter whether the network is congestion or not, it is not appropriate to WiFi network performance.
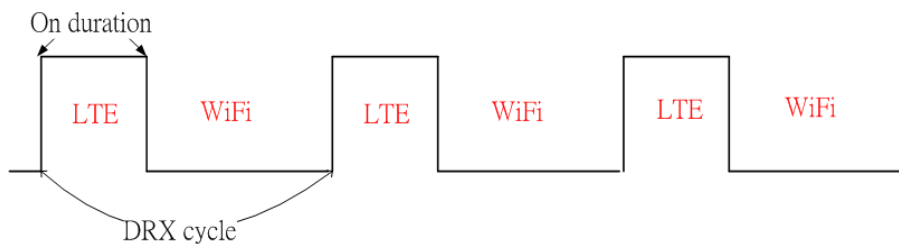

Figure 5.19: Switch between LTE and WiFi on DRX scheme.

Because the WiFi can only use on DRX Off-duration as shown in Fig. 5.19, the WiFi
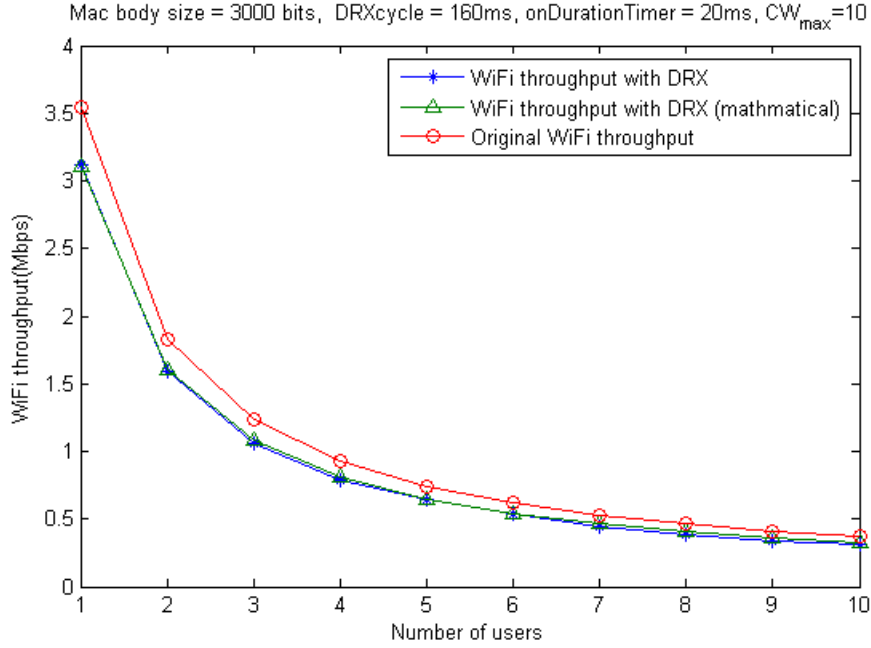
Figure 5.20: WiFi throughput with DRX for derivation and simulation, T_{on}=20ms.

throughput with DRX $T_{\text{WiFi}}^{\text{DRX}}$ can be (5.42)

$$T_{\text{WiFi}}^{\text{DRX}} = \frac{E[P]}{T_{\text{WiFi}}^{\text{theoretical}}} \cdot \frac{T_{\text{DRX}} - T_{\text{on}}}{T_{\text{DRX}}} \tag{5.42}$$

where $E[P]$ is constant packet size(3000bits), $T_{\text{WiFi}}^{\text{theoretical}}$ is transmission time interval of a packet from theoretical derivation (5.30). T_{DRX} is time interval of DRX cycle which we set 160ms in below simulations and T_{on} is time interval of DRX On-duration. We will simulate WiFi throughput for different T_{on} as follows

We show the simulation result for different DRX parameters from Fig. 5.20 to Fig. 5.24. The theoretical simulation result from (5.42) will close to real simulation result for each DRX cases from Fig. 5.20 to Fig. 5.24. And we combine the figures from Fig. 5.20 to Fig. 5.24 together to obtain Fig. 5.25.

Fig. 5.25 compares theoretical WiFi throughput with real WiFi throughput for different DRX parameters. We can observe that the WiFi throughput will increase when the DRX on duration decreases. The reason is that when the DRX on duration decreases
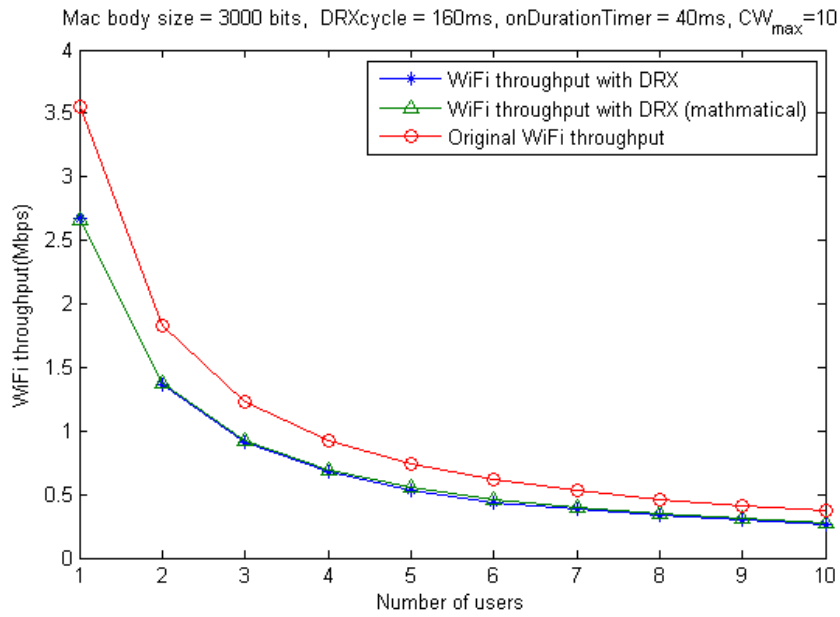
Figure 5.21: WiFi throughput with DRX for derivation and simulation, T_{on}=40ms.
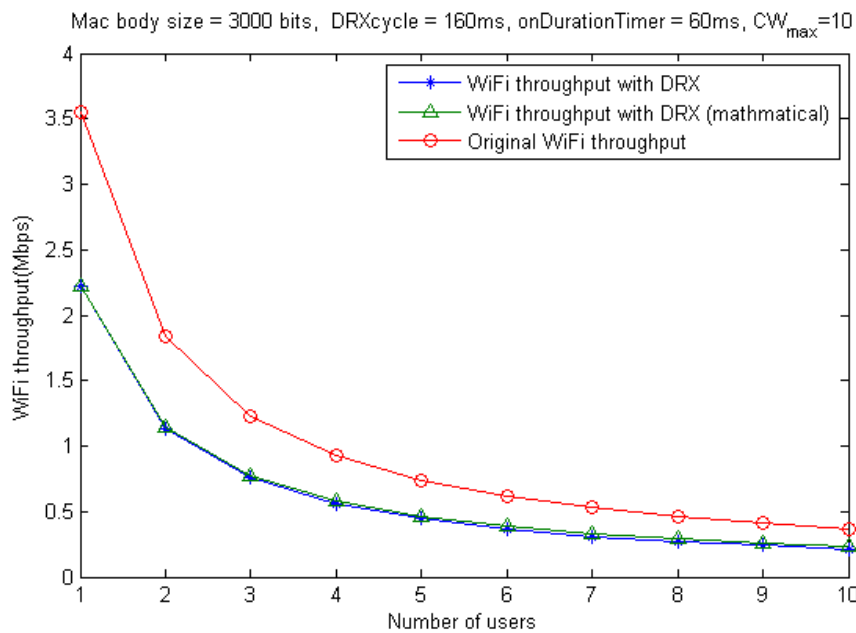

Figure 5.22: WiFi throughput with DRX for derivation and simulation, T_{on}=60ms.
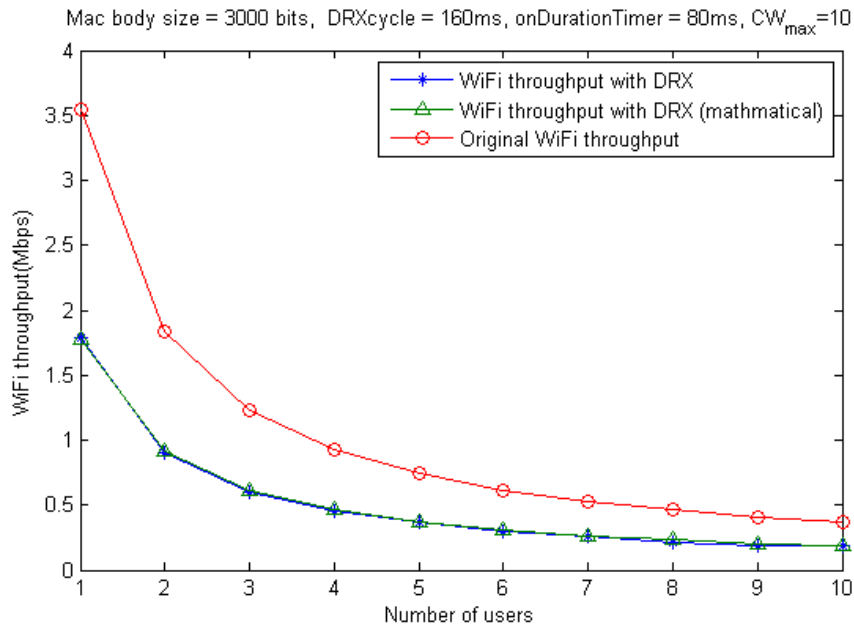
97

Figure 5.23: WiFi throughput with DRX for derivation and simulation, T_{on}=80ms.
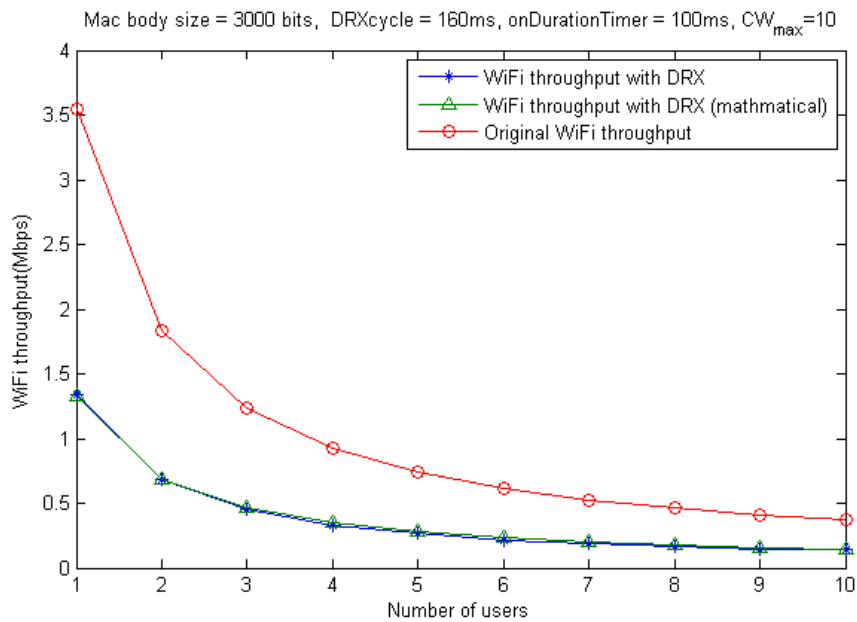

Figure 5.24: WiFi throughput with DRX for derivation and simulation, T_{on}=100ms.
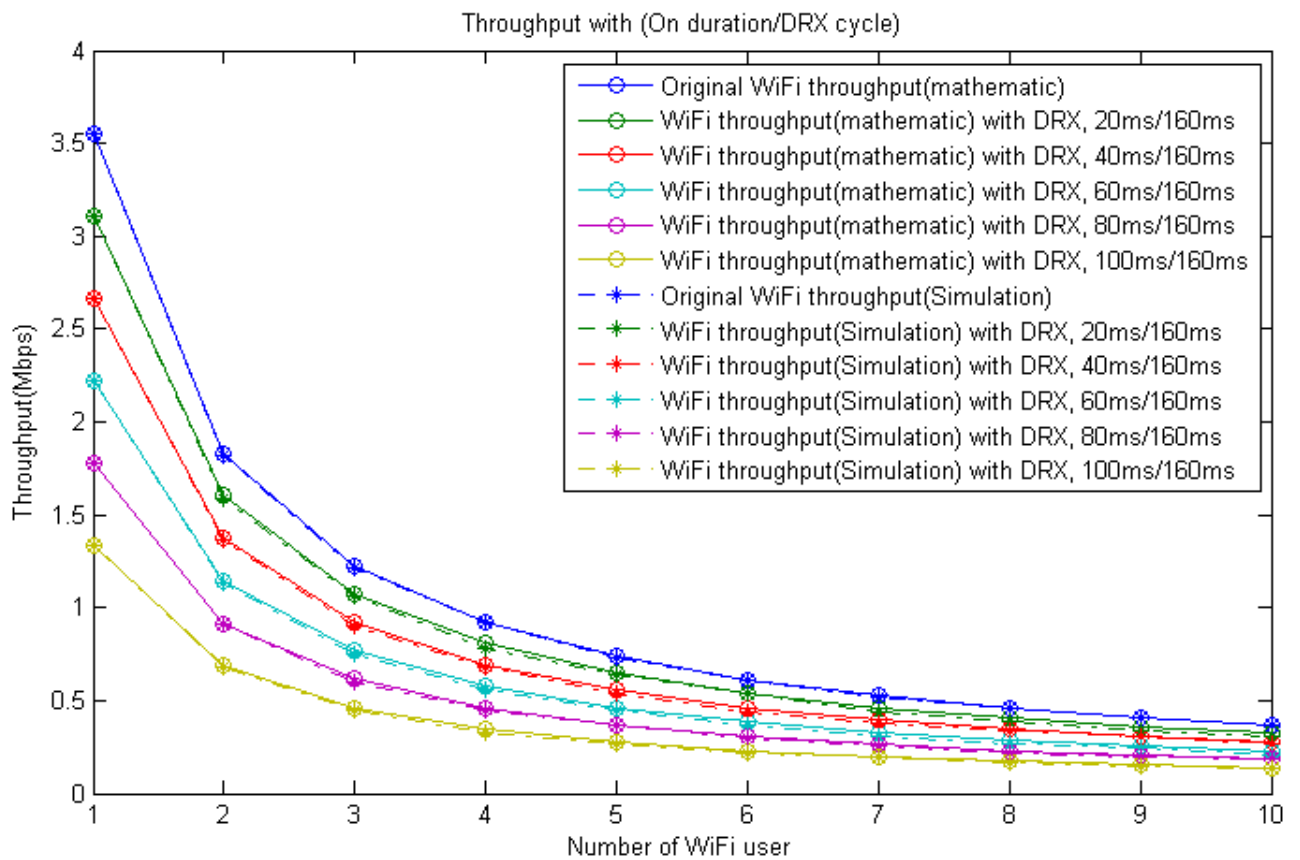
Figure 5.25: WiFi throughput with different DRX parameters.

the time resource for WiFi will increase. We can discover that theoretical results are close to simulation results. The ratio between remaining time and DRX cycle period is also equal to the ratio between WiFi throughput with DRX and WiFi throughput without DRX.

5.3 LTE throughput analysis

5.3.1 Introduction of scheduling scheme

There are many scheduling schemes for eNB to allocate resources to user based on considering to maximize the total network throughput and to remain the minimal requirement of each user. We adopt the scheduling scheme from [15], which called frequency domain proportional fair (FD-PF). Because the based unit of the resource is a resource block (RB) for each user in LTE system, FD-PF will decide one of these users to use this RB to magnify system throughput as possible as it can do and remain the Quality of Service (QoS) of each users. The average throughput $T_k(t)$ it used from [15] is computed after all the allocation of RBs are finished in this subframe, and it may induce all RBs in this subframe will allocate the IDC user once the DRX turn Off-duration to On-duration because average throughput is small after the DRX Off-duration and the allocated RBs can't refresh the average throughput immediately. So we will use $T_{k,j}(t)$ to refresh the average throughput once the RB is allocated to user k. $T_{k,j}(t)$ means average throughput at j RB from time frame 1 to time frame t, it can be expressed as

$$T_{k,j}(t) = \begin{cases} (1 - \frac{1}{t_c \cdot N_{RB}})T_{k,j}(t-1) + \frac{1}{t_c \cdot N_{RB}}R_{k,j}(t) & \text{for} \quad k \text{ is served at time } t \text{ and } j\text{-th RB} \\ (1 - \frac{1}{t_c \cdot N_{RB}})T_{k,j}(t-1) & \text{for} \quad otherwise \end{cases} \tag{5.43}$$

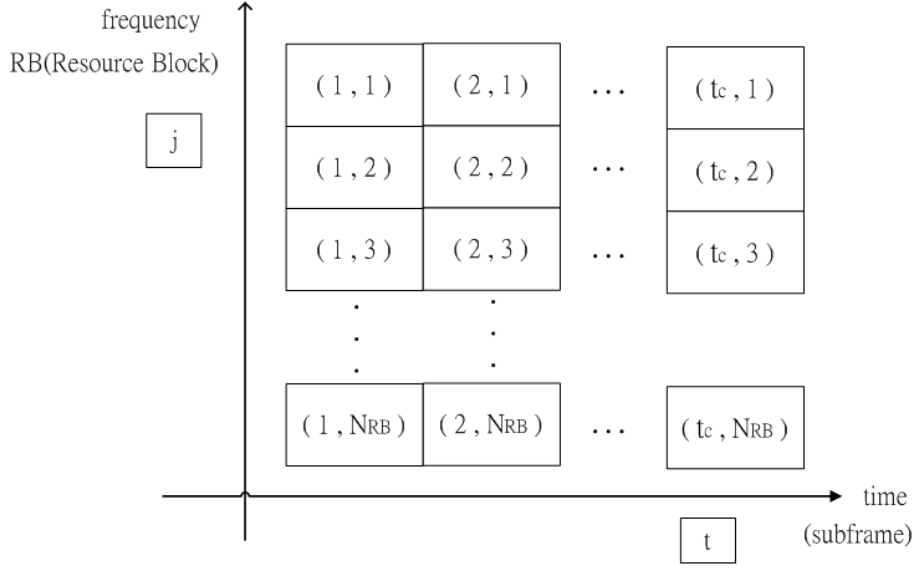The $R_{k,j}(t)$ is current provided throughput, it can be expressed as

Figure 5.26: WiFi throughput with different DRX parameters.

$$R_{k,j}(t) = k = \arg_n \max \left(\frac{R_{n,j}(t)}{T_{n,j}(t)} \right) \tag{5.44}$$

k is the user who get the j-RB at subframe t

and $T_{k,j}(t)$ is average throughput from 1 RB, 1 subframe to j RB, t subframe in k user. This scheduling scheme will allocate RB to the user which current throughput is better than average throughput to maximize total system throughput when average throughput of each users are similar and allocate RB to the user which average throughput is lower than other users average throughput to equalize all users throughput when current throughput of each users are similar. The resource can be expressed as Fig. 5.26, t_c is total number of subframes, N_{RB} is total number of RBs in frequency domain.

When the time is in the end t_c, we derive from average throughput per RB, $T_{k,j}(t_c)$ to average throughput $T_k(t_c)$ by (5.45)

$$T_k(t_c) = N_{RB} \cdot T_{k,j}(t_c) \tag{5.45}$$

$T_k(t_c)$ is final average throughput for each k user.

101

and the scheduling procedure will be

$$\text{for loop of subframe index from 1 to } t_c, \text{ t}$$

$$\text{for loop of frequency index 1 to } N_{RB}, \text{ j}$$

$$\text{for loop of user index 1 to } N_{user}, \text{ n}$$

$$k = \arg_n \max \left(\frac{R_{n,j}(t)}{T_{n,j}(t)} \right)$$

$$\text{if n is equal to k}$$

$$(1 - \frac{1}{t_c \cdot N_{RB}}) T_{k,j}(t-1) + \frac{1}{t_c \cdot N_{RB}} R_{k,j}(t)$$

$$\text{else}$$

$$(1 - \frac{1}{t_c \cdot N_{RB}}) T_{k,j}(t-1)$$

$$\text{end if}$$

$$\text{end for loop of user index}$$

$$\text{end for loop of frequency index}$$

$$\text{end for loop of subframe index} \tag{5.46}$$

5.3.2 Scenario

We assume that the Base station (BS) is separated by 3 sectors, BS will beamform the data into one sector and the LTE users will be uniform distribution in this sector. We consider three cases in Fig. 5.27 as follows

We consider the scenario of Macro Urban, and the BS cover range will be 1200 meters. The number of users is 20. As can be seen from Fig. 5.27, the IDC user is red square point, the blue star points are WiFi users distributed in the sector and one of them is IDC user. and the distance between IDC user and BS is respective to be 200, 800 and 1100 meters for case 1, case 2 and case 3.

The probability of distance between LTE user located from BS shows in Fig. 5.28.
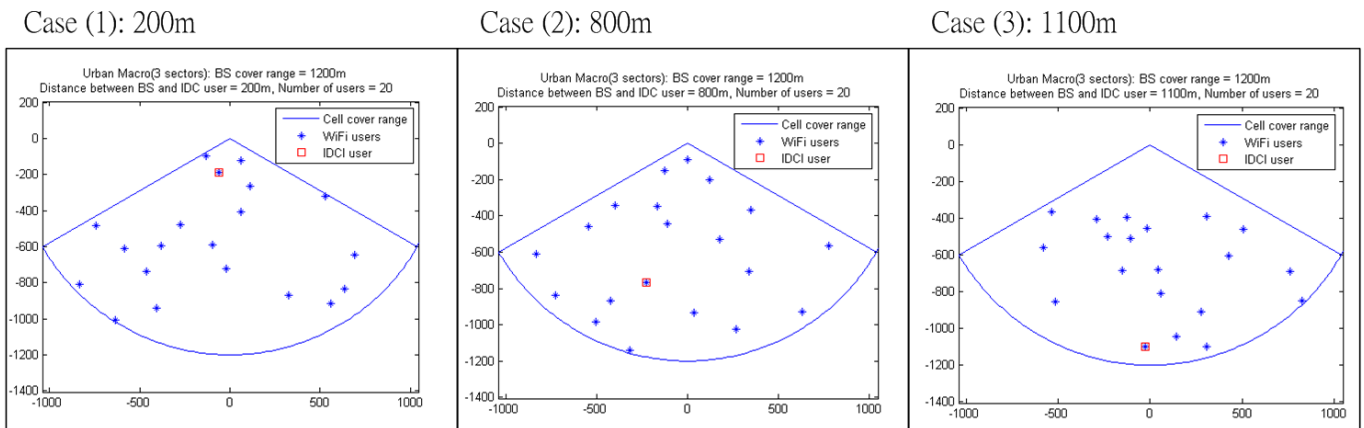
Figure 5.27: Cases for different distance between BS and IDC user.
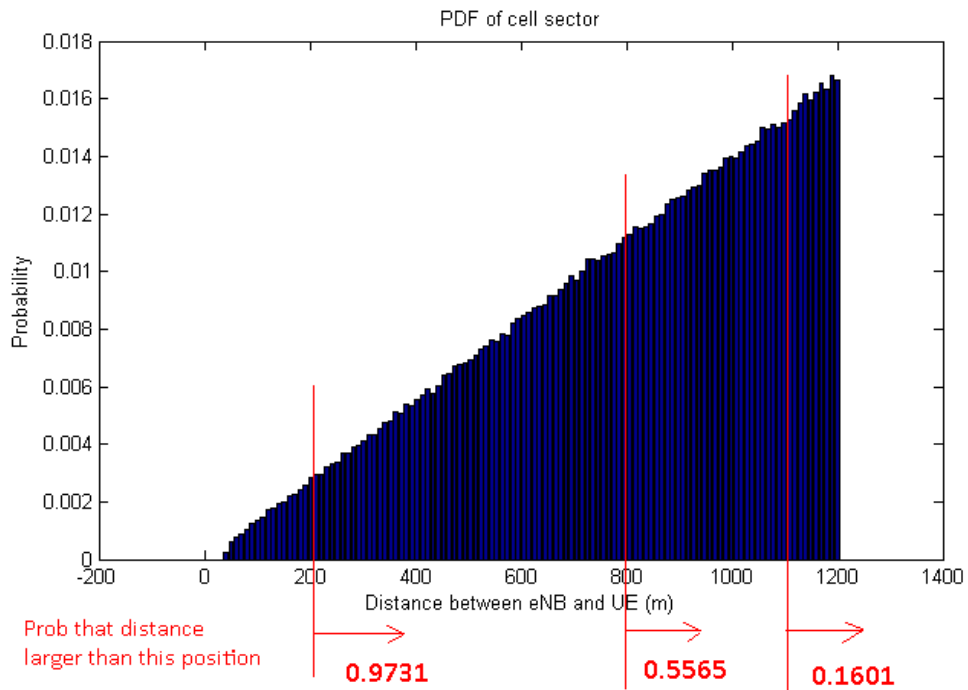

Figure 5.28: The probability density function with different distance when users appear.
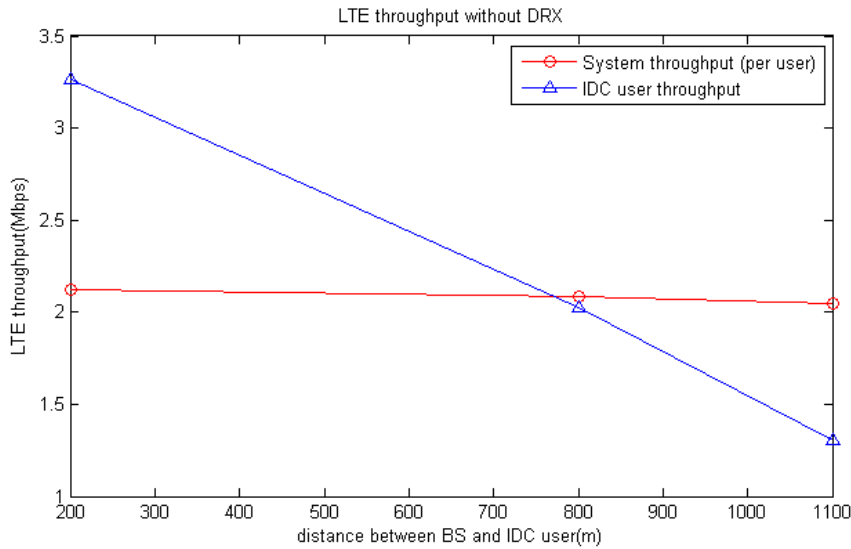
103

Figure 5.29: Compare LTE throughput with DRX and without DRX in different distance of BS.

The percentage for users which distance are larger than 200 meters is 97.31, and larger than 800 meters is 55.65 and larger than 200 meters is 16.01. The distance will affect the SNR, if the LTE user is close to BS the SNR will be very well and the LTE throughput will also be very well. This phenomenon will display on simulation as following section 5.3.3.

5.3.3 Simulation result for LTE throughput

We assume that the bandwidth of BS is 20MHz, it include 100 RBs, the number of users N_{user} is 20. One of users is IDC user which will active DRX scheme to avoid interference from WiFi, and the BS will allocate RBs to IDC user only it operates on On-duration of DRX. Other LTE users don't be limited by DRX which means they can always be scheduled by BS. We use the FD-PF scheduling scheme in section 5.3.1 to get the result as follows

Fig. 5.29 compares IDC user throughput with system throughput in distance 200m,
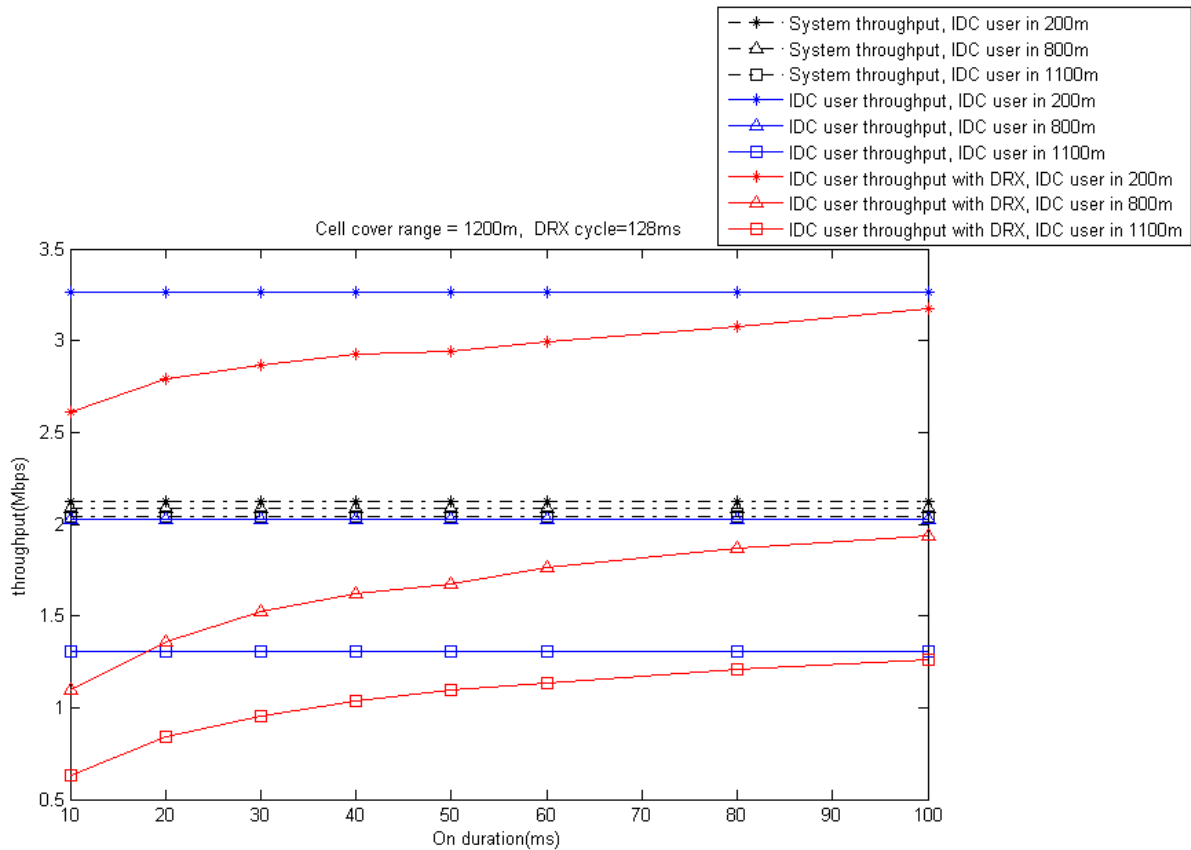
Figure 5.30: Compare LTE throughput with DRX and without DRX on DRX cycle 128ms.

800m and 1100m. It makes sense that it shows that the IDC user throughput will be larger when its location is close to BS and vice versa. The system throughput also consider the IDC user throughput so it will degrade slightly when IDC user distance become more far.

We show the LTE throughput for different DRX parameters from Fig. 5.30 to Fig. 5.33, and DRX cycle is respective to be 128ms, 160ms, 256ms and 320ms. On duration is 10ms, 20ms, 30ms, 40ms, 50ms, 60ms, 80ms and 100ms for each figure. We can observe that IDC user throughput will degrade when DRX is active, and IDC user throughput with DRX will increase not linearly from On-duration because the scheduling scheme that the BS will keep allocate RB to IDC user on the begin of On-duration but other
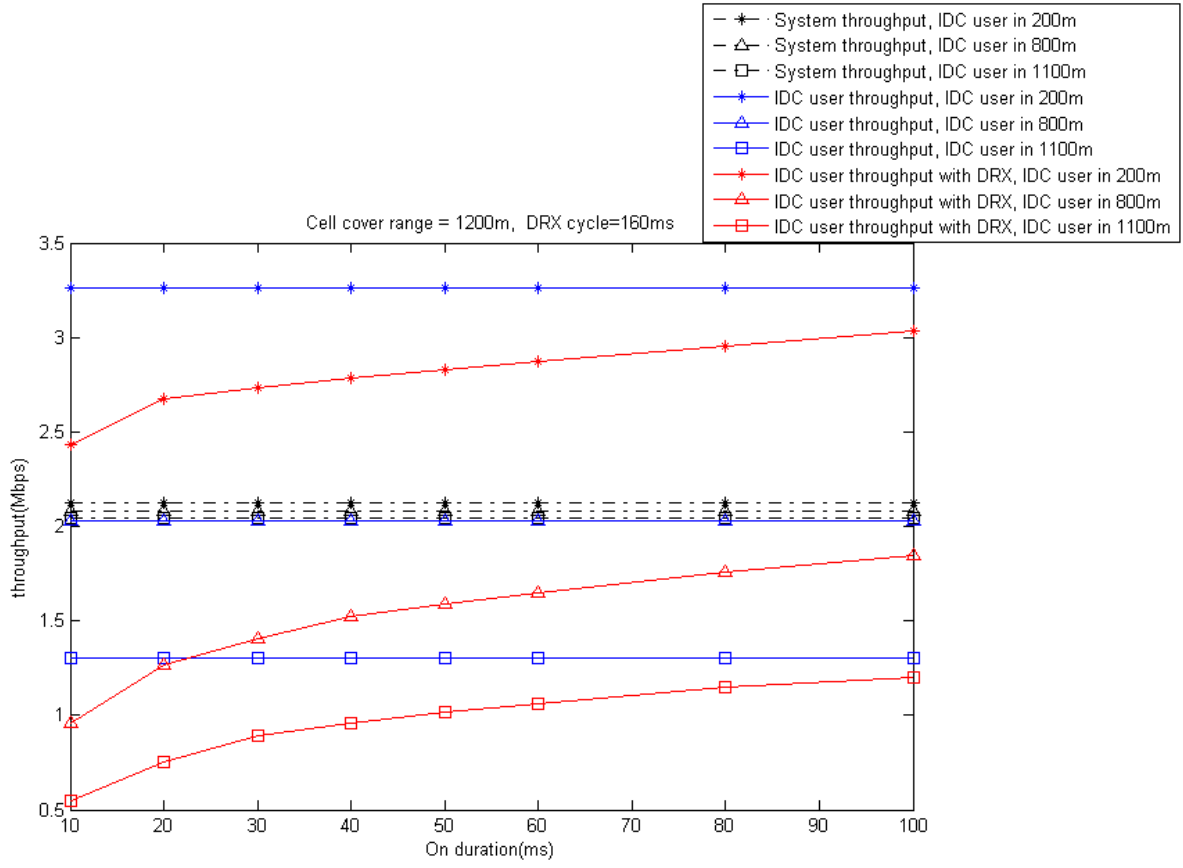
Figure 5.31: Compare LTE throughput with DRX and without DRX on DRX cycle 160ms.

users average throughput $T_{n,j}(t)$ will degrade and soon after BS will allocate RBs to other users following equation (5.44). Compare with different figures, the difference between IDC user with DRX and IDC user without DRX will be larger when DRX cycle is larger because it means the LTE usable time ratio from DRX is smaller.

We compare all different DRX parameters in one figure for different distance 200m, 800m and 1100m from Fig. 5.34 to Fig. 5.36. We can see the throughput will increase when On-duration increases in different DRX cycles, the system throughput will almost fixed in different DRX parameters. In Fig. 5.34, the IDC user throughput will be larger than system throughput mostly even if DRX scheme is on because the IDC user is close to BS. If we compare IDC user throughput with system throughput in Fig. 5.35 and
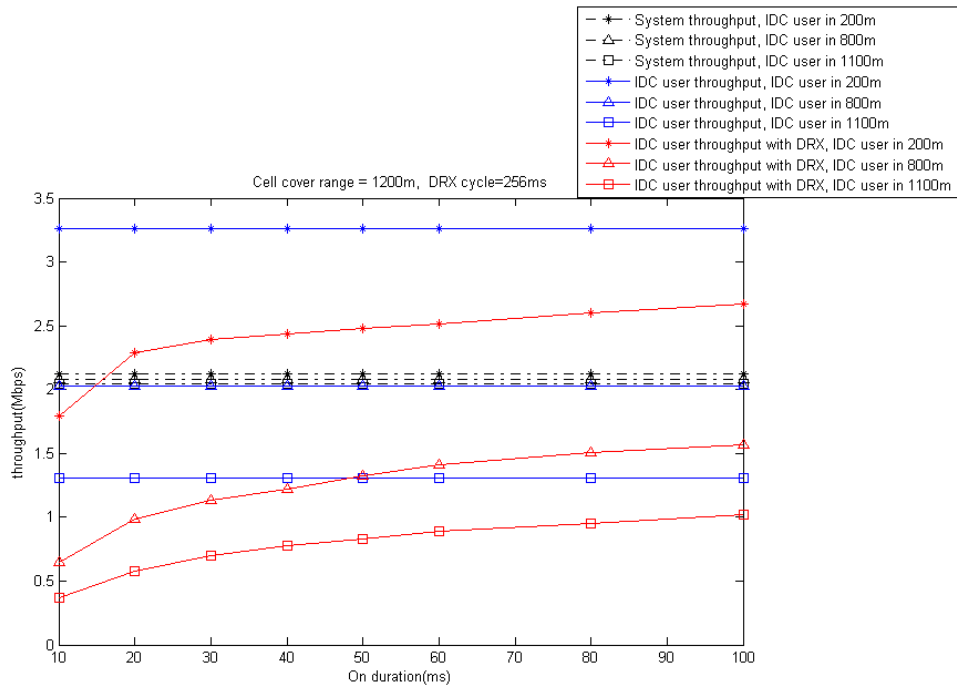
106

Figure 5.32: Compare LTE throughput with DRX and without DRX on DRX cycle 256ms.
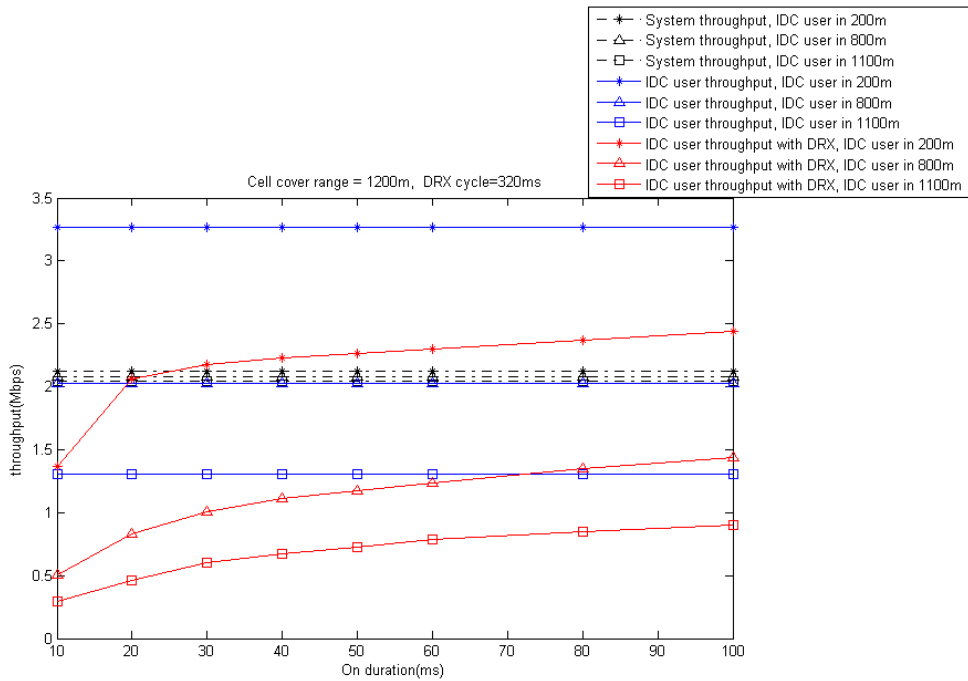

Figure 5.33: Compare LTE throughput with DRX and without DRX on DRX cycle 320ms.
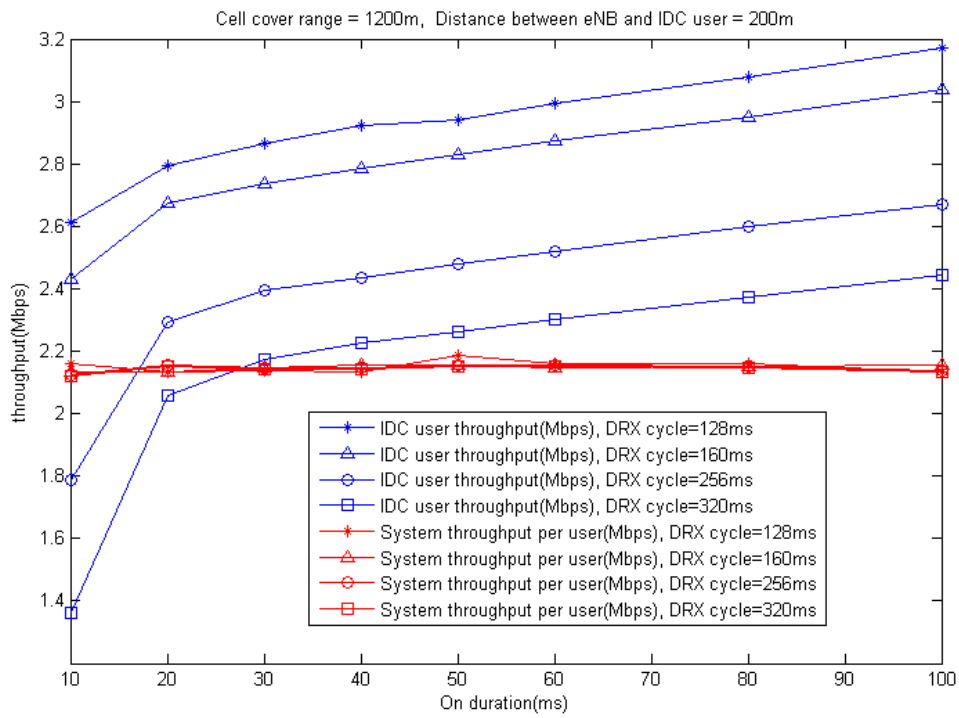
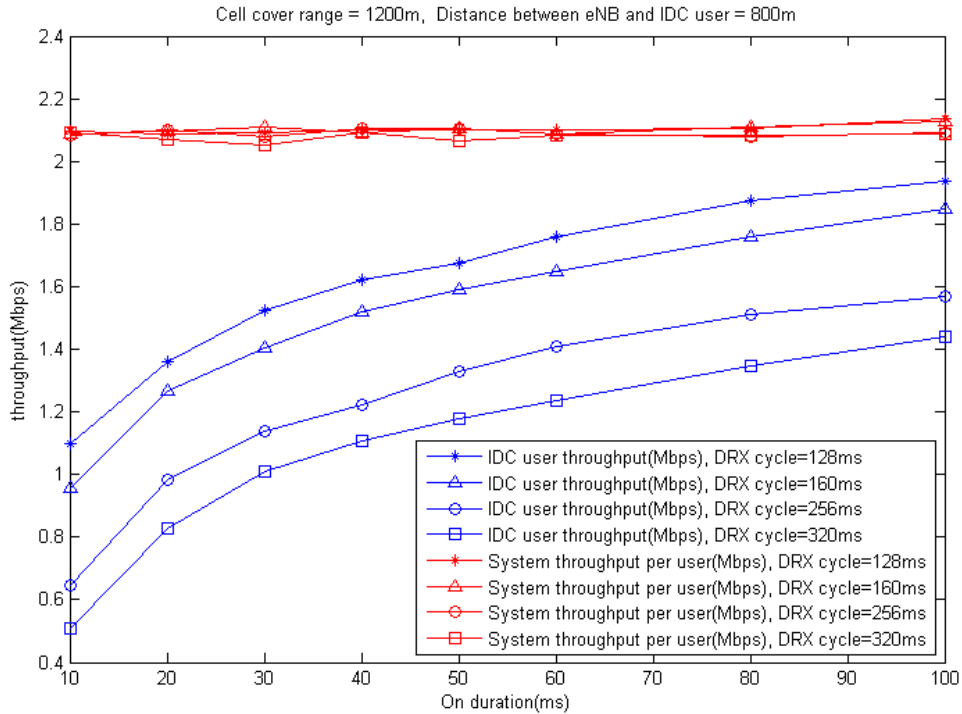Figure 5.34: On duration vs. throughput for different DRX cycle on distance 200m.

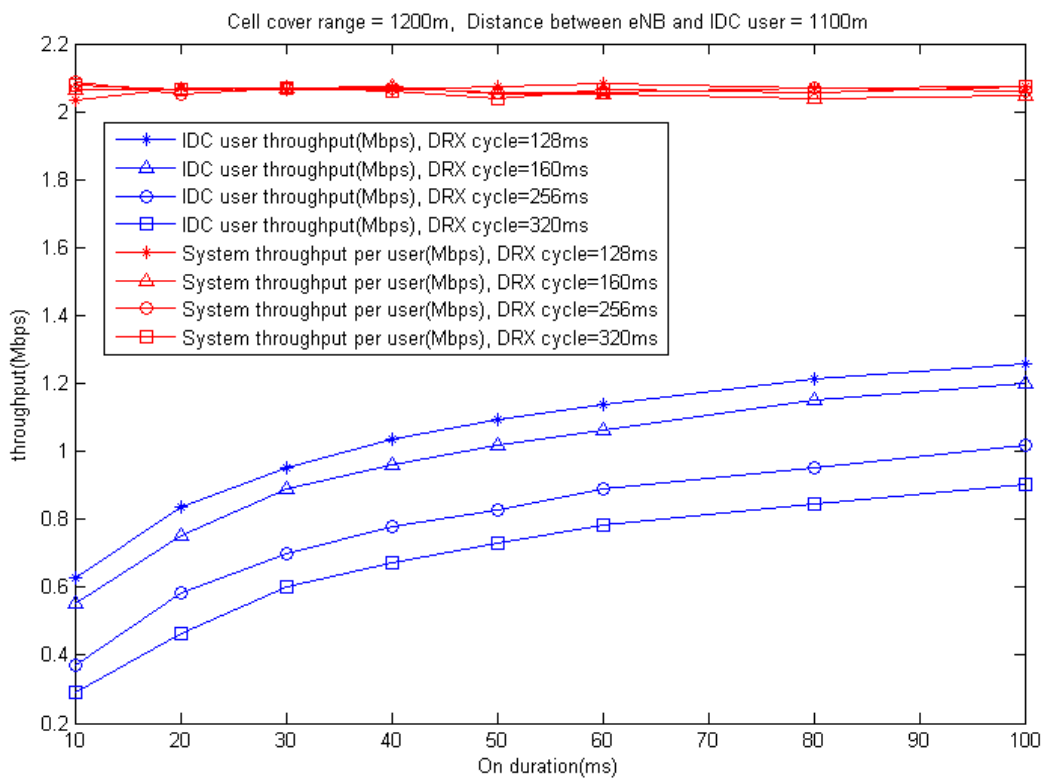Figure 5.35: On duration vs. throughput for different DRX cycle on distance 800m.

Figure 5.36: On duration vs. throughput for different DRX cycle on distance 1100m.
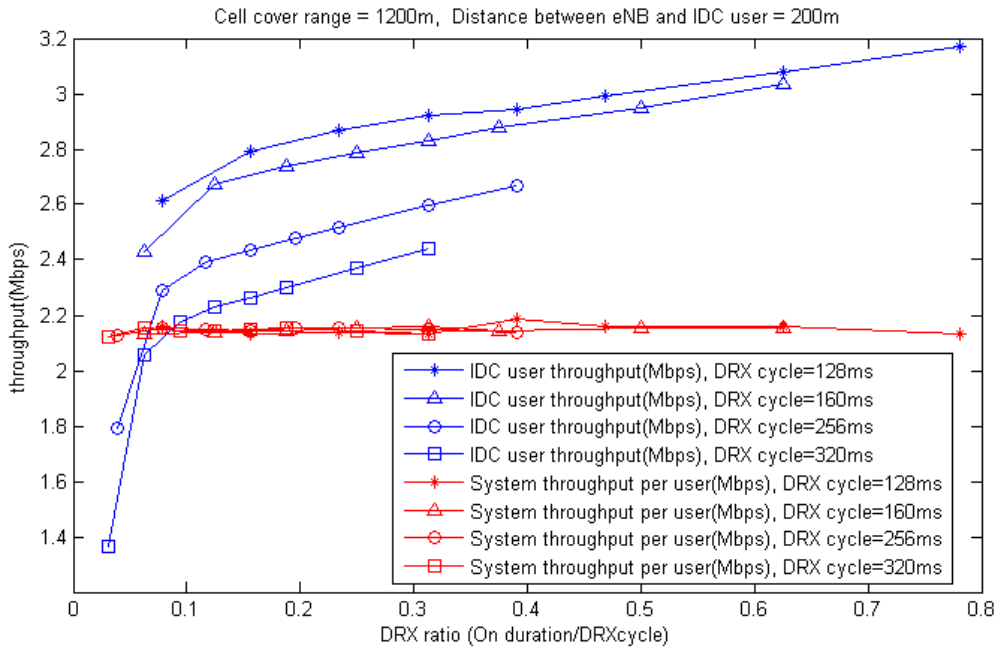
Figure 5.37: DRX ratio vs. throughput for different DRX cycle on distance 200m.

Fig. 5.36, the IDC user throughput will always be lower because distance become much far.

In Fig. 5.37 to 5.39, we compare LTE throughput with DRX ratios with all different DRX parameters for different distance 200m, 800m and 1100m. From these figures, we can observe that IDC user throughput will be larger if DRX cycle is smaller in the same DRX ratio. This is because that BS will allocate RBs to IDC user more urgently when DRX operates at On-duration in larger DRX cycle no matter this RB for the IDC user is good or not and it will degrade IDC user throughput. We can observe that they also have the same tendency related to distance from BS as like as Fig. 5.34 to Fig. 5.36. There is a situation that IDC user throughput will be closer each other for different DRX cycle when the distance between IDC user and BS become larger, because the scheduling scheme will allocate more RBs when IDC user close to BS, and it results in the difference between different DRX cycle being larger.

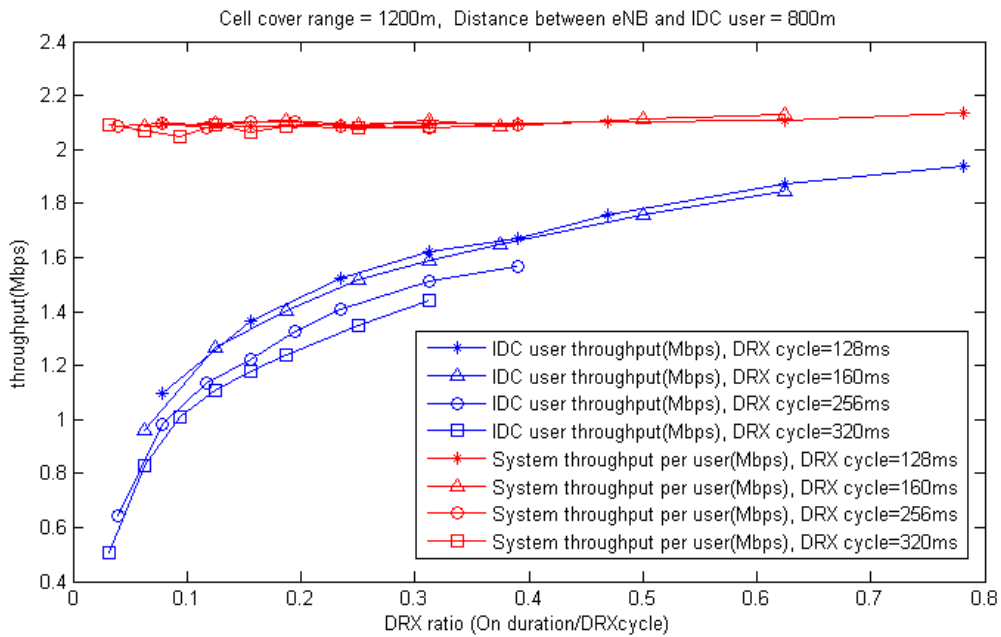As shown in Fig. 5.40, we show the average throughput effects throughout different

Figure 5.38: DRX ratio vs. throughput for different DRX cycle on distance 800m.
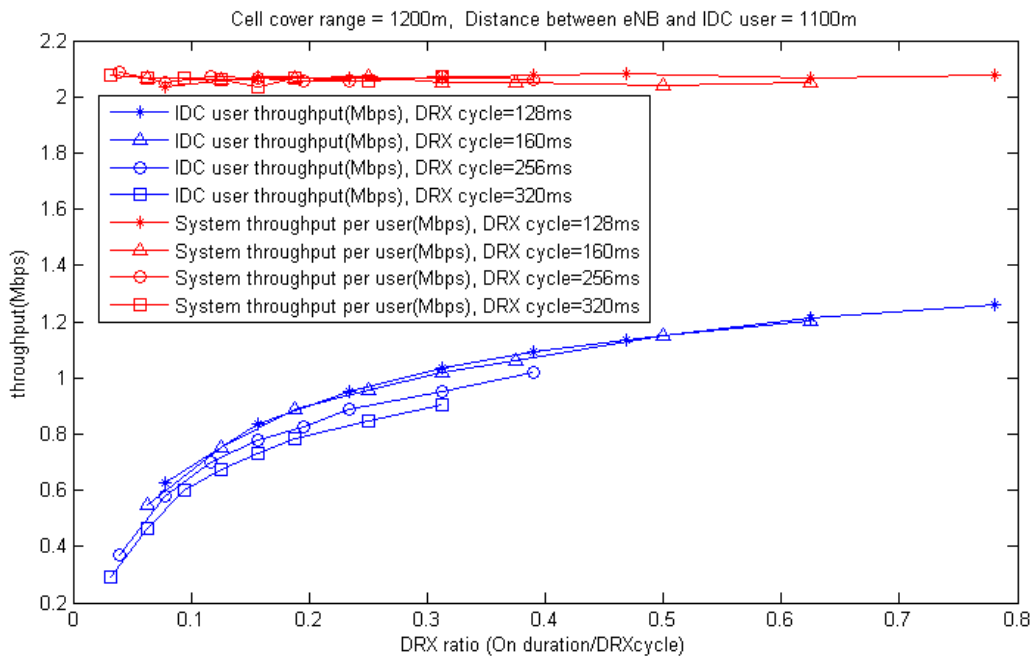
Figure 5.39: DRX ratio vs. throughput for different DRX cycle on distance 1100m.
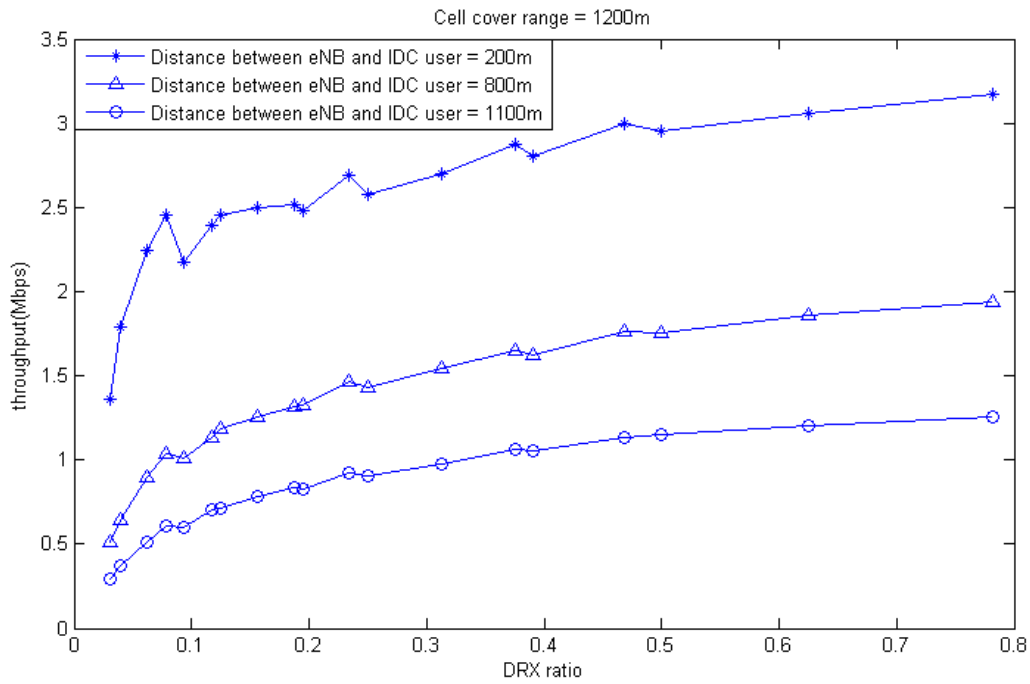
Figure 5.40: DRX ratio vs. throughput.

DRX ratio. The discontinue property of the curve comes from different throughput from different DRX cycle in the same DRX ratio for example Fig. 5.37, some DRX ratio will not appear on some DRX cycle pattern, and it results in the discontinue property of the curve. The tendency of throughput will be larger if the DRX ratio become larger because IDC user usable time ratio will also increase.

From simulation results, they conform the anticipation that the throughput gain come with increasing On-duration and DRX ratio and decreasing eNB-IDC user distance. In the scenario with large DRX cycle, eNB is likely to schedule RBs to IDC user urgently even if the physical channel corresponding to these IDC user RBs is in bad condition, thus its LTE throughput is inferior to the case with small cycle when fixing the same DRX ratio. Following these figures, user can select appropriate DRX parameters to fit its requirement.

Chapter 6

Conclusion

The IDCI issue related to the co-existence of LTE-TDD and WiFi transceivers is studied in this thesis. Methods for selecting appropriate reporting parameters of TDM and FDM based IDCI solutions have been proposed. To comply with existing LTE standard, the TDM solution has invoked the DRX mechanism. It is shown that judicious choices for the DRX triggering time and related parameters is of paramount importantance in optimizing the LTE and WiFi throughputs.

The best trigger condition depends on both WiFi uplink ratio and the corresponding interference level. We investigate different LTE and WiFi system parameter settings and study their effects on the respective throughput performance. We ind that increasing the number of WiFi users reduces the traffic of the coexistent WiFi uplink user of concern and results in lower WiFi interference level whence improves the LTE downlink throughput. On the other hand, if we increase the DRX active ratio, the LTE downlink throughput increases as well because the effective time for LTE to have collision-free transmission becomes longer if the DRX-based solution is properly triggered. When the WiFi uplink transmission rate increases, its buffer is emptied shortly and its interference reduces whence the LTE downlink throughput increases.

We propose a scheme which triggers and deactivates the DRX mode in proper epoches so as to maximizes LTE downlink throughput while meeting the LTE and WiFi throughput constraints. To find the optimal activate and deactivate times, the device has to be

able to estimate the associated SINR accurately. SINR estimate is also needed for FDM message reporting. We use a model-based method to jointly estimate the channel and SINR using a proper observation block size. As our SINR estimate becomes unreliable when the real SINR falls below 0 dB, an UE shall use the desensitization table to determine which frequency bands are usable, if the estimated SINR is less than or equal to 0 dB. The estimated usable and unusable bands whether they are determined by SINR estimator or by table look-up, shall be reported to eNB for FDM solution.

We analyze the WiFi and LTE throughput with/without DRX-aided scheme to help an IDC user selecting proper DRX parameters. The theoretical WiFi throughput value as a function of the number of WiFi user, n, the contention window size, W, and the maximum retry number of contention window, m. We derive the characteristic function of the WiFi packet transmission time and evaluate the corresponding mean and variance, assuming a fixed packet size. By inverting the characteristic function, we obtain the pdf of the packet transmission time with which the DRX-activated WiFi throughput is computed. The WiFi throughput is maximized by adjusting the packet size given that the WiFi transmitter knows perfectly the remaining available transmission time during a particular off-duration. The resulting throughput is hence equal to the unconstrained throughput times the off duty factor. The mean packet transmission time and the associated variance predicted by our analysis are verified by computer simulations.

As for the LTE IDC user throughput, we find that, for a fixed DRX cycle, it is an increasing function of the DRX on-duration and the DRX ratio but a decreasing function of the distance between user and BS. However, the IDC user throughput is nonlinearly related to the on-duration. The BS scheduling policy tends to allocate more RBs to an IDC user but less to other non-IDC users at the begin of an on-duration. The fairness requirement, however, will force the BS to gradually allocate more RBs to non-IDC users according to their rate specifications. Our simulation also indicate that, with a fixed DRX ratio, the IDC user throughput is a decreasing function of the DRX cycle and it

is insensitive to the DRX cycle when the distance between IDC user and BS is large. The last observation is due to the fact that the scheduler often allocate more RBs to an IDC user when it is close to the BS. These throughput performance trends are useful guidelines for us to select appropriate DRX parameters to satisfy the requirements of an IDC user.

Bibliography

[1] 3GPP TR 36.816 V11.2.0, Evolved Universal Terrestrial Radio Access (E-UTRA); Study on signalling and procedure for interference avoidance for in-device coexistence," ., in (Release 11).

[2] 3GPP TS 36.321 V10.4.0, Evolved Universal Terrestrial Radio Access (E-UTRA); Medium Access Control (MAC) protocol specification,"., in (Release 10).

[3] M. X. Chang and Y. T. Su, ModelVBased Channel Estimation for OFDM Signals in Rayleigh Fading," *IEEE Trans. Commun.*, vol. 50, no. 4, Apr. 2002, pp. 540V44.

[4] Nokia Corporation, "R2-121525: Details on IDC indication," *3GPP TSG-RAN WG2 meeting 77bis*, Jeju, South Korea, 26 - 30 Mar. 2012

[5] Pantech, "R2-116047: IDC trigger procedure," *3GPP TSG-RAN WG2 Meeting 76*, San Francisco, USA, 14th- 18th Nov. 2011

[6] CMCC, "R2-115839: On the procedure of interference avoidance for IDC," *3GPP TSG-RAN WG2 Meeting 76*, San Francisco, USA, 14-18 Nov, 2011

[7] Ericsson, ST-Ericsson, "R2- 121645: Measurements and triggers for IDC indication," *3GPP TSG-RAN WG2 77bis*, Jeju, South Korea, Mar 26-30, 2012

[8] 3GPP TR 25.996 V10.0.0, "Spatial channel model for Multiple Input Multiple Output (MIMO) simulations ," in (Release 10) 2011-03

[9] R. H. Jian and K. H. Liao, "Wireless Local Area Network, WLAN," *Chuan Hwa Publishing Ltd.*Press, Jan. 2007

[10] F. Khang, "LTE for 4G Mobile Broadband, Air Interface Technologies and Performance," Cambridge, U.K.: Cambridge Univ. Press, 2009.

[11] S. Sesia, I. Toufik, and M. Baker, "LTE, The UMTS Long Term Evolution: From Theory to Practice, Secomd Edition ," John Wiley and Sons, 2011.

[12] 3GPP TS 36.211 V10.4.0., "Evolved Universal Terrestrial Radio Access (E-UTRA); Physical Channels and Modulation,"., in (Release 10).

[13] 3GPP TS 36.331 V10.3.0., "Evolved Universal Terrestrial Radio Access (E-UTRA); Radio Resource Control (RRC); Protocol specification ,"., in (Release 10).

[14] G. Bianchi.,"Performance analysis of the IEEE 802.11 distributed coordination function "*IEEE J. Select. Areas Commun.,* vol. 18, pp. 535V547, Mar. 2000.

[15] K. C. Beh, S. Armour, and A. Doufexi, Joint Time-Frequency Domain Proportional Fair Scheduler with HARQ for 3GPP LTE systems, *Proc. IEEE Veh. Technol. Conf. (VTC),* Calgary, Canada, Sept. 2008.

.

作者簡歷

一、個人資料

姓名	賴勇先
生日	1988/08/16
出生地	台中市
E-mail	lai77816@yahoo.com.tw
永久地址	40744 台中市西屯區至善里 14 鄰逢甲路 339 號
通訊地址	300 國立交通大學電信工程學系 811 實驗室
電話	(03)5712121 轉 54571
現職	國立交通大學電信工程研究所 系統組 碩士班二年級

二、學歷

高中	國立台中第一高級中學	2003/09-2006/06
大學	國立中山大學 電機工程學系	2006/09-2010/06
研究所	國立交通大學 電信工程研究所碩士班	2010/09-2012/08

三、擅長工具

C/C++	Matlab	Mathematica
Office	Latex	Windows

四、參與培訓課程與研討會

單位	培訓課程/研討會 名稱
台北大學通訊工程研究所	2011 消息理論及通訊春季研討會暨國科會成果發表會
中山大學通訊工程研究所	2011 消息理論及通訊秋季研討會暨國科會成果發表會
交通大學電機工程學系	RF4206 LTE PHY 系統技術簡介
交通大學電信工程研究所	國外學者短期課程 Cross Layer RRM for Next Generation Wireless Networks Speaker: Professor Vincent Lau